ON MODELLING RESPIRATORY ARRHYTHMIA OF HEART RATE

English Translation of a
Masters Thesis in Psychology
at the Eberhard-Karls University of Tübingen
by

HANS STRASBURGER

MUNICH 1979

English translation April 2025

This publication is a translated version of my diploma thesis (masters thesis)
‘Zur Modellierung der respiratorischen Arrhythmie’
(http://dx.doi.org/10.15496/publikation-102954)
which was submitted in autumn 1979 for the diploma examination in psychology at the
Eberhard-Karls University of Tübingen

Preface to the English Translation

When, in the nineteen-seventies, I joined the psychophysiology research group, led by Rupert Hölzl and Roman Ferstl at the Munich Max-Planck Institute for Psychiatry, Rupert Hölzl had come across an exciting earlier cybernetic study of Martin Clynes (then at Rockland State University, NY), who had shown that respiratory arrhythmia of heart rate (RSA) was well described by a non-linear system sensitive to the direction of breathing (Clynes, 1960, 1962, 1969). The interesting property of Clynes' model was that – unlike many other non-linear biological systems – it could not be approximated by a linear system, even at small amplitudes. Yet by taking the direction of breathing into account, i.e. by introducing a simple non-linearity, a system composed of two linear systems (one for inhalation and the other for exhalation) worked perfectly. This held the promise to uncover the reason for many contradictory results on RSA, e.g. whether breathing-in or breathing-out would accelerate or slow-down heart rate. Contradictory results were also obtained for the orienting response (OR) of heart-rate, a major topic in psychophysiology at the time, which might also have stemmed from the RSA, acting as a confounding variable. Similar puzzling results on the RSA and OR still seem to exist today. Clynes also showed a similar, direction-sensitive behaviour for another physiological system, control of the pupil of the human eye (Clynes, 1962). To describe such systems, Clynes coined the terms *unidirectional rate sensitivity,* and later *rein control* (Clynes, 1969), where – unlike in a linear system – an effect in a subsystem can only be exerted in a single direction, similar to pulling the reins in horse riding.

Shortly before I joined, the psychophysiology research group had acquired a state-of-the-art analogue computer, made by Electronic Associates Inc. (EAI), and, together with a PDP-8 running FORTRAN and assembler – an excellent digital laboratory computer system for real-time applications – and also extensive psychophysiological hardware, the lab was well-equipped for real-time physiological simulations. I was hired to implement, verify, and extend Clynes' RSA work, and work towards applications in, e.g., behaviour therapy. Indeed, by 1979 we had a running and verified RSA-simulation in real time, with individualised system parameters for a number of subjects, documented in my unpublished thesis.

Clynes' (1960) paper was seminal for unraveling the workings of respiratory arrhythmia of heart rate, with reference to it even today

(Wang & Zhu, 2025). More than thirty studies have since explored its dependence on important factors, including respiration rate, tidal volume, vagal tone, lung volume, breathing patterns, subject age, and interindividual differences (see Grossman & Taylor, 2007, for a review). An application as a measure of vagal tone which we envisaged, important in assessing relaxation from stress, has indeed come true (e.g. Goldberger, Challapalli, Tung, Parker, & Kadish, 2001).

Research on RSA has thus indeed advanced enormously. However, what we considered Clynes' ground breaking new achievement – showing the non-linear, unidirectional character of RSA and other biological systems – appears to have rarely been explored further. Hirsch & Bishop (1981), e.g., who cite Clynes (1960), show Bode diagrams of RSA vs frequency, which presupposes linearity. Saul et al. (1991), who also cite Clynes (1960) and even have *transfer functions* in their paper's title, use that term in a colloquial manner (1991, p. 1231) to mean the amplitude and phase response, ignoring that converting these to a transfer function requires linearity of the underlying system. Indeed, the main message of Clynes (1960) is that this is *not* the case.

One exception to the above is the work of F. Foerster in Freiburg (1978, 1984). As a mathematician, he published (in German) a unidirectional-rate-sensitive third-order digital filter along the model of Clynes, with transfer functions derived from step responses, *separately for inhalation and exhalation* (Foerster, 1978). He later implemented the model in a collection of programs for biosignal analysis for further use (Foerster, 1984).

Notes on the translation. After all this time, the topic of respiratory arrhythmia has lost none of its topicality. Clynes' (1960) paper remains seminal and is widely cited. At the same time, however, its main message – the RSA's removable non-linearity – has been, except for Foerster (1978, 1984), fully neglected in the literature I have reviewed. I therefore decided to transfer my type-set thesis to machine readable form and make it available online (Strasburger, 1979). In the corresponding English translation here, the figures are mostly left unchanged to preserve the character of the time, and are only occasionally annotated in English for readability. Equations were converted to current layout for legibility, however. Footnotes are from the original, except for a few (set in a different font) that refer to the translation.

Munich, March 2025

References

Clynes, M. (1960). Respiratory control of heart rate. Laws derived from analog computer simulation. *IRE Transactions on Medical Electronics*(1), 2-14.

Clynes, M. (1962). The non-linear dynamics of unidirectional rate sensitivity illustrated by analog computer analysis, pupillary reflex to light and sound, and heart rate behavior. *Annals of the New York Academy of Sciences, 98*(4), 806–845.

Clynes, M. (1969). Cybernetic implications of rein control in perceptual and conceptual organization. *Annals of the New York Academy of Sciences, 156*, 629-664.

Foerster, F. (1978). Zur psychophysiologischen Methodik: Phasische Herzfrequenz-Reaktionen unter Berücksichtigung der respiratorischen Arrhythmie [Psychophysiological methodology: Phasic heart rate reactions with consideration of respiratory arrhythmia]. *Zeitschrift für Psychologie, 186*, 518-528.

Foerster, F. (1984). *Computerprogramme zur Biosignalanalyse*. Berlin: Springer.

Goldberger, J. J., Challapalli, S., Tung, R., Parker, M. A., & Kadish, A. H. (2001). Relationship of heart rate variability to parasympathetic effect. *Circulation, 103*(15), 1977–1983.

Grossman, P., & Taylor, E. W. (2007). Toward understanding respiratory sinus arrhythmia: Relations to cardiac vagal tone, evolution and biobehavioral functions. *Biological Psychology, 74*, 263-285.

Hirsch, J. A., & Bishop, B. (1981). Respiratory sinus arrhythmia in humans: how breathing pattern modulates heart rate. *American Journal of Physiology - Heart and Circulatory Physiology, 241*(4), H620-H629.

Saul, J. P., Berger, R. D., Albrecht, P., Stein, S. P., Chen, M. H., & Cohen, R. J. (1991). Transfer function analysis of the circulation: unique insights into cardiovascular regulation. *American Journal of Physiology-Heart and Circulatory Physiology*, H1231-H1245.

Strasburger, H. (1979). *Zur Modellierung der respiratorischen Arrhythmie [On modelling respiratory arrhythmia of heart rate].* Max-Planck Institute for Psychiatry, München, and Department of Psychology, University of Tübingen, 208 pp., dx.doi.org/10.15496/publikation-102954.

Wang, C., & Zhu, H. (2025). *Universal Behavior Computing for Security and Safety. Chpt. 1, Overview of universal behavior computing*.

Preface

The present work was carried out in the Psychology Department of the Max Planck Institute of Psychiatry in Munich under the supervision of Dr. R. Hölzl (MPI of Psychiatry) and Prof N. Birbaumer (University of Tübingen).

I would like to thank Dr Rupert Hölzl for his support and his many valuable suggestions and discussions. To Dieter Klenk (Dipl. Psych.) I owe the suggestion for the principle of the breath analyser, Peter Bolsinger helped me with questions of systems theory. The manuscript was typed by Miss A. Wörl; Mrs Sylvia von Gienanth helped me with its completion. My sincere thanks go to all of them.

Munich, May 1979 Hans Strasburger

TABLE OF CONTENTS

ABBREVIATIONS USED

ECG: Electrocardiogram

EHR: Evoked heart rate response

HR: Heart rate

HRR: Heart rate response

IBI: Interbeat interval, distance between two R-waves of the ECG orienting response

RSA: Respiratory (sinus) arrhythmia

Note: Symbolism of the circuit diagrams according to SCS Standards Committee

1. INTRODUCTION

The inspiration for the present work comes primarily from two areas of psychophysiological research: studies on the orientation response (OR) of the heart rate, and studies on heart rate (HR) biofeedback.

There are a large number of studies on the habituation of the heart rate orienting responseresponse to neutral and stress stimuli, which have produced contradictory results, both with regard to the course of the orienting response itself and with regard to the dependence of the speed of habituation to various parameters. Standard procedures for the exact determination of individual habituation processes would be important in the field of psychosomatic research, because when comparing response patterns of different subjects, a particularly slow habituation in certain physiological "channels" of the subject can provide indications of the susceptibility to stress of the respective organ systems (organ specificity). This would possibly provide a means of prognosis of the therapeutic success of biofeedback techniques and related procedures.

However, recording the heart rate response is not easy, as its course is initially largely masked by the physiological noise of the heart rate measurement. Various averaging methods can be used to eliminate the noise. In principle, there are the two possibilities of averaging: within a subject over different stimuli, or over different subjects with a fixed stimulus. If the time courses are averaged within a subject, with repeated presentation of the stimulus, there is a risk of blurring the information on habituation; the course of habituation becomes dependent on the number of responses included in the averaging (see Fig. 1.1 and 1.2). The answer to the question of when the habituation is "complete" obviously depends on the success of noise suppression. Statements in this direction should therefore be viewed with caution (see SCHANDRY, LUTZENBERGER and BIRBAUMER 1977).

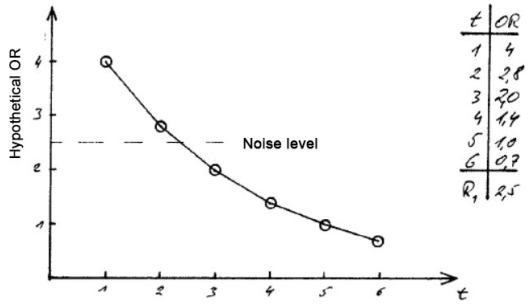

Fig. 1.1: Hypothetical "true" course of habituation

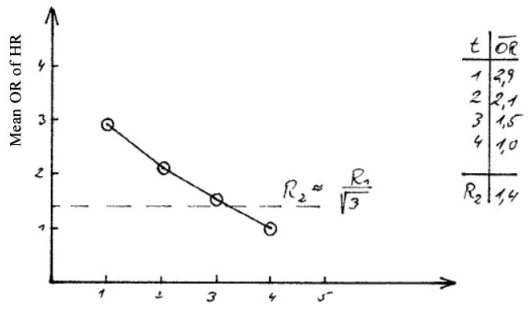

Fig. 1.2: Course of habituation after averaging three successive responses.

The other possibility: averaging the responses of different subjects to the same stimulus is questionable, as the averaged response is possibly no longer representative for the individual processes. FERSTL and HÖLZL (1979) were able to distinguish at least three types of responses, which, when superimposed, would almost cancel each other out in the averaged HR response (see Fig. 1.3). The only possibility is to reduce the error variance in the real-time signal.

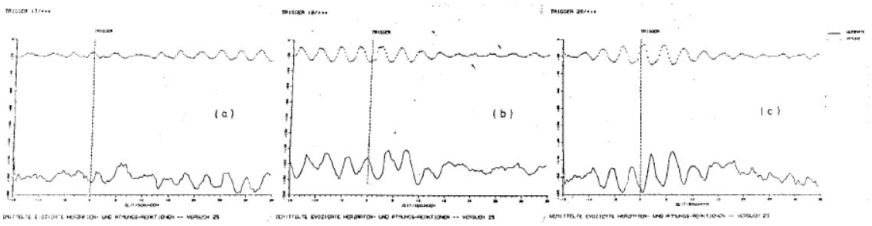

Fig. 1.3: HR response types according to FERSTL and HÖLZL (1979)

Now, a considerable part of the error is by no means stochastic but consists of a pronounced fluctuation in the rhythm of breathing, the so-called respiratory (sinus) arrhythmia (RSA). It usually amounts to approx. 10 beats per minute (bpm), but can increase up to 70 bpm (CLYNES 1959). Its severity depends, among other things, on the depth and speed of breathing as well as on the general level of the subject's activation. It varies greatly from person to person, and is particularly pronounced in people under 30; it can also be completely absent.

In the past, various attempts have been made to eliminate this influence from the data. They are discussed in Chapter 2.2. What they all have in common is that they make incomplete use of the regularity of the RSA. The relationship can be mathematically described quite accurately; a corresponding analogue computer model for simulating the RSA was already created by CLYNES in 1959. In the present context, however, his work, as well as the remarkable further developments by

MIYAWAKI et al. (1966) and LUCZAK and RASCHKE (1975), remained unnoticed until very recently. Almost 20 years later, independently of the present work, the CLYNES model was taken up and applied as a digital model for extracting the RSA (FÖRSTER 1979, in press).

In addition to investigating the OR, a second possible application of a HR freed from the influence of breathing is in biofeedback experiments: Conditioning of central autonomous control of HR can only be spoken of properly if the feedback signal contains predominantly central nervous information components. If the feedback is dependent, in part, on mechanisms such as the RSA, which have a secondary modifying effect on the HR, then these moderating processes are possibly conditioned instead. Although central autonomous learning can take place, it is difficult to prove. In all previous attempts at HR conditioning, great care had to be taken to subsequently exclude the effectiveness of moderating processes as the main cause.

A further difficulty lies in the possibility of "superstitious" learning: if, for example, cardiac acceleration is to be trained, short R-R intervals must be rewarded; these occur preferentially during inspiration, then inspiration will be rewarded regularly and the subject will either breathe faster in order to receive more reinforcement or breathe more slowly and deeply in order to remain in the reinforcement zone for longer. Since faster breathing, in contrast to deeper breathing, does not change the mean HR (SROUFE 1971), the effective impact on the HR can be quite different. A detailed discussion of the methodological problems associated with biofeedback of the heart rate can be found in HÖLZL (1976).

Direct feedback of central nervous components of the HR information is further desirable because there are some indications that direct autonomous conditioning has a longer lasting success (BELMAKER 1972).

Measurement of the evoked heart-rate response (EHR) and of HR in biofeedback experiments are two important applications in which the RSA represents a confounding variable. In addition, however, there has recently been increasing evidence that the RSA – contrary to earlier belief – could itself contain important information. Low RSA, for example, appears to be associated with a higher risk of cardiac death (see KATONA and JIH 1975 for literature references). HARRER

(1977)[1] investigates connections between RSA and disorders of the autonomic nervous system, e.g. in spinal processes. In addition to an extraction of the RSA, procedures should therefore be endeavoured which allow the HR to be broken down into respiratory and central-nervous mediated components and to determine the two independently of each other. Approaches to this could be derived from the systems theory viewpoint adopted in this work.

Such a decomposition of HR into different components has an even more general significance: it can serve as an example of the possibility of separating interacting or superimposed variables using system theoretical methods in order to arrive at more specific statements about psychophysiological mechanisms. Other obvious variable interactions for which a similar approach would be possible are found, for example, between the EEG and EOG (electrooculogram).

The present thesis deals with the extraction of the RSA using system-theoretical methods. With the help of a dynamic model[2], the course of the RSA is predicted at each point in time and is subtracted from the natural HR. Such a model can be realised in digital or analogue form. In both cases, there are several options available for implementation, which differ in terms of their circuitry or programming complexity, critical behaviour, working speed, the effort required to derive their structure, etc. Which is the best method? The best method must be decided for each specific application. The more advanced the analysis of the system behaviour is, the more flexible one will be in the choice of the respective method.

For a linear system, the simplest and most direct way on the digital computer uses direct convolution. In biological systems its use was pioneered by FÖRSTER (1979). The efficiency of this method was demonstrated in a study on the orienting response (OR), in which stimulus-induced HR changes after RSA extraction became independent of breathing manipulations.

---

[1] HARRER, G. (1977): (1977): Unpublished lecture at the 6th Workshop for Psychophysiological Methodology in Heidelberg.

[2] Dynamic model: A dynamic model is a system whose output signal depends not only on the current values of the input signals, but also on its past. Its behaviour can be described by a differential equation system, for example. In contrast, in static models only the current value of the input signals affects the output; if, for example, the current output value is a linear combination of the current input signals, the parameters can be determined by multiple linear regression. A more recent introduction to the theory of dynamic systems is, e.g., the book by UNBEHAUEN (1971); a detailed description of digital simulation is provided by ROSKO (1972).

In the present work, the system analysis is to be taken one step further. The empirically determined step response of the HR was used to determine third-order transfer functions, which are the prerequisite for the realisation of an RSA model on the analogue computer (for explanations of terms, see Chapter 2.8.2). The reason for this was that an analogue computer was available in our lab, which was acquired to free the digital computer, a PDP-8, from signal pre-processing tasks. If, namely, in a psychophysiological experiment several variables are to be pre-processed, recorded, checked, and simultaneously output to influence the course of the experiment, and the experiment is further to be controlled, even powerful laboratory computers are quickly overloaded. Tasks therefore will need to be decentralised. In addition to analogue pre-processing, digital pre-processing should also be considered. In this case, also, knowledge of the transfer function is desirable, as it enables the construction of recursive filters, which are considerably superior to direct convolution in terms of the required computing time.

For the routine use of RSA extraction in psychophysiological research and practice, the aim should be miniaturising the necessary circuitry. Analogue methods are currently still cheaper and simpler to implement. In psychophysiological laboratories, in addition, the monolithic "digital analogue computers" that are already available today, can be considered for use. These are microcomputers with internal digital data processing, but analogue inputs and outputs.

With digital RSA extraction, data acquisition, processing, simulation, and data output are all carried out on the digital computer, making all that essentially a software-based task. The use of an analogue computer brings with it a whole series of additional methodological and technical difficulties, which will be described in the course of this work. The interface between digital and analogue computers requires amplitude and time scaling, synchronisation of the computers, the sources of noise signals are increased and data input and output are made more difficult. These tasks have been solved here with a complex laboratory installation system, the structure of which will be described elsewhere (STRASBURGER, in preparation).

Overview of the thesis

In a first theoretical section, the role that RSA plays in psychophysiological research is described. An overview of the current state of research into the physiological mechanisms underlying RSAwill give an impression of the diagnostic information that can be

expected from it and the extent to which the procedures for the treatment of the HR signal appear appropriate. A brief discussion of these procedures is intended to illustrate the purpose of the RSA simulation attempts undertaken. This includes first and foremost the pioneering work of M. CLYNES, in particular his concept of "unidirectional rate sensitivity". After a summary of the points of criticism of CLYNES and a discussion of physiological implications, more recent modelling attempts are touched on. The application of analogue and digital simulation for HR correction is then presented. Criteria are discussed with which the quality of the correction methods can be determined. An excursus on the problems of definition and collection of the HR measure concludes this part.

The subsequent experimental part is divided into two subject areas: Problems of respiration measurement and problems of RSA simulation.

After having tried various common techniques for indirect respiration measurement which turned out to be unusable for the purpose at hand, it became necessary to develop a measurement method of our own. In our research group we therefore built temperature-compensated opto-electronic belts for breathing measurement by measuring chest and abdomen circumference. By multiple linear regression with the intercept forced to zero, it was possible to combine the circumference measurements into a reliable respiratory volume measure. Next, the method’s applicability for *paced respiration* is described (in *paced respiration* the subject is shown their breathing pattern on a visualisation device and is asked to match it to a predefined pattern).

Various methods from the theory of dynamic models are available for creating an RSA model. In addition to the classical methods of frequency response and transfer function analysis, probabilistic methods have been used more recently. Firstly, I will therefore justify the selection of the method used. In order to carry out the selected transfer function analysis, the response of the HR to stepped breathing is examined. To obtain reliable HR responses, 10 – 20 step responses are obtained from which an average time course of the HR is calculated. The respiratory amplitude and the step-shaped time course are kept constant with paced breathing. The experiment is described and the results discussed.

One of the main results is the confirmation of CLYNES' "unidirectional rate sensitivity": heart rate responses to inhalation and exhalation steps are not mirror images of each other, as would be expected in a linear system, but are almost identical. This means that one of the main

precondition of the usual averaging methods is violated: Breathing-related errors in the HR response do not average out, but can add up. This result suggests a critical review of other studies on the evoked HR response.

In addition to determining the step response, the experimental set-up and associated software form a flexible and comfortable system for analysing the average HR response to any shape of the course of breathing, or other stimuli.

In the next step, a model was created that has a step response similar to that of the real HR. A graphical analysis of the step response led to parameter estimates for a second-order model[3]. An implementation on the digital computer of the expected step responses of second- and third order systems provided a simplified identification of parameters and an overview of how parameter changes affect the behaviour of the step response in an ideal system. The results on the digital computer led to a direction-dependent third-order system on the analogue computer. To determine the parameters on the analogue computer, the average real step response is output in analogue form at increased speed, and compared with the step response of the analogue computer model.

The fitted model response shows very good agreement with the real HR response. Finally, the properties of the model are discussed, as well as the differences to CLYNES' and FÖRSTER's models. In an outlook, the further development of the work with regard to standard application in psychophysiological experiments is outlined.

The appendix provides technical details: circuit diagram and structure of the breathing measurement belts, presentation of the variant of multiple linear regression for obtaining a breathing volume measure from the circumferential measurements, a comparison of transfer functions up to the third order and their corresponding step responses, a compilation of basic analogue computer circuits, as well as the description of the programme system.

To streamline the presentation of the work, technical details for readers interested in systems theory, as well as introductory systems theory principles, are summarised in footnotes and excursuses.

[3] The order of a linear system is the number of its storage units, on the analogue computer the number of integrators involved, in the descriptive differential equation the highest degree of the time derivative, in the transfer function the degree of the denominator polynomial, and in the step response the number of exponential functions.

2. THEORETICAL PART

2.1 Physiological principles of respiratory arrhythmia

Although respiratory arrhythmia has been studied since the beginning of the century, physiologists have not yet been able to reach a consensus as to which of the possible mechanisms plays the main role in the development of RSA. Four mechanisms are mainly considered:

(1) During inspiration, stretch receptors in the lungs and thorax inhibit the cardiac inhibition centre (dorsal nucleus of the vagus) of the medulla oblongata via the afferent vagus, thereby reducing the activity of the afferent vagus, which in turn decreases HR. The heart thus beats faster (GANONG 1972).

(2) According to the current view, the baroreceptors of the carotid sinus and aortic arch are further involved in the generation of the RSA.

The baroreceptors are the sensors of the control circuitry which ensures that the correct blood pressure is maintained under varying physiological conditions. Higher blood pressure is signalled to the vasomotor centre by the baroreceptors through increased activity of afferent nerves. This, in turn, is signalled back to the medulla oblongata and leads, reflexively, to a reduction in blood pressure by lowering peripheral vascular resistance, lowering HR, and (at higher heart rates) possibly lowering contractility (force of contraction). With regard to the heart, under resting conditions the vagus is mainly active, which influences HR only – not contractility.

The pressure fluctuations in the thoracic cavity that occur during breathing are now transmitted to the veins and arteries within it. The negative pressure during inspiration thus increases the filling of the right ventricle. At the same time, the lungs suck blood back from the left atrium, which leads to poorer filling of the left ventricle and a drop in aortic pressure. However, this initial drop in aortic pressure is soon equalised (after 1 to 2 heartbeats) and even overcompensated by the blood that has passed through the lungs in the meantime. (DALY 1930, DAVIES and NEILSON 1967; KOEPCHEN 1972, p. 214, however, is of a different opinion here). Reflexive compensation of blood pressure via the baroreceptor mechanism should therefore lead to a reduction in HR.

However, FREYSCHUSS and MELCHER (1976) were unable to find a negative correlation between blood pressure and HR. They therefore (among other things) ruled out the baroreceptor mechanism as the main

cause. They use the pressure of the brachial artery (measured continuously with a catheter) as an aortic pressure reference measure. However, whether this is a valid measure seems questionable to us: due to the Windkessel effect of the arterial system, rapid pressure fluctuations of the aorta, in particular, will no longer be clearly visible on the arm. The time delay of the arterial pressure increase of approx. 2 seconds found by FREYSCHUSS and MELCHER could be the peripheral effect of the aforementioned short-term drop in aortic pressure during inspiration. Such rapid changes in blood pressure are not negligible, since it is known that the baroreceptors are strongly influenced by the *speed* of blood pressure changes, and in different ways for rise and fall (KATONA and BARNETT 1969, STEGEMANN and TIBES 1969). Simple correlations of measures are unsuitable for recording such temporal dependencies; clarification can only be expected from a dynamic approach (LUCZAK & RASCHKE 1974, DAVIES & NEILSSON 1967). In such an approach, the mean increase in HR during inspiration is not set in relationship to the mean increase in blood pressure (which then would not be explained by the baroreceptor mechanism), but the initial rise in HR can be explained as a response to the brief drop in blood pressure mentioned above, and the further course as the decay of this response. This biphasic course of the HR (acceleration/deceleration) was found by DAVIES & NEILSON (1967) as a response to isolated inhalation (as previously by CLYNES 1959). For responses to inhalation and exhalation to be considered in isolation, it is necessary to separate them sufficiently far in time from one another. Otherwise the responses overlap, so that the outcome can even be reversed with rapid breathing. FREYSCHUSS & MELCHER also paid no attention to this dependence of the RSA on breathing frequency which ANGELONE & COULTER (1964) described. The role of the baroreceptor mechanism in the development of RSA is therefore still controversial.

Intrathoracic fluctuations are furthermore not only proportional to the filling state of the lungs, but above all to the breathing speed: the intrathoracic positive or negative pressure serves to overcome the airway's flow resistance ; higher flow speeds therefore require higher pressure differences. (Since psychological factors can change the airway's resistance, the assumption of constant resistance is not entirely self-evident.) Therefore, if pressure fluctuations in the thoracic cavity play a causal role in respiratory arrhythmia, the latter must be expected to be dependent on the speed of breathing.

(3) Reflex responses to stretching of the veno-atrial junction, the

ventricles, the pulmonary vein and the left atrium are considered as further mechanical-neuronal mechanisms (FREYSCHUSS & MELCHER 1976).

(4) The persistence of RSA after switching off the respiratory movements (by neuromuscular blockade) shows that, in addition to the mechanical effects, central couplings between the respiratory and circulatory centres also play a role (KOEPCHEN & THURAU 1952, VALENTINUZZI & GEDDES 1974). (Needless to say, the absence of RSA during breath-holding is not an argument against the effectiveness of central factors, as DAVIES & NEILSON (1967, p. 953) suggest, since the respiratory centre does not emit any impulses during breath holding.) There is really only agreement that the RSA is mediated almost exclusively via the vagus nerve. It is even possible to quantitatively determine the effectiveness of the vagus on the heart via the extent of the RSA: KATONA & JIH (1975) define "parasympathetic control" (PC) as the difference in HR before and after pharmacological vagus blockade; they were able to demonstrate a correlation of $r = 0.969$ between PC and the extent of the RSA.

In summary, the development of RSA can be explained by mechanical effects in the thoracic cavity and homeostatic mechanisms involving the cardiovascular centres and the respiratory centre of the brainstem.

The control model shown in Fig. 2.1 may serve as an overview. However, neuronal activity that carries psychological information originates from higher centres (cortex, hypothalamus, limbic system). Their influence is rather to be understood as by changing the setpoints and boundary conditions of the homeostatic and mechanical processes than by directly adjusting peripherally measurable parameters such as HR, blood pressure, etc. Since this neuronal activity cannot be measured directly (and will not be measurable in the foreseeable future), it is only possible for now to estimate its influence by describing the regularity of the homeostatic processes in sufficient detail and using this information to draw conclusions. From this point of view, the recently created complex cybernetic models, such as the blood circulation model of LUCZAK & RASCHKE (1975), are not only of physiological but also of psychophysiological interest.

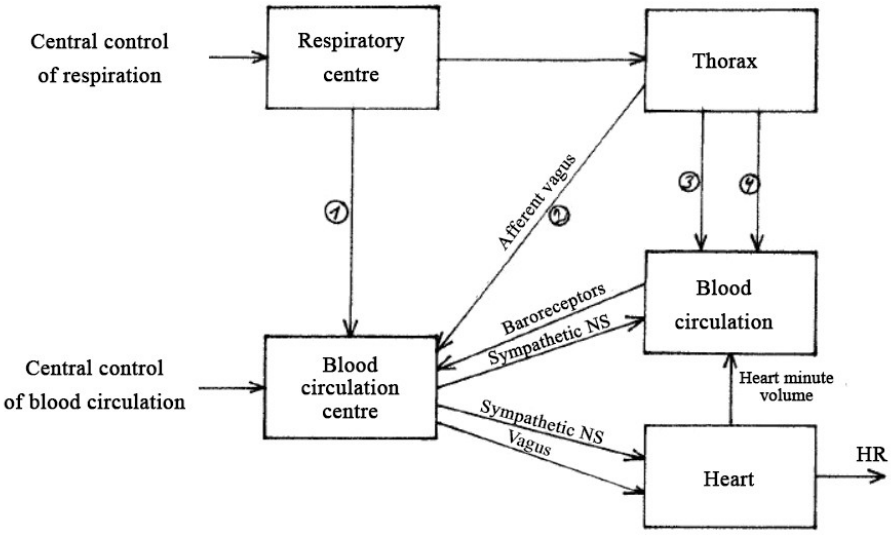

Fig. 2.1: Interaction between respiration and circulation

Legend:

(1) Coupling of inspiratory centre and circulatory centre

(2) Activity of the lung's and thorax's stretch receptors

(3) Mechanical effect of the thorax on the veins of the thoracic cavity: It changes the venous ventricular filling and thus the cardiac output, and subsequently the heart rate via a compensatory reflex (Valsalva test).

(4) Mechanical effect of the thorax on the arteries of the thoracic cavity: It results in pressure fluctuations synchronous to respiration in the entire high-pressure system. These are regulated by baroreceptors and lead reflexively to changes in heart rate.

2.2. Previous treatment of heart rate data

A brief overview of the data handling methods used to date is intended to make their possibilities and limitations understandable and to help assess what improvements an RSA model can deliver.

As already indicated, disturbances in the heart rate measurement have so far essentially been eliminated by various averaging methods. In principle, there is the possibility of time averaging and sample averaging.

2.2.1 Time averaging

Since it is not possible to average over the entire past of a time series, one can look at a sliding time window of constant length extending into the past, or to simulate such a window by allowing data further back in time to be weaker in the averaging. The first option is called moving time averaging.

Moving time averaging

The time window has the length T (T must of course be longer than a breathing period). Between the current time t and t-T, let the n measured values HR(t) have been recorded at the times t. The averaged heart rate is then

$$\overline{HR} = \frac{1}{n} \sum_{t-T \le t_i \le t} H(t_i) .$$

With continuous measurement, this becomes

$$\overline{HR} = \frac{1}{T} \int_{t-T}^{t} HR(\tau)\, d\tau .$$

In real time, the sliding time averaging can be implemented via an analogue or digital shift register, or with an analogue filter with an approximately rectangular impulse response.

Advantages: Data available in real time; simple realisation on the digital computer.

Disadvantage: The better the suppression of interference should be, the larger the time window must be chosen. This renders the measure insensitive to rapid changes, as these receive comparably less weight than the previous data.

Weighted moving time averaging

Simple low-pass filtering is more convenient in real time. This results in a weighted moving average over time, in which values further in the past are weighted less by weighting with an exponential function:

$$\overline{HR} = \int_{-\infty}^{\infty} e^{a(\tau - t)} HR(\tau)\, d\tau$$

Because of the circuitry used, e.g., on an analogue computer, this averaging is also called "RC-averaging"; in older papers the filter is referred to as a "leaky integrator" (see Fig. 2.2). Low-pass filtering is used, for example, in simple pulse meters. The disadvantages are the same as those of unweighted averaging.

2.2.2. Sample averaging ("coherent averaging")

When it can be assumed that a heart rate response follows a certain internal or external stimulus in a stereotyped manner, several measurements can be made and interpreted as a random sample of the

response. If HR(t) is the course of the response to the i-th stimulus given at time t_i, the mean time course is

$$\overline{HR} = \frac{1}{n}\sum_{i=1}^{n} HR_i(t - t_i)\,.$$

The responses are thus averaged in a time-synchronous manner. You can either average over the responses of different subjects or average over several responses within a subject. In the second case, it is also possible to reduce the weighting of responses further back in time; this is referred to as sliding coherent averaging. The advantage of the latter method is that it can also be used to detect short-term changes in HR.

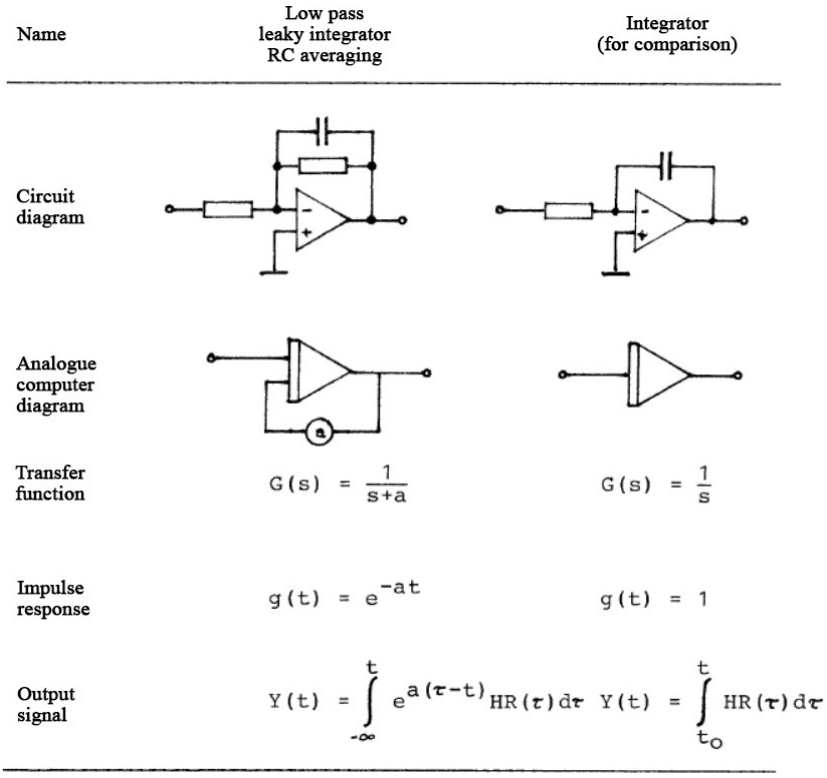

Fig. 2.2: Low-pass filter and integrator

Time-synchronous averaging is therefore used, for example, in studies on the orienting response and habituation. A disadvantage is that the results are available only after several measurements; one-off processes, such as heart rate responses to internal stimuli in therapy situations, can still not be detected.

To eliminate the RSA in the HR signal, the stimuli are either set

independent of the respiratory phase, or are set alternatingly at the respiratory maximum and minimum. For the noise to be removed by averaging and that no systematic signal distortion occurs, it must be assumed that noise is additive to the signal, that there is no interaction with the signal, and that, with increasing number of responses, the mean of the noise vanishes. None of these preconditions are generally fulfilled in the RSA, however. On the one hand, all authors who have analysed the influence of inhalation and exhalation separately agree that inhalation and exhalation have different effects, which therefore do not cancel each other out on average. On the other hand, the size of the RSA is lower with a higher mean HR, so its influence cannot be described by simply adding a constant signal course. This is also physiologically plausible: at higher heart rates, the vagus nerve, via which the RSA is mediated, is increasingly less involved in heart rate control; this task is then taken over by the sympathetic nervous system. FERSTL & HÖLZL (1979) have provided direct evidence that, in studies on the OR of HR, the RSA is not removed by averaging. Which systematic signal distortions in averaging stem from the fact that the necessary preconditions are not fulfilled, in particular the extent to which the OR of respiration is also involved in studies on the OR of HR, would still have to be investigated.

The averaging methods discussed here are always justified when eliminating unforeseeable (stochastic) interferences. If, however, as in the present study the interference is quantitatively predictable, it should be possible to improve data handling by using this information.

2.2.3 Extrapolation (HART 1975)

Even if the conditions mentioned in (2) are generally not fulfilled, additivity of the RSA effect can be assumed as a first approximation for small HR excursions. If one further takes the size of the RSA as constant over short periods of time, i.e. in particular as being independent of momentary other causes of HR fluctuations, one way of at least partially freeing short-term HR responses in real time from the RSA is the method of extrapolation, as used by HART (1975), for example.

HR and respiration are recorded in a preceding control period (15–20 sec); this control HR is subtracted from the HR obtained under the subsequent experimental conditions. Since the influence of breathing should not change between the control period and the experimental period, it should cancel out.

The restrictions have already been discussed in (2). Furthermore,

breathing must not change during the measurement, otherwise the course of the RSA will change.

2.2.4 Filtering

Since the RSA has a defined frequency range, essentially that of the respiratory frequency, the interfering fluctuations can simply be filtered out with an appropriate bandstop, as long as one is not interested in other information in this frequency range. WOMACK (1971), for example, describes the use of a digital bandstop. With digital filtering, the distortions by phase shifts at the cut-off frequencies with analogue filters can be avoided. It would also be conceivable to use adaptive filters whose cut-off frequency is controlled by the momentaneous respiratory frequency. However, as the HR-OR typically has frequency components in that critical range, we do not consider these options.

2.3 The simulation of CLYNES

At the beginning of the 1960s, Manfred CLYNES reported on simulations of various physiological systems on an electronic analogue computer. Among other things, he created a model of the RSA, which will be discussed in more detail, as essential parts of it are used in my simulation attempts.

2.3.1 On the concept of "unidirectional rate sensitivity"

Under the heading of "unidirectional rate sensitivity", CLYNES explained a property of physiological systems that had previously received little attention.

The meaning of the term is briefly explained using a particularly illustrative example, namely pupil regulation (see Fig. 2.3). The purpose of pupil adjustment is to keep the light intensity reaching the retina constant. Increasing light intensity should therefore lead to a smaller pupil diameter (Fig. 2.3a). Surprisingly, however, briefly switching off the light also leads to pupil constriction (Fig. 2.3b)! The puzzle is solved, if you look at the step responses: Switching off the light leads to a slow pupil enlargement (Fig. 2.3c). Switching on the light leads to a pupil constriction, which is characterised by a strong overshoot (Fig. 2.3d). This response can be described as the sum of a slow response (which is the mirror image of (c)) and a response to the rising flank (arrow in (e)).

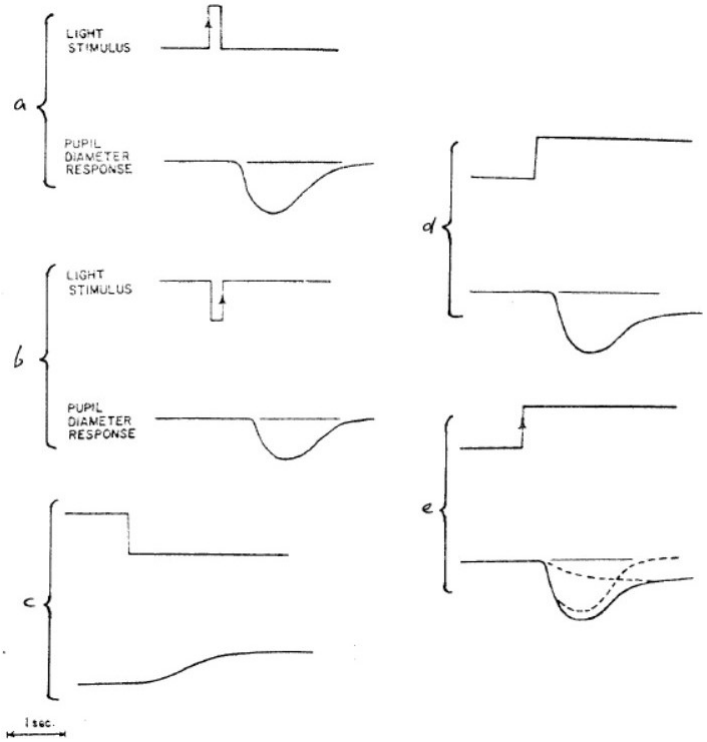

Fig. 2.3: On "unidirectional rate sensitivity" (From: CLYNES, 1961)

The pupil therefore reacts not only to light intensity, but also to its change; the fact that the pupil only shows this behaviour with positive rising edges is the aforementioned "rate sensitivity".

With short light pulses ((a) and (b)), the slow response does not have time to form. What remains is the response to the rising edges (arrow in (a) and (b)).

In control engineering, the slow rise is known as "proportional behaviour with delay" (so-called "PT1 elements"); the dependence on the slew rate is called “differential behaviour”.

With respect to the RSA, ’unidirectional rate sensitivity’ means that, besides the state of breathing, its speed in particular has an influence on HR, and that this effect depends on the direction of breathing. The discussion of the physiological mechanisms led us to expect such a dependence on breathing speed. It may be the indirect expression of the effectiveness of intrathoracic pressure fluctuations. The directional dependence means that positive and negative pressure do not have mirror-image effects on HR.

However, CLYNES himself attributes the speed dependence to the differential behaviour of stretch receptors (CLYNES 1960, p. 13). (For

criticism of the physiological interpretation given by CLYNES, see Chap. 2.4.)

2.3.2 Description of the model

CLYNES' model is based on the physiologically given facts (see Fig. 2.4).

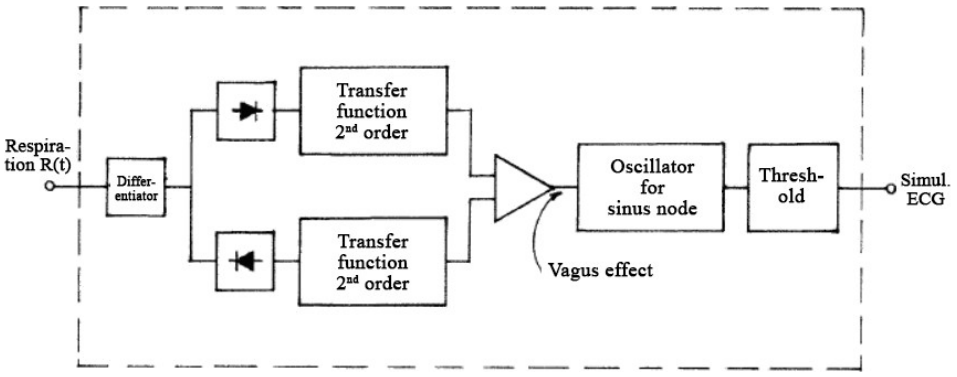

Fig. 2.4: Principle of the CLYNES model of respiratory arrhythmia

Breathing acts with a second-order (during inhalation) or third-order (during exhalation) transfer function on the "efferent vagus nerve". The described differential behaviour is included in these transfer functions. For its part, the vagus exerts an inhibitory influence on a sinus oscillator that simulates the heart's sinus node. In order to obtain an ECG-like pulse sequence from its modulated sinus oscillation, a threshold-value element with pulse shaper is connected downstream. This pulse sequence is finally fed into a cardiotachograph. Fig. 2.5 shows the complete model (after CLYNES 1960, p. 10; with more modern symbols).

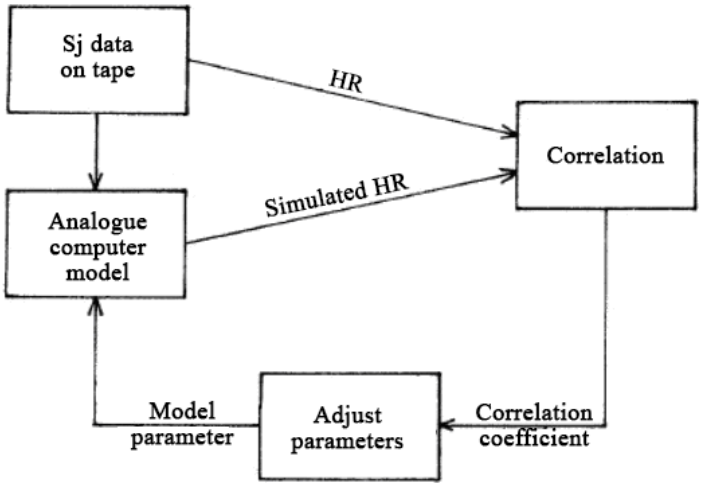

Fig. 2.6: Adjustment of the model parameters

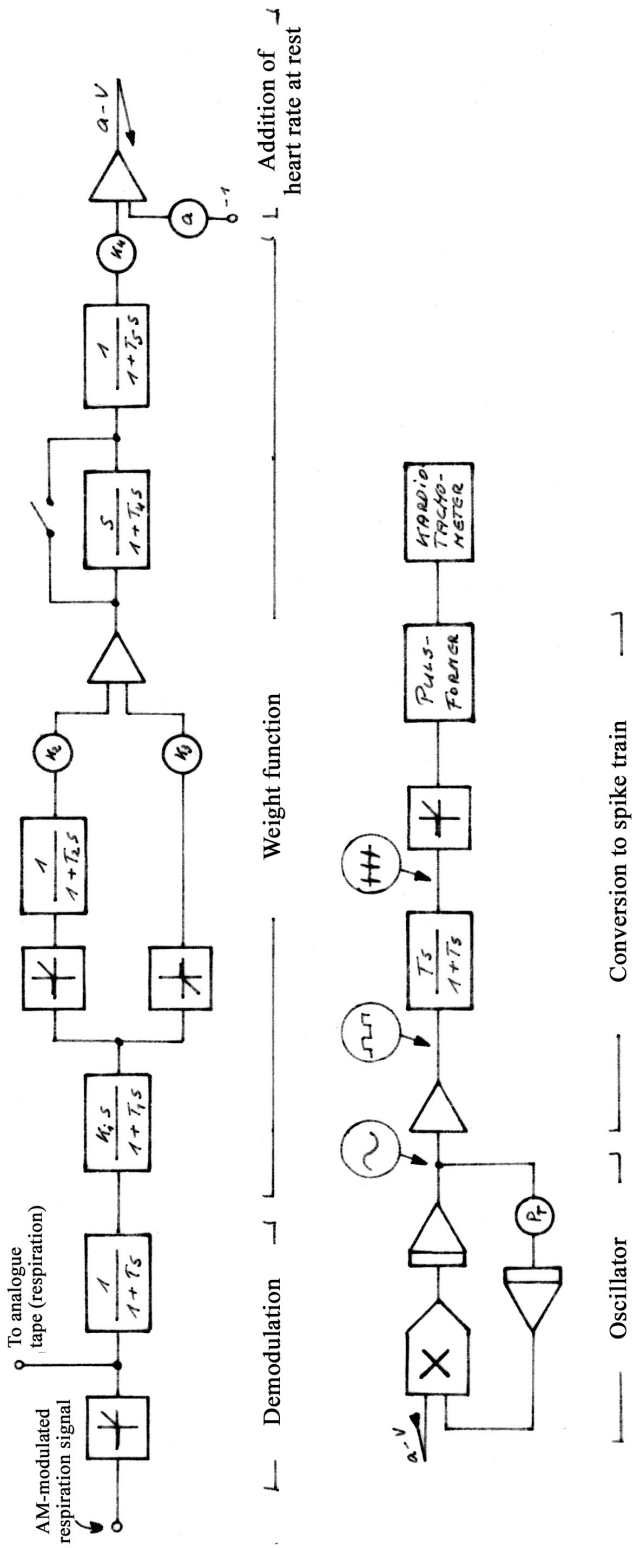

Fig. 2.5: CLYNES' RSA model. From: IRE Transactions on Med. Electron. ME-7, 1959, p. 10

2.3.3 The mathematics of the model

During normal cardiac activity, the cardiac vagus nerve – in contrast to sympathetic cardiac nerves – has a resting activity around which fluctuations occur in a positive and negative direction. The vagus control of the HR thus does not contain a rectifier effect, and it makes sense in the modelling to use the directional property of the vagus nerve early on in the processing chain. The transfer function that describes the relationship between respiration and vagus activity is therefore set to being dependent on the direction of breathing:

$$\frac{V(s)}{R(s)} = \begin{cases} \dfrac{k \cdot s^2}{(1+T_1 s)(1+T_2 s)} & \text{for } \dfrac{dR}{dt} \geq 0 \\ \dfrac{k \cdot s^2}{(1+T_1 s)(1+T_2 s)(1+T_3 s)} & \text{for } \dfrac{dR}{dt} < 0 \end{cases}$$

V(s) = Laplace transform of vagus activity
R(s) = Laplace transform of respiration

The sine oscillator is described by a second-order differential equation:

$$\ddot{y} + (a - V(t)) \cdot \dot{y} = 0$$

For constant vagus activity V, this equation has the solution

$$y = A \cdot \sin(2\pi r t), \quad \text{with}$$

$$r = \frac{1}{2\pi}\sqrt{a - V}$$

The resulting relationship between oscillator frequency and vagus activity is not linear. It is plotted in Fig. 2.7.

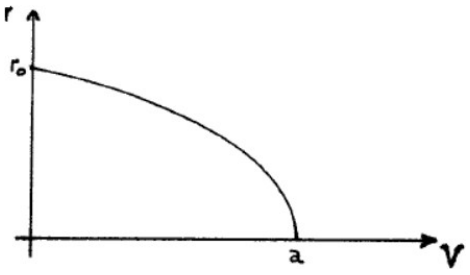

Fig. 2.7: Dependence of the oscillator frequency r on the vagus activity V

In accordance with physiological facts, higher vagus activity lowers the frequency. The maximum vagus activity is given by V = a. It means cardiac arrest. The frequency

$$r_0 = \frac{1}{2\pi}\sqrt{a} \quad \text{for } V = 0$$

is what CLYNES calls "basic heart rate". In his case, it is approx. 60 bpm, so it is not the same as the heart rate in the absence of vagus activity, which is approx. 100 bpm in humans. V = 0 therefore does not correspond to a lack of vagus activity, but to the average vagus activity at rest. The minimum vagus activity does not emerge from the equation; it is expected to be approx. –a, so that V(t) is symmetrical around the zero line.

At higher cardiac base rates (i.e., larger a), the same change in vagus activity causes a smaller variation in HR. This corresponds qualitatively to the physiological conditions.

2.3.4 Conclusions from the model

For a better understanding of the model, a number of implications are derived from it and discussed.

The course of the HR results from the superimposition of the responses to inhalation and exhalation. Positive "impulse breathing" (short inhalation and immediate exhalation) should produce essentially the same HR response as negative impulse breathing, as both are composed of an inhalation and exhalation jump (with a slight time shift and from different resting levels). Whether the HR response normally observed during exhalation is actually a consequence of exhalation, or whether it is an offshoot of the inhalation response, can only be decided if inhalation and exhalation are sufficiently far apart in time. My results show that the responses only fade out after approx. 15 seconds.

Whether an inhalation leads to acceleration or deceleration of HR can thus only be determined if the respiratory rate is known. Such statements in relevant physiology textbooks are therefore misleading (see e.g. GANONG 1972, p. 505). Empirical material on the frequency dependence of the RSA is provided by ANGELONE & COULTER (1964) (see Fig. 2.8). They had subjects breathe sinusoidally at fixed frequencies between 1 and 40 breaths/min and determined the amplitude and phase of the RSA. The 0° phase shift was defined as the relative position of the HR and breathing curves at extremely low breathing frequency. At this frequency, the maxima of the HR occurred at the inspiratory maximum. At the normal breathing frequency of approx. 10 breaths/min, the situation is reversed (=180°). Remarkable in the subject shown is the pronounced maximum of the RSA amplitude at 6 breaths/min.

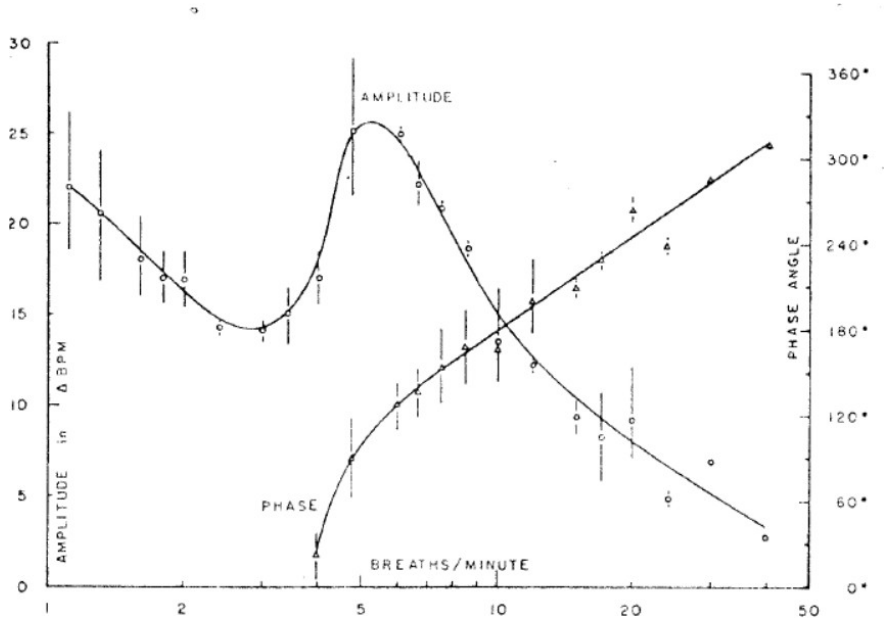

Fig. 2.8: Dependence of the RSA amplitude and phase on the respiratory frequency in a subject (from ANGELONE & COULTER 1964, p. 481)

2.3.5 Interaction of the RSA with other influences on HR

The CLYNES model does not yet specify how the RSA interacts with other influences on HR (orientation response and habituation, physical and psychological stress). Additive models are insufficient for larger HR variations, as the RSA decreases with both physical and psychological stress (for physical stress, see, e.g., LAURIG, LUCZAK & PHILLIP 1971; for psychological stress: LUCZAK & LAURIG 1973).

One possibility would be to add other influences to the vagus activity; this amounts to defining the parameter a as a function f(x) of other influences. This would take account of the RSA decrease at higher activation (higher a). The resulting dependency

$$r = \frac{1}{2\pi}\sqrt{f(x) - V}$$

is based on pure speculation, however, and would first have to be substantiated by quantitative comparison with actual dependencies. For the time being, therefore, the coaction between the RSA and other factors is still assumed to be additive:

$$HR(t) = HR_0(t) + RSA(t)$$

$HR_0(t)$ = back-calculated HR course.

2.4 Discussion of CLYNES' approach

2.4.1 Criticism of the model

CLYNES' model was criticised by DAVIES & NEILSON (1967):

(1) They found no detectable effect of expiration.

(2) They found a significantly lower response to inspiration.

There are two possible reasons for the discrepancies:

(1) CLYNES may have used much larger breathing amplitudes. This cannot be verified as he did not use a calibrated breathing volume measurement.

(2) CLYNES did not ensure that during breath-holding the glottis was open. This can result in unwanted pressure effects in the thorax.

The model could be simplified if the sinus node were simulated by a linear oscillator (i.e. by an oscillator whose frequency is a linear function of the input signal). The non-linear oscillator used by CLYNES is mathematically difficult to analyse, and this analysis is not performed by CLYNES either. It only deals with the special case of V(t) being constant. The establishment of a transfer function

$$G(s) = \frac{HR(s)}{V(s)}$$

which would describe the dependence of the oscillator frequency on V(t) for any course is inadmissible, as this would presuppose the linearity of the oscillator.

CLYNES justifies the use of this oscillator e.g. physiologically: The change of gain in the oscillator's feedback loop by means of the multiplier element he says corresponds to the effect of acetylcholine in the sinus node, which facilitates the transmission of nerve impulses in an analoguous manner (CLYNES 1959). However, as there are no indications as to how the spontaneous discharge of the sinus node occurs in a way that would allow modelling by a feedback loop of the specified type makes sense, this justification remains questionable. The real reason for this probably lies more in its simple realisation due to the technical options of the time (linear voltage controlled oscillators – VCOs – are available today as integrated circuits).

Since we are not interested in a simulation of the raw ECG, but want to work with HR, the diversions via the oscillator is omitted here. The following simplified model then remains (Fig. 2.9):

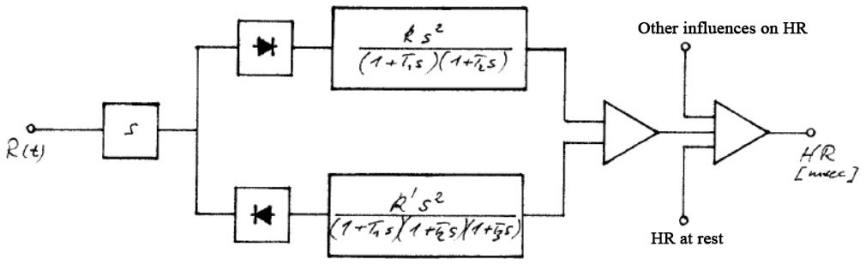

Fig. 2.9: Simplified HR simulation

2.4.2 Physiological interpretation of the model

In addition to the purely descriptive value of a dynamic model, the interesting question arises whether physiological structures can be found that can be linked to the individual components of the model. CLYNES surmises that the stretch receptors in the lungs and the thoracic cavity play a major role in the mechanism of action. Their known differential behaviour could be ascribed to a first-order term of the transfer function (i.e., s/(1+Ts)). It is further to be expected that different receptors are active during inhalation and exhalation.

CLYNES cites two main arguments against a decisive effect of the baroreceptor mechanism (1969, p. 14):

a) The HR response to a breath impulse (out-in) is greater than to step inspiration, even though in the first case, the changes in blood pressure are likely to be smaller.

b) The step responses to inhalation and exhalation go in the same direction (CLYNES does not complete this argument: Does he mean to say that the blood pressure conditions during inhalation and exhalation are likely different, and should therefore lead to different effects?)

The first thing to say about the two arguments is that the blood pressure conditions in the large arteries are by no means a reflection of the intrathoracic pressure fluctuations but are related to them in a rather complicated way. Predictions are therefore is not possible based on the intrathoracic pressure alone (see Chap. 2.1). Furthermore, the first of the two asserted statements cannot readily be inferred from the published data. Objective measures for arrhythmia are lacking. It should also be noted that DAVIES & NEILSON (1967) were unable to detect any response to exhalation.

2.5 Excursus: On the dynamic relationships between the variables involved

When following CLYNES' argumentation (1959, p. 12), some misunderstandings might arise, which should be discussed for a better understanding of the relationships.

The transfer function used by CLYNES for simulation contains a dependency of HR on the second derivative of the thoracic circumference. If the first derivative of the thoracic circumference is used as a measure of the intrathoracic pressure, as in Chap. 4.2.1.1, this implies a dependence of the HR on the first derivative of the pressure curve. CLYNES attributes to the second derivative of the thoracic circumference the dimension of a force; one is inclined to relate this to the force exerted by the thoracic musculature, as well as with the intrathoracic pressure (force/area). This would imply a dependency of HR on pressure itself, i.e. not on its derivative, as derived above.

However, the second derivative of the circumference (a length s) actually has the dimension of an acceleration ($a=d^2s/dt^2$); a connection with force is only established when it comes to the acceleration of an inertial mass ($F=m\cdot d^2s/dt^2$). Yet the force of the thoracic musculature is only used to a small extent for accelerating the air mass of breathing, lung mass, and thorax mass; at higher breathing speeds it is mainly used to overcome friction losses (PIIPER & KOEPCHEN 1972). These are proportional to the respiratory flow rate or to the square of the same. At low breathing speeds, the muscle power serves overcoming the elasticity of the lungs and the thorax.

To summarise: It is difficult to establish a relationship between the strength of the respiratory muscles and thoracic circumference or intra-thoracic pressure. Intra-thoracic pressure will be largely related to the first derivative of thoracic circumference. This is a measure of the respiratory flow velocity. Table 2.1 provides an overview of the variables involved.

2.6 Newer cardiovascular models

Two newer cardiovascular models are briefly described:

The model of MIYAWAKI et al (1966) describes the regulation of blood pressure with the control circuit: blood pressure – baroreceptors – afferent vagus – vagus centre – efferent vagus – sinus node – heart rate – heart – cardiac output – vascular system – blood pressure.

Circumference measurement	Variables of respiratory power	Intrathoracic pressure	Respiratory musculature
Circumference of thorax U(t) [cm]	Filling state of the lungs; respiratory volume [mliter]	—	Force of the muscles for inspiration acts against elasticity of the lung and thorax. At expiration in rest, muscles for expiration are used
First derivative of circumference U(t) [cm/sec]	Respiratory flow rate [mliter/sec]	Intrathoracic negative pressure [N/cm²]	At inspiration, muscle force overcomes airways' resistance; at expiration, that resistance os normally overcome by elasticity of lungs and thorax
Second derivative of circumference U(t) [cm/sec²]	(Rate of flow change)	Pressure change	

Table 2.1: Overview of correlations between respiratory mechanics variables

The RSA is introduced into the model via the effect on the baroreceptors. This means that the interaction of RSA and HR is not additive (!), as on the two non-linearities are built into the pathway (baroreceptors and sinus node). MIYAWAKI et al. also use a unidirectional rate sensitivity, whereby exhalation responses are omitted entirely. They cite a lack of statistical consistency in the exhalation response as the reason for this; they do not cite any pertinent studies. To simulate the sinus node, a model of ROSENBLUETH & SIMEONE (1934) is used, CLYNES' non-linear oscillator did not find favour.

The first physiological cardiovascular model which, in addition to resting conditions, also simulates the influence of physical and mental stress, was developed by LUCZAK, RASCHKE, LAURIG and PHILIPP at the Darmstadt Institute for Ergonomics (LUCZAK & RASCHKE 1975). The model component for blood pressure regulation basically corresponds to that of MIYAWAKI et al.; the effect of the RSA is again modelled here via the effect on the baroreceptors so is not additively superimposed on the HR. The modelling of stress additionally requires consideration of sympathetic influences on the

sinus node, stroke volume, and peripheral vascular resistance. Respiration is simulated by a sinusoidal oscillator, the frequency of which is regulated by blood oxygen debt associated with physical stress. Great importance has been attached to reproducing the actual physiological pathways in detail; almost all of the individual blocks involved have well-founded transfer behaviour from the physiological literature. Table 2.2 summarises the physiological variables occurring in the model. However, in the review of the model behaviour, only HR is considered as an output variable for now.

Input variables	Heart	Vessels
Physical stress	HR	Peripheral resistance
Psychological stress	Stroke volume	Mean arterial blood pressure
	Cardiac output per minute	State of contraction of the vascular musculature
Blood	Nerves	Respiration
Oxygen debt	Efferent vagus activity	Respiratory rate
	Afferent vagus activity	intrathoracic pressure

Table 2.2: Physiological variables in the cardiovascular model of LUCZAK & RASCHKE (1975)

2.7 Application to the measure of heart rate

As soon as sufficiently accurate parameter estimates are available for a subject and it has been demonstrated that the model describes their heart rate at rest and under changed physiological conditions with sufficient accuracy, the parameters can be assumed to be constant for this subject hereinafter. Influences of higher nerve centres on HR have been neglected until now, or were attributed to noise. In order to be able to draw conclusions on these, part of the model must be inverted: The output for simulating the HR must become the input and the "central influences" must become the output (Fig. 2.10).

The corresponding inverse model is typically not easy to determine; instead, it would be conceivable to use a suitable controller to influence the central signal in such a way that the real and simulated HR match (Fig. 2.11).

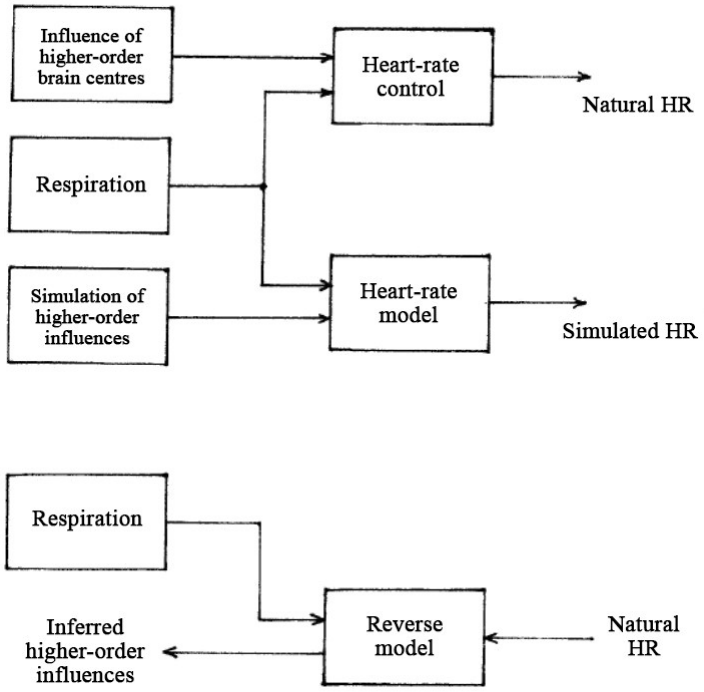

Fig. 2.10: Heart rate simulation and inverted model

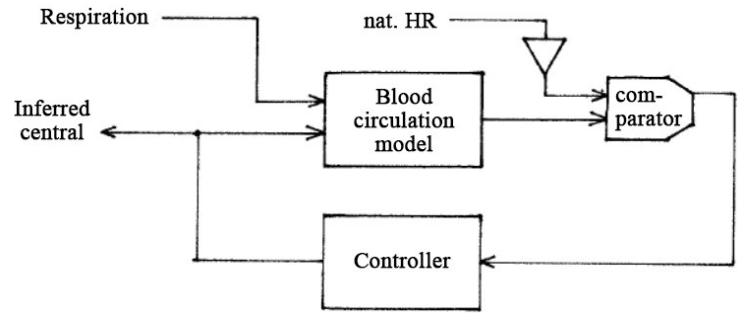

Fig. 2.11: Possible backward calculation with complicated interaction of RSA and HR

If the effect of the RSA on the HR is assumed as being additive, as in the CLYNES model, the inversion is easy: the back- calculated central influences are simply the difference between the real HR and the simulated RSA (Fig. 2.12).

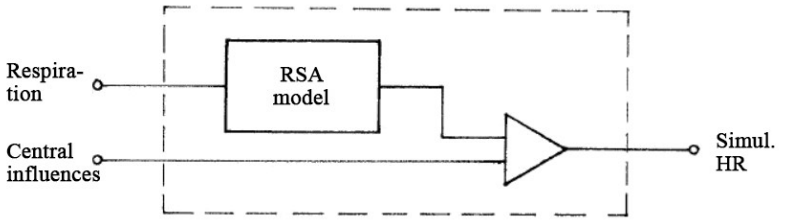

HR = RSA + central influence

⇒ central influence = HR – RSA

Fig. 2.12: Additive superposition of the RSA

Since no situations of stress are simulated in CLYNES' model, only the constant resting heart rate HR_0 corresponds to the central influences.

2.8 Digital RSA extraction

2.8.1 Overview of some methods for digital simulation

Since the days of CLYNES, the availability of digital laboratory computers has grown, while at the same time the theory of digital systems has been further developed. Digital simulation is therefore increasingly becoming a centre of interest.

If one starts from the empirically found impulse response or step response - available as a table of values with e.g. 300 values - a response of the system to any input signal can be determined using the direct (discrete) convolution. The disadvantage for an application in real time is the high computing time required: In the example, 300 multiplications and additions must be carried out per new sample point. (If the impulse response is not available as a table of values but as an equation, as in the case of FÖRSTER, it is advisable to calculate the value table of the impulse response in advance, so that this does not have to be recalculated for each sample point.

To save computing time, a non-recursive filter can first be created by utilising symmetry relationships (a so-called finite impulse response or FIR filter since the impulse response consists of a finite value table). However, the computing time can be significantly reduced further by using a low-order recursive filter (NFIR filter). This is the digital analogue of a linear analogue-computer circuit of the same order. To do this, we first look for the transfer function of a simple linear system whose impulse response approximates the empirically given one with sufficient accuracy. Using a bilinear transformation one then obtains

the coefficients of the recursive filter. (For a detailed description of the theory of digital simulation, see ROSKO 1972).

2.8.2 The RSA extraction by FÖRSTER

Since the model by CLYNES is constructed as the sum of two linear systems with upstream rectification, it can be realised digitally as the sum of two convolutions. This is the method used by FÖRSTER (1979) for RSA extraction. FOERSTER thus realised the same extraction principle digitally, independently of the present work: The respiratory signal is differentiated, rectified, fed into separate processing systems for positive and negative respiratory flow, respectively, and finally added up. The RSA simulated in this way is assumed to be additive to the HR, and subtracted for HR correction.

Fundamental differences (besides methodological differences) to the approach in this work lie in the implementation of the scaling and the determination of the step response (which is used in the convolution here instead of the impulse response; see Section 2.8.3). Since FÖRSTER uses dimensionless weighting functions (occupancy functions) instead of the real step response, the scaling of the simulated RSA must be carried out as a final step by regression to the, high-pass filtered, real HR (cf. Chapter 2.9). One advantage of using convolution is that the choice of step responses is not limited to those of simple standard linear systems, but can use the actual empirical time course. FÖRSTER does not make use of this advantage, as he does not use a method for the stable determination of step responses. Only four (mean) characteristic parameters of the step responses are used: Time points and amplitudes of the acceleration maximum and the deceleration minimum; the amplitudes are normalised to equal respiratory amplitudes. He then uses these parameters to construct weighting functions that simulate the basic biphasic course of the HR step response; the biphasic time course corresponds to a third- order system (see Fig. 2.13).

(With this, FOERSTER derives the equation

$$\varphi(t) = \frac{A+D}{(T_1-T_2)^2}[2(t^3-T_1^3)-3(T_1+T_2)(t^2-T^2{}_1)+6T_1T_2(t-T_1)-A]$$

$$\text{for } T_1 \le t \le T_2$$

which we will not need to consider here).

.

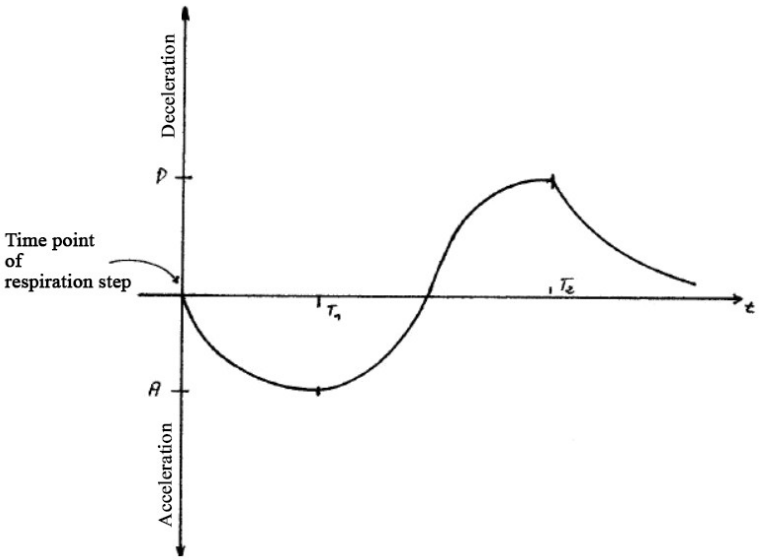

Fig. 2.13: Occupancy function in the work of FÖRSTER

Incidentally, the time points T_1 and T_2 of the extrema should not be confused with the time constants of the corresponding dynamic system (i.e. poles of the transfer function). The time constants specified by FÖRSTER

$$\left.\begin{aligned} T_1 &= 1381 \pm 131 \text{ msec} \\ T_2 &= 4613 \pm 406 \text{ msec} \end{aligned}\right\} \text{ Inhalation}$$

$$\left.\begin{aligned} T_1 &= 3812 \pm 481 \text{ msec} \\ T_2 &= 8547 \pm 715 \text{ msec} \end{aligned}\right\} \text{ Exhalation}$$

are therefore not comparable with those specified by CLYNES.

FÖRSTER refrained from determining a mean step response because, in his opinion, the RSA would be analysed under nonphysiological conditions if the required breath pacing were used. This argument appears again and again in the RSA literature, but its justification has not been empirically tested. We plan doing an experiment to this end comparing RSA responses with and without respiratory pacing. However, it seems to me that one reason for dispensing with breath pacing is that many breath measurement methods are unsuitable for this because of their DC drift.

To avoid a possible misunderstanding: When FÖRSTER speaks of digital filtering, he does not mean filtering out the RSA from the HR, but means the model that calculates the simulated HR from the respiration. The input of the filter is therefore not the HR, but the breathing. To extract ("filter-out") the RSA, this simulated HR is then subtracted from the real HR.

FÖRSTER demonstrates the success of RSA extraction in a study on the orienting response (OR). To avoid habituation of the OR, he used a complex reaction-time task as a stimulus. The success of the RSA extraction was

- a higher probability of recognising the OR
- OR amplitudes were the same for free breathing and breath holding
- the time courses of the OR during free breathing correlated with those during breath holding with 0.22 (there was no correlation before the extraction)

Digital RSA simulation using direct convolution is thus a simple and effective method for RSA extraction.

2.8.3 Excursus: Derivation of the digital form of CLYNES' model

In this section we derive the digital form of the model of CLYNES used by FÖRSTER, and explain the system-theoretical terms used in the previous section.

A linear dynamic system can be described in the time domain or in the frequency domain. The transition from one approach to the other takes place via the Laplace transform. Frequency, in this framework, is understood as a complex variable "s"

Let X(s) and Y(s) be the Laplace transforms of the input and output signals x(t) and y(t) of a system. The transfer function is defined as their ratio:

$G(s) = \frac{Y(s)}{X(s)}$, so that

(i) *Y(s) = G(s) X(s).*

By the convolution theorem we get

(ii) y(t) = g(t) * x(t), where "*" is the convolution operation:

$$g(t) * x(t) = \int_0^t g(\tau)\, x(t-\tau)\, d\tau$$

When a Dirac impulse δ- is taken as the input x(t), it follows from (ii) that the output *y(t)* is

$$\begin{aligned} y(t) &= \int_0^t g(\tau)\, \delta(t-\tau)\, d\tau \\ &= g(t) \end{aligned}$$

Function g(t) – i.e. the time-domain equivalent of the transfer function

G(s) – is therefore simply the impulse response. Conversely, its Laplace transform $\mathscr{L}$ is the transfer function:

G(s) = $\mathscr{L}$ [g(t)]

Equation (ii) can be restated as saying that the system response to a signal x(t) is given by convolving that signal with the system's impulse response function.

Fig. 2.14 provides an overview

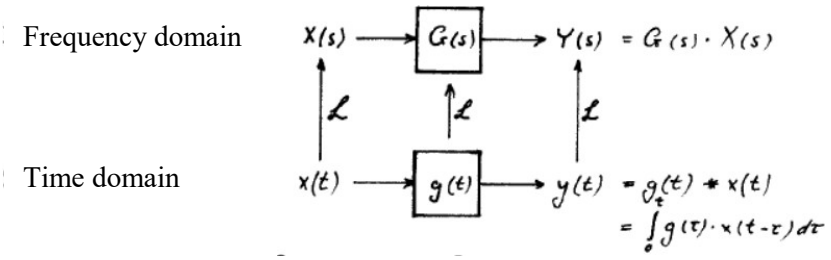

$\mathscr{L}$	Laplace transform
G(s)	Transfer function
g(t)	Impulse response
g(t) * x(t):	Convolution of g and x

Fig. 2.14: Linear system in the time and frequency domain

The discrete form of the convolution operation,

$$y(t_j) = \sum_{i=1}^{n} g(t_i - t_j)x(t_j),$$

is straightforward to realise on a digital computer and can be used for determining the system response, or, equivalently, for digital filtering. The index n in the equation is the number of samples in the impulse response g(t); as can be seen, the impulse response g(t) must be non-zero in a finite time interval only.

When a step function $U(t) = \begin{cases} 0 & \text{for } t \le 0 \\ A & \text{for t} > 0 \end{cases}$

is applied as input to a system, the output signal h(t) is called the step response. The impulse response is the first derivative of the step response:

$$g(t) = \dot{h}(t)$$

The convolution relationship can also be written in a form in which, instead of the impulse response, the step response occurs: Since the

Laplace transform maps the derivative of a function to a multiplication[4] with s,

$$\mathrm{L}\left[\dot{f}(t)\right] = s \cdot \mathrm{L}[f(t)] - f(0),$$

and since, further, a factor "s" can be grouped with X(s), it also follows from the convolution theorem that

(iii) $y(t) = \int_0^t h(\tau)\dot{x}(t-\tau)d\tau$,

in which the step response h(t) and the derivative of the input signal appear. The step response can thus be obtained from the signal's first derivative.

This is the form used by FÖRSTER. In the equation, x(t) is the respiratory flow; according to CLYNES' directional dependence, the convolution is applied separately for positive and negative flow:

$y(t) = y_1(t) + y_2(t)$

$$y_1(t) = \begin{cases} h_1(t)\dot{x}(t-\tau)d\tau & \text{for } \dot{x}(t) \geq 0 \\ 0 & \text{for } \dot{x}(t) < 0 \end{cases}$$

$$y_2(t) = \begin{cases} h_2(t)\dot{x}(t-\tau)d\tau & \text{for } \dot{x}(t) \leq 0 \\ 0 & \text{for } \dot{x}(t) > 0 \end{cases}$$

(Note the opposite range for the derivative of x(t))

This is exactly the CLYNES model: First, the respiration signal is differentiated, then rectified, fed into two separate linear systems, and finally summed-up. The heart rate at rest is omitted since only the RSA is to be simulated (see Section 2.7).

2.9 Quality of the model and assessment of the corrected heart rate

A necessary condition for the functioning of the planned correction procedure is first of all a suitable simulation. The correlation between predicted and actual HR, with free- running breathing, can serve as a measure of the prediction's accuracy. Since the correlation coefficient is invariant to linear transformations of the variables, the scaling of the simulated HR (determination of mean value and standard deviation) must subsequently (offline) be determined by regression. The

[4] Holbrook (1970, p. 61)

prediction error and proportion of explained variance can be determined from the correlation coefficient:

$$\text{Explained variance} = r^2$$

$$\text{Prediction error} = \sqrt{\text{Variance of real HR}} \cdot \sqrt{1 - r^2}$$

$$\text{Relative error variance} = \frac{\text{Prediction error variance}}{\text{Variance of real HR}} = \sqrt{1 - r^2}$$

FÖRSTER (1979), for example, proceeds in this way. He reports between 75% and 98% explained variance.

If the scaling is to be included in the quality determination, as is necessary in an online simulation, the relative error variance is used directly:

$$\text{Relative error variance} = \frac{\frac{1}{N\text{-}1}\sum_{1}^{N}(HR(t_i) - HR_0(t_i))^2}{\frac{1}{N\text{-}1}\sum_{1}^{N}(HR(t_i) - \overline{HR})^2},$$

where N is the number of samples in the period under consideration.

This direct error determination will generally result in less favourable values than the correlation: This is because the scaling is already fixed before the start of the simulation, while in the other case the scaling is optimised on the basis of the data. Thus, if the scaling obtained by regression is to be used in an online simulation, one must use the scaling from a previous experiment. Determining the error variance via the correlation then provides incorrect values, however, because the optimum scaling may have changed in the meantime.

Incidentally, since it cannot be expected that prediction error and signal are uncorrelated, additivity of the variances cannot be assumed. Explained variance as calculated by 100% minus error variance cannot therefore be applied here.

Once a sufficient model quality has been demonstrated, the model can be used for HR correction.

To interpret the corrected HR, the properties of the new measure must be analysed.Two questions, in particular, arise in its assessment: (1) What is the relationship between HR and corrected HR? (2) To what extent has one succeeded in removing the influence of respiration?

To the first question: In any case, if the breathing pattern is known, one

HR measure is completely determined by the other. The question remains as to in which parameters they correspond. For additive RSA influence, the answers are simple: If the RSA time course contains no DC component, then HR and corrected HR match with respect to their temporal and sample means:

From

$$HR(t) = HR_0(t) + RSA(t) \qquad \text{(additive approach)} \qquad \text{(i)}$$

and

$$\frac{1}{T}\int_0^T RSA(t)dt = 0 \qquad \text{(no DC component in the RSA)} \qquad \text{(ii)}$$

it follows

$$\frac{1}{T}\int_0^T HR(t)dt = \frac{1}{T}\int_0^T HR_0(t)dt \quad \text{(i.e. the temporal means are equal}$$

Under condition (ii), the sample mean of the RSA trajectories of different subjects will also vanish:

$$\frac{1}{n}\sum_{i=1}^{n} RSA^i(t) = 0, \text{ where } RSA^i \text{ is the RSA time course of subject i,}$$

and the sample means of the HR measure coincide:

$$\frac{1}{n}\sum_{i=1}^{n} HR^i(t) = \frac{1}{n}\sum_{i=1}^{n} HR_0^i(t), \text{ where } HR^i \text{ is the HR of subject i .}$$

If we follow an approach where the RSA influence is not applied additively, then the means no longer match. With a multiplicative approach, however, the means of the logarithms agree. In cases of a more complex, non- linear influence of respiration, such as in the models of MIYAWAKI or LUCZAK & RASCHKE, relations between the HR measures are difficult to predict theoretically.

To answer the last question, i.e., to what extent a reduction of breathing-related variance has been achieved, a first indicator can be a variance comparison before and after RSA extraction. However, the HR generally shows large fluctuations that are not of respiratory origin; these would first have to be filtered out. Since, according to LUCZAK & LAURIG (1973), above 0.25 Hz essentially only respiratory variance appears in the spectral analyses of HR under normal conditions, FÖRSTER (1979) suggests a variance comparison after high-pass filtering, with 0.25 Hz cut-off frequency as a standard quality measure.

For an application of the HR correction for investigation of phasic HR responses (e.g. the evoked heart-rate response; EHR), this measure of quality seems unsuitable to me. A spectral distribution such as that in Fig. 2.17 is no longer valid under such conditions. Whether the model that was used extracts slow RSA components reliably is therefore questionable. The HR step responses shown in Section 4.3.4.1 show prominent frequency components down to 0.05 Hz.

A comparison of heart rate spectra before and after RSA extraction in the application itself can be a useful procedure. From a simultaneous spectral analysis of the respiration, it is possible to determine which signal components of the HR are of respiratory origin.

2.10 Excursus: On the definition and recording of HR

The instantaneous HR is normally defined as the inverse of the respective last time interval between two R-peaks of the ECGs (in "beats per minute": bpm).

The frequency measure has the disadvantage of having a highly skewed distribution, which renders the application of common statistical methods somewhat more complicated. The R-peak intervals (R-R intervals; interbeat intervals: IBI) themselves, on the other hand, generally have an approximately normal distributions (HÖLZL 1976, p. 67, JENNINGS et al 1974, KHATCHATURIAN et al 1972). This measure is therefore preferred. (Further statistical stabilisation may be achieved by using a logarithmic transformation: log IBI. S. CHESS et al 1975.)

The tachogram is defined at a finite number of discrete points in time only, namely at each heartbeat. To obtain a more finely sampled measure, in the simplest case time points in between are supplemented by step functions. Initially, it is arbitrary which functions are used for supplementation – there is no "true" heart rate between two beats.

In a spectral analysis of the HR, the discontinuities of the step function add noise, so the tachogram is, e.g., smoothed by connecting each (n+1) measuring points with an nth order polynomial. In most cases it is sufficient to select first- order polynomials, i.e. to connect the points by a polygon (e.g. WOMACK 1971) (see Fig. 2.15).

The value between two measured values then represents the average of the neighbouring values:

$$HR(t) = \frac{t_2 - t}{t_2 - t_1} HR(t_1) + \frac{t - t_1}{t_2 - t_1} HR(t_2) \quad \text{for} \quad t_1 \le t \le t_2$$

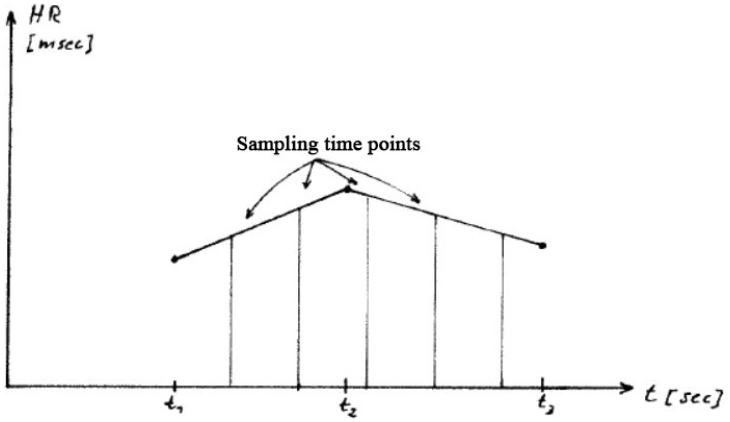

Fig. 2.15: Digitising the heart rate signal

In real time, a polygon-like curve can be obtained by sending the signal from the cardiotachograph through a low-pass filter (t≈ 0.5 sec) (see Fig. 2.16). The curve is then shifted by one heartbeat compared to the previously described polygon.

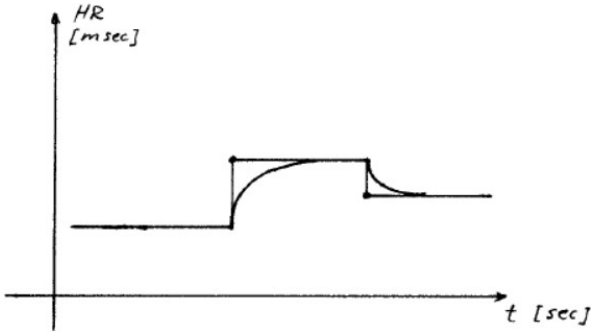

Fig. 2.16: HR signal smoothed by a low-pass filter

If several HR curves are to be averaged, polygon interpolation of the step functions can be omitted since the curve is already smoothed by averaging. (Our PDP8/E already needs 20 minutes to analyse twenty one-minute sections of heart rate data and calculate their standard deviation).

The various methodological problems that arise in the Fourier analysis of HR are discussed in detail by GALLOWAY & WOMACK (1969) and CHESS et al (1975). Fig. 2.17 shows a typical spectral decomposition of the heart rate.

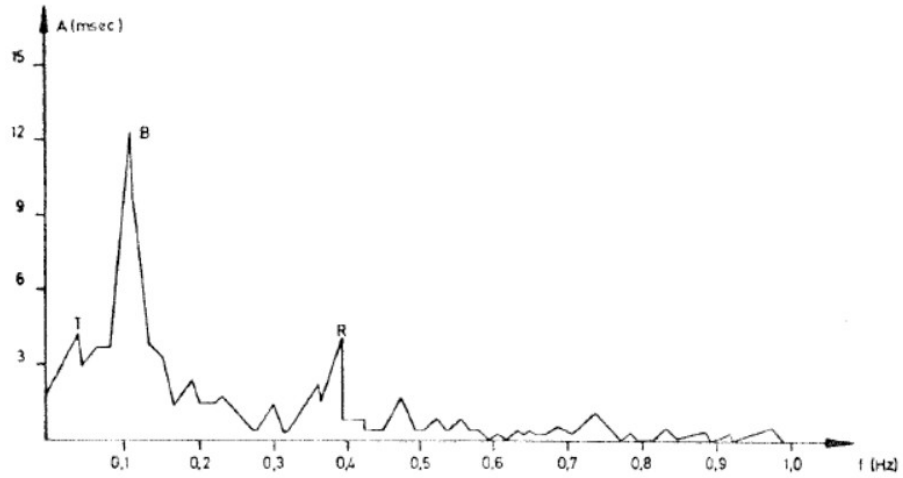

Abb. 1. Spektrum der Momentanherzfrequenz. (Nach Luczak u. Laurig, 1973)

Fig. 2.17: Spectrum of the instantaneous heart rate (after LUCZAK & LAURIG 1973)

3. BREATH MEASUREMENT

3.1 Introduction

From the discussion of the physiological mechanisms and the RSA modelling experiments, it became clear that respiratory volume and its first derivative with respect to time, i.e., respiratory flow velocity, would be the suitable input variables for a model of RSA. These variables have been measured directly in a number physiological studies using, e.g., a Fleisch pneumotachograph (developed by Alfred Fleisch in 1953). In physiological experiments, however, the necessary breathing mask would represent too great a disturbance factor; indirect methods are therefore preferable.

The reliability and accuracy of an RSA prediction naturally depends crucially on the reliability and accuracy of the breath measurement in use. Current indirect methods are not suitable for volume or flow velocity measurements; they are usually only used for determining the respiratory rate. We had therefore made attempts to modify these methods for the present work; this will be reported on briefly. Overall, however, the results were unsatisfactory, so that, eventually, a new measuring method was developed.

In a list of required properties for use in psychophysiological experiments, low mechanical dimensions and minimal inconvenience to the subject are at the top of the list.

Susceptibility to artefacts plays a subordinate role in our case for now. With regard to electrical properties, linearity of the signal conversion is desirable, but can be compensated for easily.Good repeatability of the measurement and low drift are important, however.

Increased demands are placed on the breathing measurement when attempting to steer the breathing process with the help of pacing. A prerequisite is that the subject can relate the objective measurement to their subjective, physical sensation. Non-linearities in the context do not present difficulties. However, differential behaviour, time delays and, in particular, stochastic errors with poor repeatability are highly irritating. Slow drift, e.g. due to temperature dependence, poses a particular problem: If the zero position of the signal and the relaxed expiration position no longer match, the subject is constantly forced either to breathe below the resting position with the help of expiratory muscles or is unable to fully relax when exhaling, both of which are unphysiological conditions, distorting the result. In the experiments described later, the drift of the measurement methods could further not be countered by using a high-pass filter with commonly used time constants ($\tau \leq 10$ sec), since breath holding was to be controlled for up to 20 sec.

The procedures had to be examined from these points of view. A single measure will not fulfil all requirements. One can therefore try to combine several independent measures into a more reliable and accurate overall method (see Section 3.4.3).

3.2 Measurement procedure

Indirect methods for measuring respiration can be categorised into three groups:

a) Measurement of the chest circumference and/or abdominal circumference

b) Measurement of chest impedance

c) Flow measurements with possible subsequent integration stage for the signal (an older overview can be found in BROWN 1967).

3.2.1 Circumference measurement

Chest circumference, preferably measured at the point of greatest thoracic excursion, is a fairly good predictor of respiratory volume. Even with so-called pure abdominal breathing, large deflections can still be found. However, despite their apparent simplicity, the associated measurement sensors (i.e., transducers) have considerable

deficiencies for reliable measurement.

3.2.1.1 Mercury-filled tubes

The most common method for thorax circumference measurement in psychophysiological studies uses a 10 - 30 cm long elastic plastic tube filled with mercury, with an internal diameter of approx. 1 mm. Metal pins are attached to the ends of the tube to establish electrical contact with the mercury column. These tubes are attached to a belt looped around the chest and are stretched by the thoracic excursion. The change in the electrical resistance of the mercury column caused by the change in length and cross- section serves as a measure of the change in length. The measurement needs to be carried out with alternating current to avoid electrolytic processes.[5] The resistance values are quite small, only about 2 Ω.

Advantages are the low weight of the transducer, their small mechanical dimensions and good electrical properties: low temperature drift, and high return accuracy. SHAPIRO & COHEN (1965) provide useful technical information on the construction of the transducers. However, the measuring tubes must be replaced at regular intervals. After about 3 months, small air bubbles form in the mercury column, interrupting the contact and rendering the tube unusable.

The reason for these interruptions lies in the diffusion of the mercury through the porous wall of the silicone tubes used. As mercury is a highly toxic poison that accumulates in the body, its use must be minimised. The use of these tubes must thereby be described as questionable.

After enquiring with several manufacturers, we learnt that gas-tightness cannot be guaranteed with silicone tubes. Other materials considered, e.g. Teflon, did not have the required elasticity.

3.2.1.2 Filling with other materials

Attempts were therefore made to replace the mercury with other conductive materials. The downstream circuitry for resistance measurement[6] had to be adapted in the process to the very different base resistance values. All materials tested showed high temperature drift and/or poor return accuracy, however:

[5] The Beckman "Dynograph R" system uses 6.3 V/400 Hz.

[6] We used a Beckman 9875B coupler and an improved replica that we made ourselves.

a) Two conductor pastes for electrodes showed an unacceptably high temperature coefficient

b) Saturated zinc sulphate solution: showed highest temperature coefficient of all the materials tested.

c) Graphite emulsion in distilled water: Lowest temperature coefficient, with sign opposite to zinc sulphate solution. Very high resistance (approx. 120 kΩ).

d) Pure graphite powder: Low resistance, but no reproducible values.

3.2.1.3 Strain gauges

Strain gauges are sensor devices for recording expanding and compressing deformations. They change their resistance with very small changes in length (fractions of a millimetre). The much larger changes in length of the thorax circumference must therefore be realised with suitable mechanics.[7] The high temperature drift of strain gauges precluded their use here from the outset.

3.2.1.4 Air pressure belt

An air-filled, accordion-like stretchable rubber tube forms the measuring belt for thoracic circumference. Its internal pressure is channeleld to a pressure transducer via another rubber tube, and converted into a DC voltage signal.[8] We were able to greatly reduced the initial considerable temperature drift by using a lower supply voltage than specified by the manufacturer.

The disadvantages are: The high force required to stretch the rubber bellows (approx. 1 kp or 10 N for 10 cm stretching), the susceptibility to artefacts when touching the rubber hoses, the unwieldy size, and the high price for routine use.

3.2.1.5 Potentiometric length measurement

The most obvious method for measuring length is to use a linear slider potentiometer. A suitable device was built using so-called "conductive plastic" resistor tracks[9]. As expected, this resulted in excellent linearity and repeatability, and low temperature drift. The friction force of the wiper is in the range of a few pond, so that the deflection force is given

[7] E.g. the Beckman type 7001 respiration transducer.

[8] * Manufacturer: Stoelting, Chicago. Distribution: Albrecht, Munich, Germany

[9] Manufacturer: Penny & Giles, South Wales. Distribution in Germany: Widerstands- und -Meßtechnik GmbH, Norderstedt, or Novotechnik, Ostfildern near Stuttgart.

solely by the return spring. The mechanical dimensions (20×24×207 mm) and weight (130 g) of the prototype were still a little too high. Otherwise, the use of a potentiometer appears as a simple and reliable method.

3.2.2 Chest impedance measurement

The change in the electrical impedance of the chest cavity, measured with high-frequency alternating current (approx. 100 kHz, 100 mVeff), is linearly related to the tidal volume if the measuring electrodes are suitably positioned. A large number of publications deal with breath measurement methods based on this approach; however, they will not be discussed in detail here. To summarise, the methods appear to provide useful results within certain limits (susceptibility to movement artefacts, errors duringpressed breathing as in the Valsalva Maneuver). As our working group lacked experience and equipment for chest impedance measurement, it was not initially considered in detail for this study.

3.2.3 Measures of flow

3.2.3.1 Nose thermistor

A small thermistor is placed in the nostril and attached to the cheek with an adhesive plaster; the other nostril is closed with cotton wool. The thermistor is warmed by the warm exhaled air and cooled when inhaling.

Since the measurement conditions are changed by moving the thermistor in the nose, we also use a small plastic tube in our laboratory in which the thermistor is attached so that the breathing air flows around it in a defined manner.

The dependence of the thermistor signal on breathing volume is difficult to predict theoretically: during exhalation, the warming depends on the temperature difference between the thermistor and the exhaled air as well as on the amount of air flowing past per unit of time. As a first approximation, the temperature change would therefore be linearly proportional to the respiratory flow rate. However, as the breath temperature depends on the time the air spent in the lungs, there is a further dependency on breathing speed. Furthermore, the temperature difference is related to the ambient temperature. A non-linear behaviour of the thermistor signal is therefore to be expected. For a volume measurement, it would have to be corrected via a corresponding circuitry on the analogue computer.

No data on the dynamic behaviour of the method are yet available. However, the low susceptibility to movement artefacts and low inconvenience for the test subject lets work in this direction appear worthwhile.

3.2.3.2 Direct measures of flow

Direct flow measurements, e.g. with differential pressure transducers, have so far only been used in connection with breathing masks (e.g. VANBERGEN, NOVAK & CUMMING 1970). If appropriately small transducers were used, measurement directly in the nostril would appear as a viable option.

The output signal of a flow sensor is proportional to the medium's flow velocity . To obtain a volume measurement, the signal is integrated on the analogue computer; any drift of the integrated signal is corrected by setting the integrators to zero at the times of the zero crossings of the flow during exhalation (expiratory position).

3.3 Development of the breathing belts

As a result, we[10]* developed a breathing belt that was mechanically and electrically simple and promised to solve the problems mentioned. An infrared light barrier principle is used to measure distance: A small infrared light-emitting diode and an infrared- sensitive phototransistor are glued to an elastic band approx. 3 cm wide at a distance of approx. 10 mm.[11] When the elastic band is stretched, distance between LED and phototransistor changes and with it the amount of light picked up by the latter. Although this means that the signal changes with the square of the distance, the relationship can be approximated linearly for the distance changes that occur in practice (a few millimetres).

Ambient light only interferes with the signal if it fluctuates in intensity during the measurement. If necessary, the light path must be shielded accordingly.

The belt allows stepless adjustment in length with Velcro fasteners. It is comfortable for the patient to wear and does not slip; accidental contact outside the measuring range does not interfere with the signal. The signal shows excellent return accuracy. As the only drawback, the signal drift with temperature was insufficient for volume measurements.

Temperature-compensated versions were therefore built for this work

[10] Dipl. Psych. D. KLENK and the author

[11] Hot-dried two-component epoxy adhesive has proven itself suitable.

(Fig. 3.1). In addition to the measuring section, a second, light-tightly sealed light path of constant length is added and is connected to the negative feedback loop of the tracking amplifier (see Appendix 7.1). The respective temperature responses of the measuring and compensation sections cancel each other out.

Fig. 3.1: Temperature-compensated breathing belts

In this way, the temperature response of both the light emitter and receiver are compensated simultaneously. Individual compensation with series and parallel resistors would also have been conceivable (Texas Instruments "Opto Cookbook"), but in this case the adjustment is complicated; it has to be carried out again for each individual light emitting diode and each photo transistor, and the power consumption is further considerably higher.

Against any remaining slow drift, a high-pass filter with a very low cut-off frequency was experimentally connected into the signal path (f_G = 3 mHz, corresponding to τ = 50 sec).

3.4 Combination of the circumference measurements for a respiratory volume measurement

Since chest and abdominal circumference contribute independently to breath volume, two belts were now to be used to measure these, and combine the signals to form a volume measurement.

SHAPIRO & COHEN (1965) describe a possible procedure. Based on a cylindrical model of the chest cavity, they conclude that there is a quadratic relationship between respiratory volume and circumferences:

(i) $\Delta V = k_1 \Delta U_1^{\,2} + k_2 \Delta U_2^{\,2}$

ΔV: change in respiratory volume

ΔU_1: change in chest circumference
ΔU_2: change in abdominal circumference

To determine the ratio of the weights,

$$n^2 = \frac{k_2}{k_1},$$

they have the subjects perform breath-like movements with their nose and mouth closed, and, with $\Delta V = 0$, conclude from the model:

(ii) $$\frac{k_2}{k_1} = -\frac{\Delta U_2}{\Delta U_1}$$

(The negative sign shows that in this case, chest and abdomen move in opposite directions.)

To determine the common scaling factor

(iii) $$k_1 = \frac{k_2}{n^2}$$

breath volume ΔV_R is measured continuously with a respirometer, and the difference to the volume predicted by eq. (i) is calculated on the analogue computer by

$$D = \Delta V_R - \Delta V$$

and is minimised. This corresponds to a simple linear regression of the sum calculated in (i) on the criterion variable.

The next section will show that the assumption of a quadratic relationship is not necessary. Yet if a linear model is adequate, it is simpler to predict the criterion variable by two independent variables using multiple linear regression.

3.4.1 Model of the chest cavity

If the cross-sections of the chest and abdomen are assumed being a circle, the interior of the chest can be seen as a truncated cone (Fig. 3.2). Its volume is given by

$$V = \frac{h}{12\pi}(U_1^2 + U_2^2 + U_1 U_2)$$

U_1 = chest circumference
U_2= abdominal circumference
h = conceptual height of the chest cavity

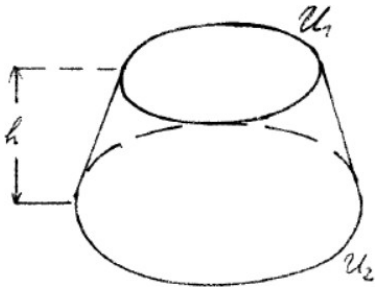

Fig. 3.2: Conceptual model of the chest cavity

During breathing, small changes ΔU_1, ΔU_2 of approx. 5% are superimposed on the circumferences U_{01}, U_{02} of the expiratory resting position:

$$U_i = U_{0i} + \Delta U_i \text{ for } i = 1,2, \quad \Delta U_i << U_{0i}$$

For small changes, we have, approximately,

$$U_i^{\,2} = U_{0i}^{\,2} + 2\Delta U_i \quad \text{for } i = 1,2 \text{, i.e.}$$

$$V \approx \frac{h}{12\pi}(U_{01}^{\,2} + U_{02}^{\,2} + U_{01}U_{02}) + \frac{h}{12\pi}(2\Delta U_1 + 2\Delta U_2 + U_1\Delta U_2 + U_2\Delta U_1$$

and with the resting volume V_0:

$$V \approx V_0 + \frac{h}{12\pi}((2+U_2)\Delta U_1 + (2+U_1)\Delta U_2)\,.$$

For the change $\Delta V = V - V_0$ of the respiratory volume compared to the resting volume V_0, we thus have

$$V \approx \frac{h}{12\pi}((2+U_2)\Delta U_1 + (2+U_1)\Delta U_2)$$

For small changes in circumference, a linear dependency of the change in respiratory volume on the height of the thoracic cavity and a weighted sum of the changes of circumference is therefore to be expected.

Ideally, a measurement of the height of the chest cavity (e.g. the distance between the upper and lower ribcage) should also be taken into account.

When you depict the relationship between breathing volume and circumferences ΔU_1, ΔU_2 as a surface over the U_1/U_2-plane, the linear model corresponds to a flat surface that intersects the coordinate origin (Fig. 3.3).

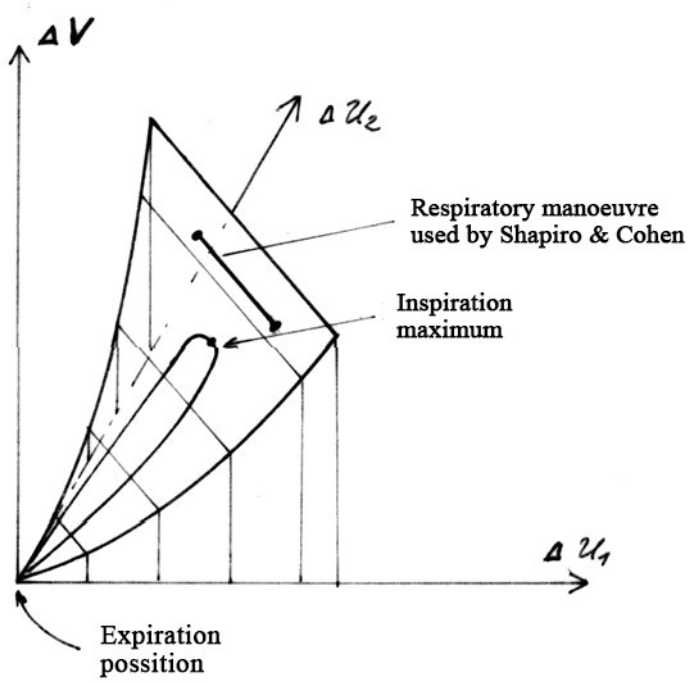

Fig. 3.3: Breathing volume as a function of chest and abdominal circumference. The breathing manoeuvre mentioned in the previous sectioncorresponds to a movement on the plane at a constant distance from the U_1/U_2-plane.

3.4.2 Parameterisation of the variables

Unfortunately, no continuously measuring respirometer with an electrical output signal was available to determine the criterion variables, we only had a mechanical model (Dräger Volumeter), in which the values had to be read at regular intervals. The easiest way to do this is to read off each at the end of the exhalation; these values (in millimetres) were assigned to the respective curve sections of the circumference measurement (Fig. 3.4).

The amplitudes of the exhalation distance (in millimetres) were then measured by hand (Fig. 3.5). The Chest and abdominal circumference values and the corresponding volume values were entered into the computer (see Fig. 3.10).

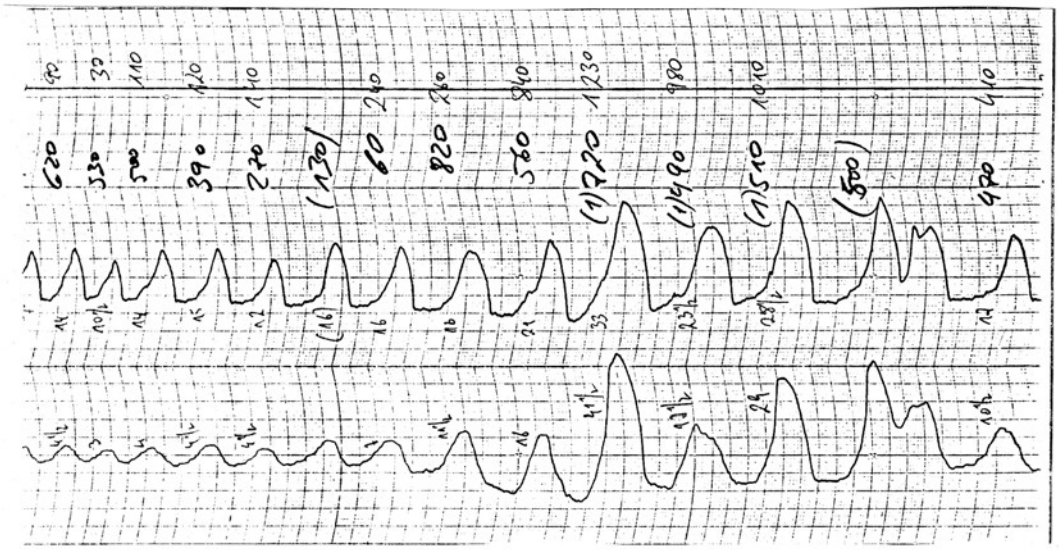

Fig. 3.4: Circumference measurement and allocation of the respiratory volumes

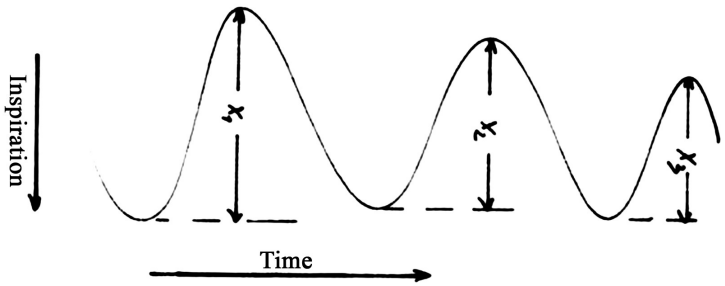

Fig. 3.5: Parameterising of the perimeters

3.4.3 Problems of regression

3.4.3.1 Sample bias

In Figs. 3.6 and 3.7, the data thus obtained from a subject were plotted as scatter plots; in Fig. 3.8, the relationship was plotted together with the two independent variables for visualisation purposes.

Unfortunately it is not possible to simply calculate a two-way multiple linear regression without further ado. It would require the samples of the variables to be representative of the population, in this case of the continuous trend.This is not the case, however. Since the digitisation takes place at the time points of the maxima, i.e. not in small regular steps or randomly, , the sample is systematically biased towards higher values.

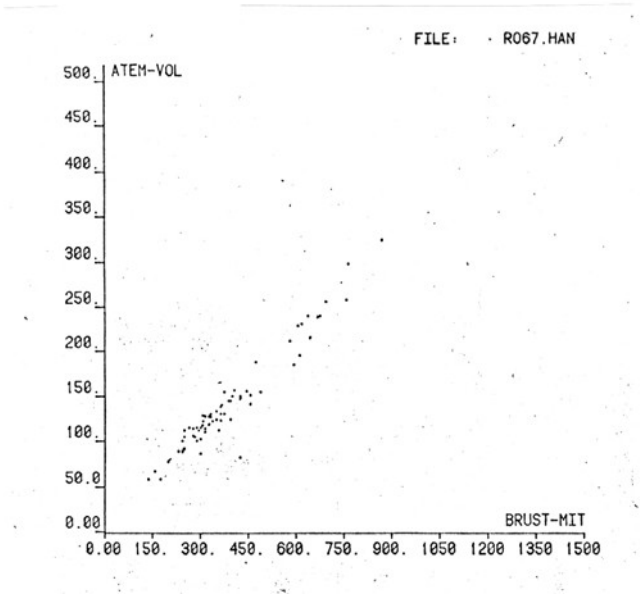

Fig. 3.6: Chest circumference and respiratory volume

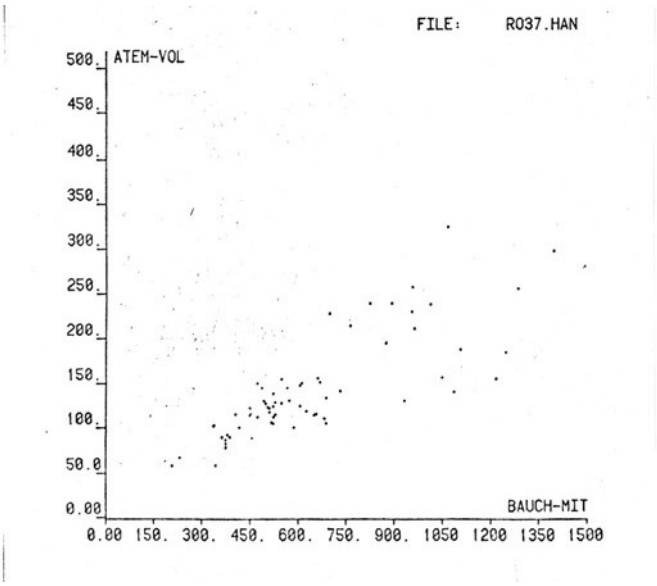

Fig. 3.7: Abdominal circumference and respiratory volume

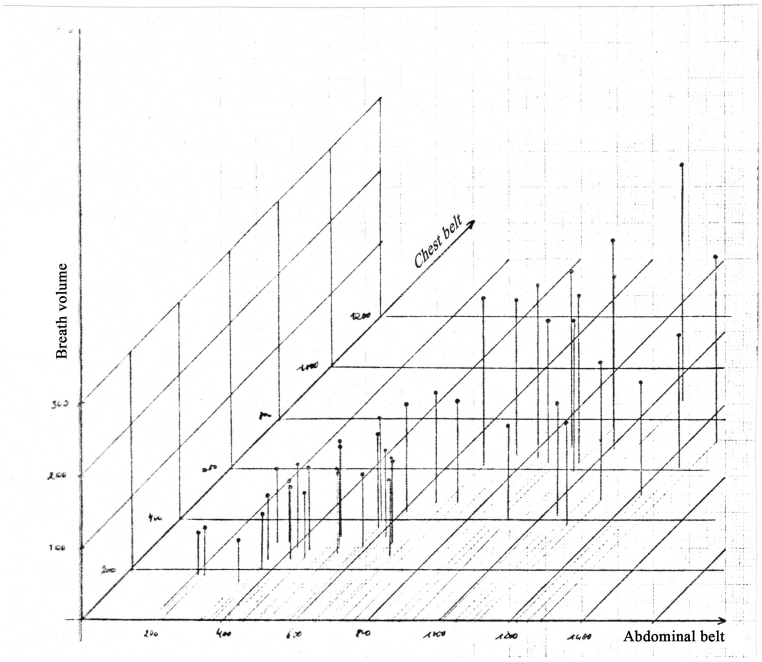

Fig. 3.8: Chest and abdominal circumference and respiratory volume

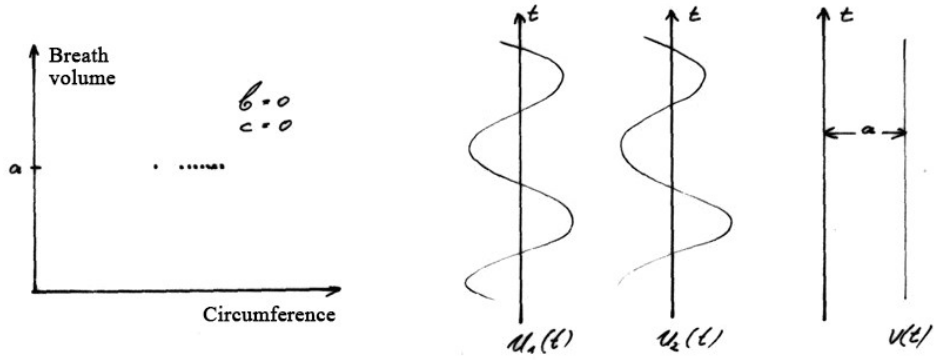

Fig. 3.9: Incorrect prediction due to insufficient variance of the independent variables

If, for example, the breathing amplitude is constant over a certain period of time, the regression will be a parallel to the circumferential axes (Fig. 3.9), which makes little sense. The predicted volume curve

$$V(t) = a + bU_1(t) + cU_2(t)$$

with

V(t) : Breathing volume at time t
U1 (t): Chest circumference at time t
U2 (t): Abdominal circumference at time t
a, b, c: Regression coefficients

would thus become a constant line at a distance a from the time axis.

In the distributions of Figs. 3.5 and 3.6, the distortion is expressed by the fact that no measured values occur below a certain limit (50 ml).

3.4.3.2 Modification of the regression model

Indeed, the regression approach in (i) is too general: Since missing changes in circumference are synonymous with missing changes in volume (i.e., correspond to holding one's breath), the constant a of the regression equation must be zero. In order to maintain the usual approach, it would be conceivable to add the missing zero crossings to the sample, i.e. to add as many value triples (0,0,0) as there are measured values.

However, this is a dubious approach. It is more correct to formulate the approximation task anew and to adjust the regression model accordingly: We are looking for a linear prediction

(ii) $V(t_i) = bU_1(t_i) + cU_2(t_i), i = 1...n$

with minimum quadratic deviation, which results in zero for diminishing values of the independent variables. I.e., sought for is a regression forced through zero.

The optimisation criterion is therefore the standard estimation error

(iii) $S_{V.U_1U_2} = \sqrt{\frac{\sum_1^n (V_i - V_i')^2}{n-1}}$, with

V_i: criterion's value at time t_i
V_i': predicted value at time t_i

The conditionalequations for the regression weights are derived by partial differentiation as in standard multiple regression. To look at the properties of the modified regression model we wrote Fortran computer programmes to calculate the weights and the usual statistical parameters (the routines are called HSMREG & HSMRE1).

In standard multiple linear regression, the correlation R between predicted and criterion values is referred to as the multiple correlation coefficient; it can be used to calculate the achievable standard error of the estimate, i.e. the smallest prediction error that can be achieved with appropriate scaling of the weights:

$S_{V.U_1U_2} = S_V \cdot \sqrt{1 - R^2}$, with

S_V: Standard deviation of the criterion volume values

The same correlation can be calculated for the regression with a forced zero intercept; beware, however, that the relationship with the standard error of the estimate applies no longer: The standard estimation error is greater than the correlation coefficient would suggests:

$$S_{V.U_1U_2} > S_V \cdot \sqrt{1-R^2}$$

The coefficient of determination R^2 therefore no longer indicates the proportion of explained variance. As it lacks a simple interpretation, it is not further considered here. Instead, the relative error variance of the prediction is calculated directly:

$$s_{rel\%}{}^2 = \left(\frac{s_{V.U_1U_2}}{s_V} \right) \cdot 100$$

The routines further calculate the 95% confidence intervals, for assessing the prediction accuracy:

$$CI = \pm 1.96 \cdot \frac{s_{V.U_1U_2}}{\sqrt{N}} .$$

To illustrate the relationships between standard error, relative error variance, and correlation with the criterion, simple and multiple linear regression, as well as multiple linear regression with forced zero intercept, are calculated in Table 3.1 using the calibration data of two subjects. Fig. 3.10 shows a print-out of calculating the regression. On the analogoue computer, the linear approach according to equation (ii) corresponds to a linear summing circuit as shown in Fig. 3.11. The standard error is the RMS value of the difference between the weighted sum V'(t) and the respirometer signal V(t). The regression condition requires the output signal of the RMS meter (a so-called "true RMS converter") to be minimised.

The addition of the regression constant, a, would correspond to a DC voltage shift of the signal V'(t) on the analogue computer. Since $U_1(t)$, $U_2(t)$ and V(t) are all pure AC-voltage signals (i.e. their time average is zero), the use of a continuously measuring respirometer will likely result in only small values for the constant, even with the conventional regression model. However, the DC voltage shift in the expiratory rest position is distorting in any case and a regression with forced zero intercept is thus preferable.

Example No.	Constant a	Weight chest belt b	Weight abdominal belt c	Standard error $s_{V.U1U2}$	Standard error expected from R $s_{V.U1U2}$	Relative error variance $s_{rel\%}^2$	Correlation with criterion	Comments
Data set AR 0903.DA								
1	–180.22	8.81	20.73	145.36	145.36	16.5%	0.9137	Standard multiple regression $s_{V.U1U2} = s_{V.U1U2}$
2	0	–4.78	20.9	148.6	148.2	17.3%	0.9101	Regression through zero $s_{V.U1U2} = s_{V.U1U2}$
3	0	–9.56	41.8	684.6	148.2	366%	0.9191	Regression weights doubled R is unchanged Standard error quadrupled
4	0	0	1	650	146.53	330%	0.9122	Abdominal belt only R increased. Large error because of wrong choice of weight
5	0	0	19.18	150.90	146.53	17.8%	0.9122	Weight optimal; single regression through zero $R=r_{U1U2}$ as expected (inf.)
6	–80.39	0	21.29	146.53	146.53	16.8%	0.9122	Standard single regression
Data set AR 0604.DA								
7	–437.74	39.89	46.99	114.81	114.81	8.7%	0.9558	Standard multiple regression
8	0	31.59	24.67	197.6	116.9	225.9%	0.9536	Multiple regression through zero
Data AR 0903.DA								
$r_{chest/vol.} = 0.4299$				Std. dev. of volume $s_V = 357.67$				
$r_{abdomen/vol.} = 0.9122$								

Table 3.1: Prediction of respiratory volume from chest and abdominal circumference with different forms of linear regression

```
ATEMGUERTEL-EICHUNG
*******************

DATEN AUS FILE AR0604.DA

KOMDATEN

BRUST [MM]          BAUCH [MM]          ATEMVOLUMEN [MLIT]
X( 1)=    5.5       Y( 1)=   13.0       Z( 1)=  430.0
X( 2)=    6.0       Y( 2)=   12.0       Z( 2)=  370.0
X( 3)=    6.0       Y( 3)=   12.0       Z( 3)=  480.0
X( 4)=    6.5       Y( 4)=   12.0       Z( 4)=  460.0
X( 5)=    5.5       Y( 5)=   12.0       Z( 5)=  160.0
X( 6)=    3.5       Y( 6)=   13.0       Z( 6)=   80.0
X( 7)=    3.5       Y( 7)=   13.0       Z( 7)=  280.0
X( 8)=    5.0       Y( 8)=   13.5       Z( 8)=  110.0
X( 9)=    3.0       Y( 9)=   10.5       Z( 9)=  110.0
X(10)=    2.0       Y(10)=   11.0       Z(10)=  110.0
X(11)=    1.5       Y(11)=   11.5       Z(11)=  100.0
X(12)=    1.5       Y(12)=    9.0       Z(12)=  140.0
X(13)=    4.5       Y(13)=   24.0       Z(13)=  950.0
X(14)=    7.0       Y(14)=   24.0       Z(14)= 1100.0
X(15)=    9.5       Y(15)=   25.5       Z(15)= 1150.0
X(16)=   12.0       Y(16)=   23.0       Z(16)= 1240.0
X(17)=   10.0       Y(17)=   27.0       Z(17)= 1160.0
X(18)=   12.0       Y(18)=   25.5       Z(18)= 1110.0
X(19)=   12.0       Y(19)=   25.0       Z(19)= 1240.0
X(20)=    6.0       Y(20)=   10.0       Z(20)=  340.0
X(21)=    5.5       Y(21)=   11.0       Z(21)=  340.0
X(22)=    6.0       Y(22)=   12.0       Z(22)=  370.0
X(23)=    4.5       Y(23)=   11.0       Z(23)=  100.0
X(24)=    4.0       Y(24)=   12.5       Z(24)=  360.0
X(25)=    7.0       Y(25)=   12.0       Z(25)=  370.0
X(26)=    4.0       Y(26)=   11.0       Z(26)=  300.0
X(27)=    6.0       Y(27)=   13.5       Z(27)=  420.0
X(28)=    5.0       Y(28)=   11.0       Z(28)=  390.0
X(29)=    7.5       Y(29)=   13.5       Z(29)=  540.0

MITTELWERT & STANDARDABWEICHUNG

MX=   5.97      MY=  14.83      MZ= 496.90
SX=   2.88      SY=   5.09      SZ= 388.40

REGRESSION

Z = 31.59 * X  +  24.67 * Y
***************************

KORRELATIONEN

KORR. D. UNABH. VARIABLEN UNTEREIN: RXY = 0.7524
KORR. M. KRITERIUM: RXZ = 0.8326    RYZ = 0.9357

MULTIPLER KORR.-KOEFF.: 0.9535
STANDARDSCHAETZFEHLER:  197.59
RELATIVE FEHLERVARIANZ: 25.88%
KONFIDENZGRENZEN:    +-  71.92
```

Fig. 3.10: Calculation of the regression

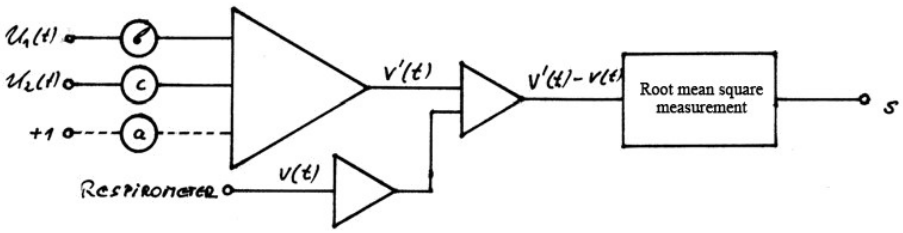

Fig. 3.11: Equivalent of multiple linear regression on the analogue computer

3.5 Results and application for paced breathing

Initial results from 10 subjects are available to date. The relative error variance of the volume determination is between 15% and 25%. The confidence limits of the measurement are below 80 millilitres, with breathing amplitudes of approx. 500 ml ± 350 ml. It should be noted

that these values refer to the prediction of the maxima in the time course (see Chapter 3.4.3.1). When the entire time course is taken as a basis, better values can be expected, as the sample variance is then greater.

The calibration procedure with manual measurement of the curves takes approx. 45 minutes. An automatic evaluation is in preparation for routine use.

The measurement method proved to be excellently suited for paced breathing. Fig. 3.12 shows the attempts of untrained subjects to "re-breathe" sine, triangle and square wave curves generated by a function generator; see also the step-breathing curves in Figs. 4.3, 4.4 and 4.10 et seq.

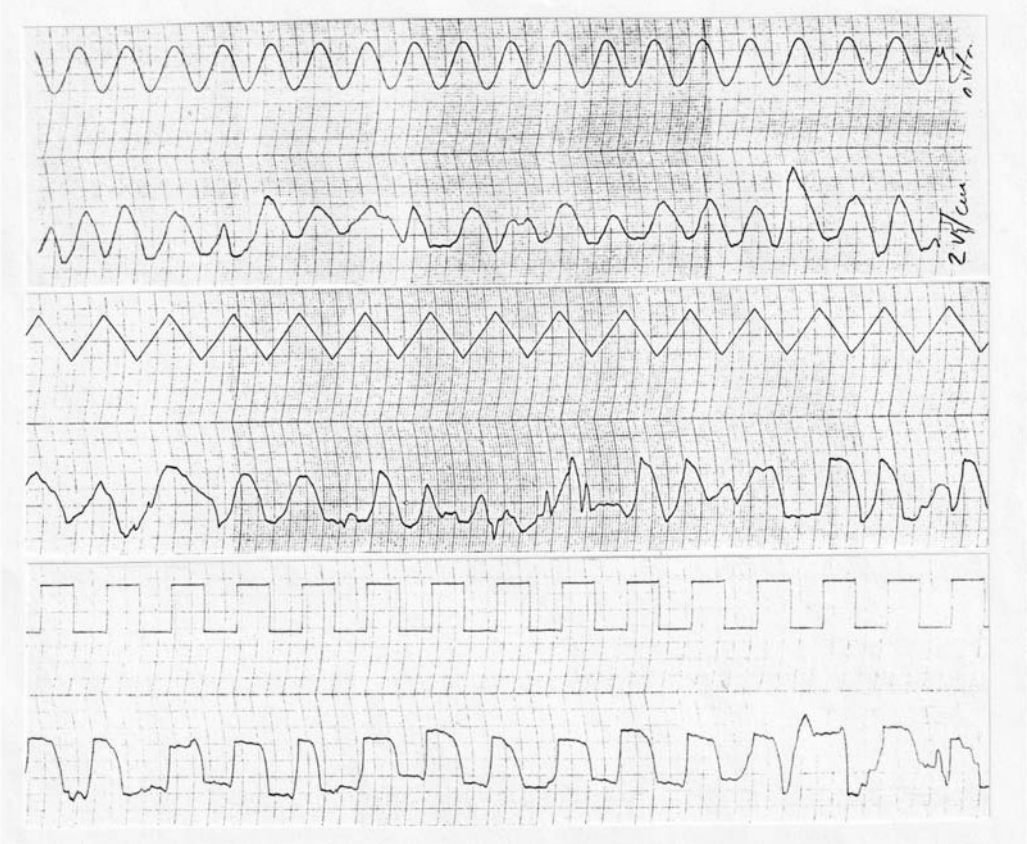

Fig. 3.12: Breathing in various waveforms

The paced breathing experiments showed that the use of the 50-sec high-pass filter (Section 3.3) in interaction with the subject's responses led to zero-point shifts rather than to their elimination. Therefore, the unfiltered respiratory signal was later used; occasionally, the zero line needed to be readjusted manually (approx. every 20 minutes).

3.6 Discussion

For judging the gain in measurement accuracy when using two belts instead of just one, a comparison of the respective correlations will be misleading. Often, the correlation with only one belt was already so high that the multiple correlation coefficient was only slightly higher in comparison. Yet which one is the belt with higher correlating cannot be said beforehandbecause it is not clear from the outset whether, during the measurement, the subject will use more chest breathing or more abdominal breathing. If, in particular, as with paced breathing, a particular willed beathing activity is required, the use of either chest or abdominal breathing can become a conscious decision on the part of the subject. Particular manoeuvres can then easily reverse the correlation of the movement with a belt, e.g., the subjects can learn to draw-in their stomach when breathing-in.

Let us therefore return to a causal view: since breathing is composed of two movements whose contribution can be changed both voluntarily and involuntarily, two independent measurements must also be used, and combined suitably way. A linear model is the simplest way to do this.

The relative contributions to the overall measure can be determined using a special breathing manoeuvre, as in SHAPIRO & COHEN (1965), for example. However, the resulting values are only accurate for a small variety of possible breathing movements, and there is as yet no validation for normally occurring movements. We thus believe it is better to optimise of the weights in the summation with regard to the criterion, i.e. to use a multiple linear regression approach

Overall, the respiratory volume measurement method described above is very easy to use thanks to the small dimensions of the transducers and their simple and inexpensive manufacture, the stability of the measured values and their relative accuracy, even with altered respiratory movements in psychophysiological experiments. It appears superior to most other indirect methods of respiration volume measurement.

4. DEVELOPMENT OF THE RSA MODEL

4.1 Introduction

Creating a cybernetic model requires analysing the natural system to be modeled, from which then a suitable model structure is derived and its parameters are determined. The methods available for this purpose are

found in the area called "system identification". The methods differ in particular in the type of input signals used to stimulate the natural system, in this case respiration; A main distinction is between periodic and stochastic stimulation.

Classical frequency response analysis uses periodic sinusoidal functions with various distinct frequencies or continuously variable frequency for excitation, is the latter being the closest approximation to natural breathing. With single excitations, simple test functions are fed into the system – step function, impulse function, ramp function, etc. To improve the signal-to-noise ratio, several system responses are then averaged in a time-coherent manner.

More recently, stochastic identification methods have been used which make a virtue out of noise, so to speak, and are thus particularly well adapted to analysing natural systems (“white noise approach”).

All of the above identification methods assume that the system is linear; however, if the signal amplitudes are small enough, a non-linear system can often be approximated by a linear model.

The non-linearity of respiratory sinus arrhythmia found by CLYNES, however, can be directly analysed by determining the step response. This approach was therefore initially favoured in the present work. However, in order to verify the model, it will later be necessary to also compare its behaviour with that for other excitation functions. The experimental set-up for determining the step response was therefore designed to be flexible enough to allow easy adaptation to other identification methods.

In the physiological and psychophysiological literature, systems theory analyses have so far been largely new territory. In the case of RSA, authors have not reached agreement on the simple question of whether exhalation has an effect on HR. The neglect of the exhalation response in the models of MIYAWAKI et al. (1966) and LUCZAK & RASCHKE (1975), for example, does not seem to me to be sufficiently empirically justified. The uncertainty as to which system properties of the RSA are to be expected I attribute this to the fact that either frequency response analysis was used – which is not very adequate given the non-linear behaviour of the RSA and the presumably high required respiratory amplitudes (for an adequate signal-to-noise ratio), or were step or impulse responses from singular HR responses determined more or less by inspecting the responses, whereby reliable information on the respiratory amplitudes and forms used is lacking. The determination of a stable and reproducible step response with the

aid of time-coherent averaging ("averaging") has so far only been carried out by DAVIES & NEILSON (1967).

My goal was therefore to use paced breathing and coherent averaging, thereby determine stable RSA responses with various stimulation patterns, to provide a better basis for modelling.

After an overview of the properties of various possible analysis methods, I will first describe the experiment for determining the step response. A programme package developed for data acquisition, data control, data processing and presentation, will be discussed in detail. This is followed by a presentation and interpretation of the measurement results and a comparison of these with the heart rate responses found by DAVIES & NEILSON (1967).

4.2 Selecting the method of analysis

As various procedures for system identification have already been mentioned in the previous section, I would like to go into more detail about the properties of these procedures with regard to the present application.

4.2.1 Frequency-response analysis

A frequency response analysis is easy to perform and interpret. Using a frequency response's Bode diagram, a transfer function having the same frequency response can be read-off from the diagram..

However, the transfer function is only fully determined once the phase response has been taken into account (i.e., the phase shift of the input and output signal as a function of the frequency). In the case of the RSA, the frequency range from approx. 4 to 20 breaths/minute is of interest, which corresponds to 67 mHz up to 0.3 Hz. The excitation with the highest and lowest frequencies of that range is problematic, however, because the oxygen levels in the blood could change and the system properties would be altered as a result. The results would then be valid for prolonged very fast or very slow breathing, but not for short-term slow or fast signal components.

Another disadvantage of a frequency-response analysis is the relatively high breathing amplitudes that are necessary for a good signal- to-noise ratio of the output signal. The RSA will certainly be operated outside its linear range. With low signal amplitudes, it is possible to analyse the output signal using correlative methods (as in Section 4.2.3), but the simplicity of the procedure is lost.

Another disadvantage of the method is that it takes a relatively long

time to carry out, as it is necessary to wait for the system to settle at each new excitation frequency.

Frequency-response analyses of the RSA have been carried out by ANGELONE & COULTER (1964) and WOMACK (1971). To my knowledge, excitation with sliding frequencies (sometimes called "wobbling") has not yet been attempted.

4.2.2 Transition function analysis

Analysis of the step function response is quicker to carry out in comparison because it is the system's transient response that provides the information (incidentally, such one-off processes are referred to as "transients").

Analysis of the step response is the only method in which CLYNES' directional dependence can be determined directly: When the inhalation and exhalation stages are separated in time to the point that they no longer overlap, one can describe the two responses separately as a linear system. By superposition of the responses, the responses to other test functions – e.g. impulse or rectangular functions - can then be predicted.

At any given amplitude, the step function has the highest energy content of all test functions in the low frequency range and is therefore particularly suitable for determining the slow system properties. The energy content at higher frequencies depends on the realisable steepness of the edge, but decreases rapidly with frequency in any case. Periodic square-wave excitation is therefore generally used to investigate the behaviour at higher frequencies (ISERMANN 1971). However, according to the above, this does not readily work here.

4.2.3 Stochastic identification

Auto- and cross-correlation functions are the dynamic analogue of the well-known (product-moment) correlation coefficient; they have the property of making linear correlations visible in statistical noise. Stochastic identification methods utilise the properties of these functions.

The system is stimulated with noise[12] that is as broadband as possible.

[12] **Noise:** In the case of deterministic signals, their value is predetermined at all times; stochastic signals, on the other hand, can only be described by statistical parameters. This means that stochastic signals can also be subjected to a spectral analysis. The bandwidth of a signal is the difference between the highest and lowest frequency at which the power density has dropped by 6 dB. So-called "white noise" has constant power density across all frequencies, i.e.

For natural systems, the natural noise at the input may be sufficient. The transfer function is given by the Laplace transform of the quotient of the cross-correlation between the output and input signal, and the autocorrelation of the input signal (see e.g. ISERMANN 1971, MILSUM 1966, MCFARLAND (1971).

For ideal white noise at the input, the autocorrelation becomes a Dirac impulse, its Laplace transform a constant. In this case, the transfer function is simply the Laplace transform of the cross-correlation between the output and input signal. The frequency response is the Fourier transform of the same and can be determined using the Fast Fourier Transform (FFT) algorithm for example. White noise is in practice often approximated by so-called PRBS noise (pseudo-random binary-signal noise); this is a sequence of rectangular pulses with seemingly random, but predetermined, time intervals.

The method could be used for subsequent system identification when, for example, respiration and HR are available on tape in a completed experiment. However, it is difficult to predict what effects the non-linearity of the system has on the result. It would therefore be interesting to apply stochastic identification to the CLYNES model set up on the analogue computer and to compare the resulting model parameters with those actually used.

4.3 Determination of the step response

4.3.1 Experimental set-up

Fig. 4.1 shows a block diagram of the experimental set-up. Two of the breathing belts described in Chapter 3 are used to measure the breathing volume. The signals are high-pass filtered to avoid DC drift (cut-off frequency 8 mHz corresponding to T = 20 sec, 6 dB steepness); filtered and unfiltered signals are fed into a Beckman Dynograph R (standard AC/DC coupler type 9806). Optionally, high-pass filtered or unfiltered respiratory signals are switched through to the analogue computer (EAI 380) via an analogue crossbar switch, are summed-up in a weighted manner there, and, via the crossbar switch and a 1:5 attenuator, fed into an analogue input of the PDP8/E.

The ECG enters the Beckman amplifier via the connection panel and an electrode selector, where it is high-pass filtered so that only the R-

---

has infinite bandwidth. Since the energy content of white noise is therefore infinite, only band-limited noise can be realised in practice (FISCHER 1969, ISERMANN 1971).

waves remain visible, and is fed to the Schmitt-trigger input of the PDP8/E's programmable clock via the crossbar switch.

The digital outputs of the PDP8/E are used to control the analogue switches of the EAI, which generate the target signal for paced breathing. This, together with the totalled breathing signal, is presented to the subject on a Philips storage oscilloscope. The patient sees her own respiration signal and the target signal move across the screen at approx. 0.5 cm/sec (Fig. 4.2). On the Beckman system's 8-track paper chart recorder, the high-pass filtered and unfiltered chest and abdominal respiration signals, their weighted sum, and the breathing target signal, are recorded/plotted, as well as the (high-pass filtered) ECG. Fig. 4.3 shows a typical section of the recording.

The programme execution can be influenced by the teletype unit of the PDP8/E. To check the recording, the Tektronix X/Y display shows the points in time of the R-spikes, the calculated tachogram (in msec), and the respiration signal (see Fig. 4.4).

Particular emphasis was placed on the scaling of the breath recording: In order to achieve a good signal- to-noise ratio, all elements of the signal path should be operated close to their maximum level, but at the same time, no element may overdrive at practically occurring signal levels. Table 4.1 shows the conversion factors in the signal path. Table 4.2 compares the level control at an assumed maximum respiratory amplitude of 1.5 litres with the range limits of the devices. With the settings used, a breathing volume of 1 litre in the computer corresponds to a fixed-point number of 724 (decimal). In the recording monitoring on the Tektronix display, a calibration line of the appropriate length is drawn on the display (see Fig. 4.4).

For respiratory pacing, two patterns 0 and 1 were prescribed 20 times each, in random order (Fig. 4.5). They were divided into five segments: pattern 0: 30 sec free breathing for recovery, 5 sec preparation, 3 sec breath holding in expiration status, fast inhalation and 10 sec holding in inspiration status, fast exhalation and holding in expiration status. Pattern 1: By A small-amplitude sinusoidal oscillation, superimposed on the signal, indicated to the subject the range within which they should steer their breathing signal.

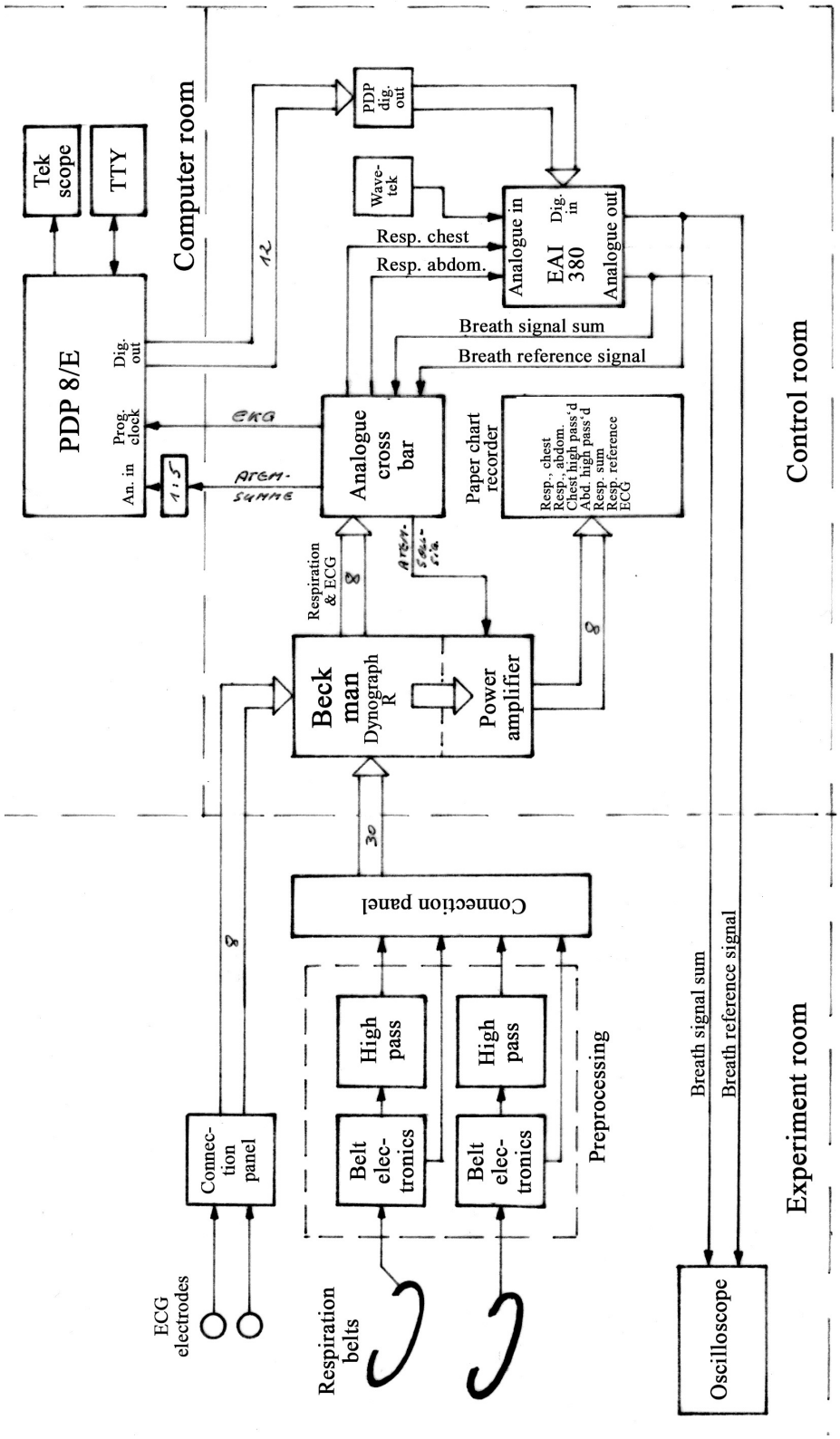

Fig. 4.1: Block diagram of the experimental set-up

Fig. 4.2: Paced breathing (subject: Sylvia v. Gienanth)

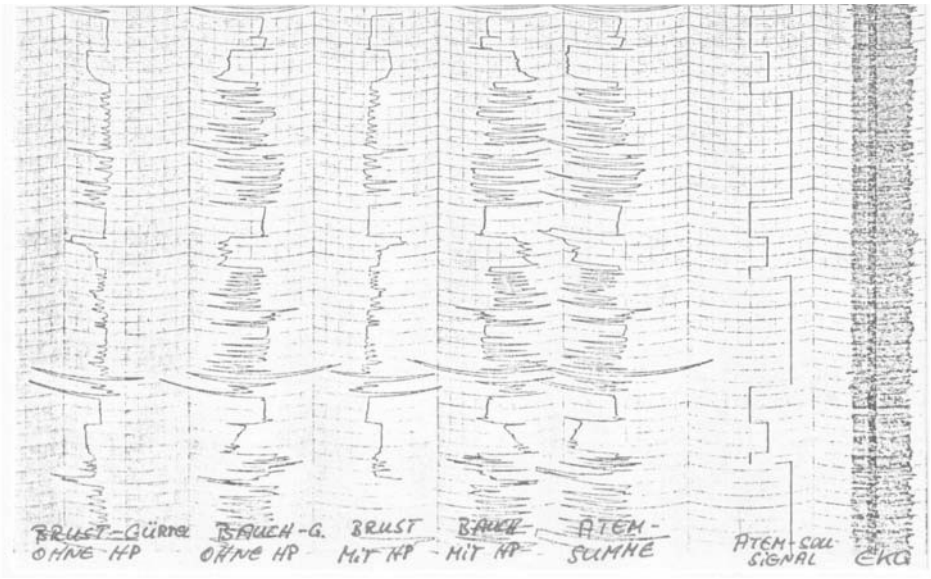

Fig. 4.3: Typical section of the respiration signal recording

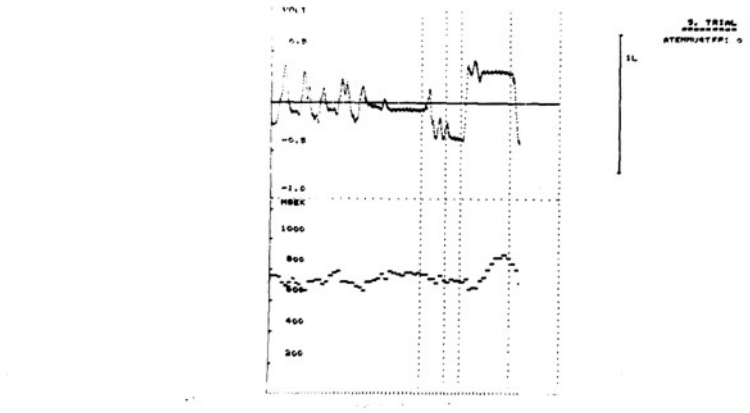

Fig. 4.4: Monitoring of the recording on the Tektronix screen

Signal point	Setting	Size
Breath volume	–	1 litre
Breathing belt output	–	e.g. 400 mV (chest) 1000 mV (abdomen)
Beckman recorder	Chest: 100 mV/cm Abdomen; 200 mV/cm	400 mV (chest) 1000 mV (abdomen)
Beckman Aux Out	As above	4 · 0.707 V 5 · 0.707 V
EAI sum	a=20, b=4, i.e. a/10=2, b/10=0.4	2 · (4·0.707 V) + 0.4 · (5·0.707 V) = 10 · 0.707 V = 10 · 0.707 V
Oscilloscope for subject	2 V/cm	3.65 cm
Beckman paper recorder	2 V/cm	3.65 cm
After the 1:5 divider at the PDP8/E Analog-In	–	7.07/5 V = 1.414 V
PDP 8/E	1V = 512	724 decimal
PDP Scope	1:2	362 points

Table 4.1 Amplification factors during breath recording

Device	Amplitude	Range
Breath	1.5 l assumed	Breath volume:
Beckman Recorder	± 2 cm	± 2.5 cm
EAI sum	± 5 V	± 10 V
MUX	± 5 V	± 10 V
PDP D/A converter	± 1 V	± 1 V
PDP integer range	± 512	± 2048
PDP Scope	± 256 points	± 256 points

Table 4.2: Breathing signal level at full scale

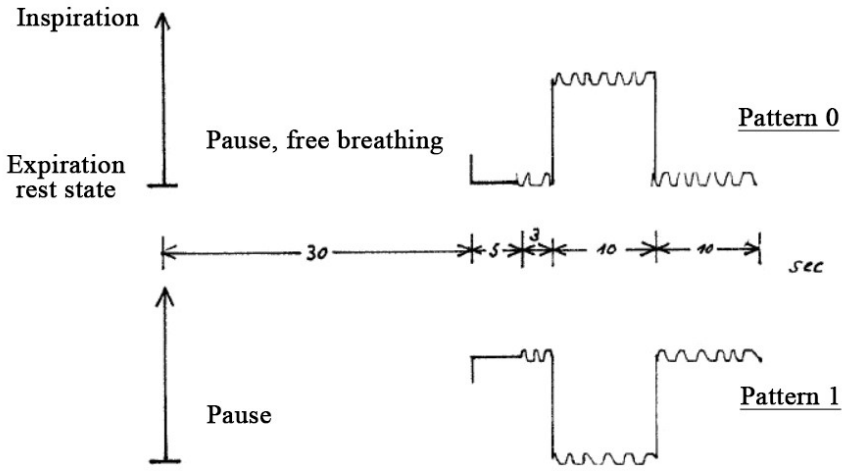

Fig. 4.5: Breath target signals

As the experiment analysis showed that the heart rate response had not yet subsided after 10 sec, another experiment, with 20 sec breath holding, was carried out. The pattern in Fig. 4.6 was used for this, alternating with 58 sec pauses:

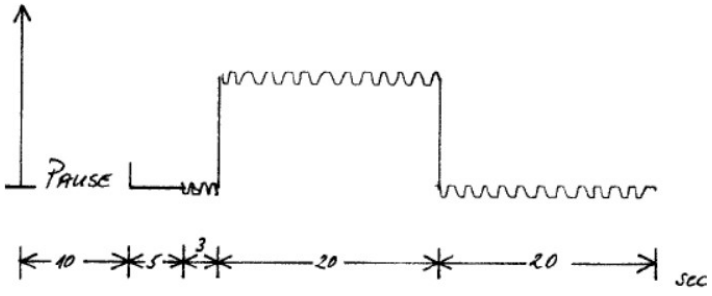

Fig. 4.6: Breath target signal for 20/20 sec step responses

The target signal is generated on the EAI with 3 analogue switches and a summing integrator (Fig. 4.7).

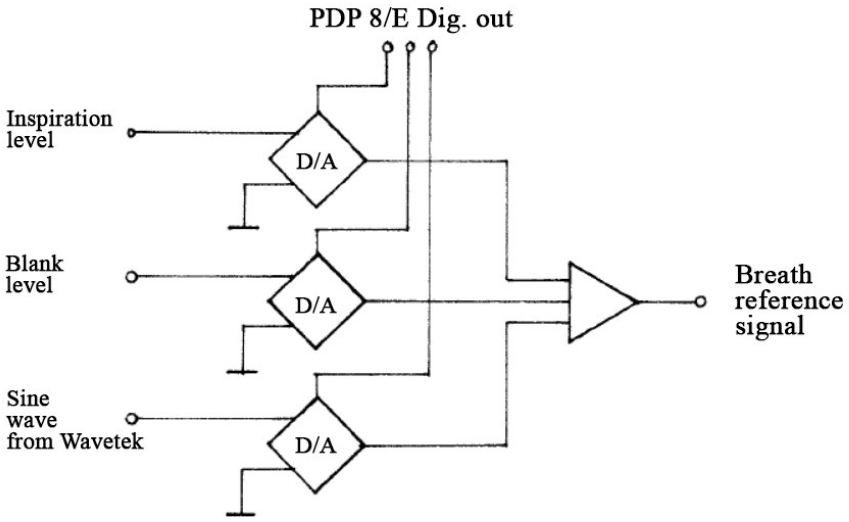

Fig. 4.7: EAI circuit for generating the paced breathing target signal

4.3.2 Carrying out the experiment

After the technical preparations of initialising the computer and the crossbar switch, checking the signal pathways, warming up the Beckman etc., the ECG electrodes are attached to the patient and the belts are put on. The chest belt is attached at the level of the largest chest circumference, the abdominal belt at the level of the navel. The subjects were only lightly clothed during the experiment (shirt, T-shirt) so as not to obstruct the breath measurement. The measurements were taken in the supine position.

After setting up the Beckman amplifier, the breath calibration procedure was carried out first (see Chapter 3). While the belt summing weights were being determined on the computer, the subjects waited and kept the belts on, since the output signal of the belts per cm of length expansion depends on the mechanical pretension of the rubber when applied.

To carry out the paced breathing, the position of the feedback breathing signal in the relaxed expiration position must correspond to the zero line of the target signal. For this purpose, the offset controls of the Beckman amplifier were first set such that the breath signals at the recorder are symmetrical to the centre line in order to obtain the full dynamic range of the Beckman final amplifier, pen recorder, and EAI. Then the necessary DC shift is set only for the feedback signal on the oscilloscope using the Y-position control. In this way, the expiration position in the digitised stored breath signal does not match the zero line, so this correction must be made later during data playback.

This is followed by a training phase for the paced breathing. During this time, the threshold of the Schmitt trigger is set to safe triggering by the ECG. The subject is instructed to keep the glottis open while holding the breath; whether the subject complies can be checked by the slight fluctuations around the breath-holding position that then occur. At the end of the training phase, the person is told to continue doing this for 40 minutes, but to please take breaks if it gets too strenuous.

The control programme is switched to the "Recording" position during that time. The position of the breathing zero line must be checked occasionally during the test. The programme completes the recording after 40 trials and stops generating a breathing target signal.

4.3.3 Storage and evaluation

4.3.3.1 Recording and evaluation

The sampling rate for the respiration signal was 20 Hz; the Nyquist frequency is therefore 10 Hz, which is approximately the 33rd harmonic of the normal respiratory frequency of 0.3 Hz. This high sampling rate would not have been necessary, but the correspondingly good resolution is pleasant for inspecting the course of breathing.

The interbeat intervals of the ECG are determined to an accuracy of 10 msec. In order to conserve memory space, the current value of the tachogram is not stored at every digitisation time of the respiration, but is only registered, together with the current number of the digitisation time, if a new ECG pulse has arrived in the meantime (see Fig. 4.8). The times of the IBI registration are therefore slightly shifted from the actual times. After each section, the data are written to the disc, which takes about 4 sec time.

At the beginning of the data file there is a header block with 256 parameters that can be used to characterise the test; there is further a block with 20 parameters before each section for characterising it . A final block concludes the respective data recording. There are 1160 respiratory values and up to 200 pairs of HR values per section. With 40 sections, that are 54,400 values corresponding to 212 ½ storage blocks on the disk (an empty DEC RKØ5 disc holds 6469 blocks in total).

4.3.3.2 Assessment of the measurement results

Before heart rate and breathing time courses can be recorded, the following points must be checked:

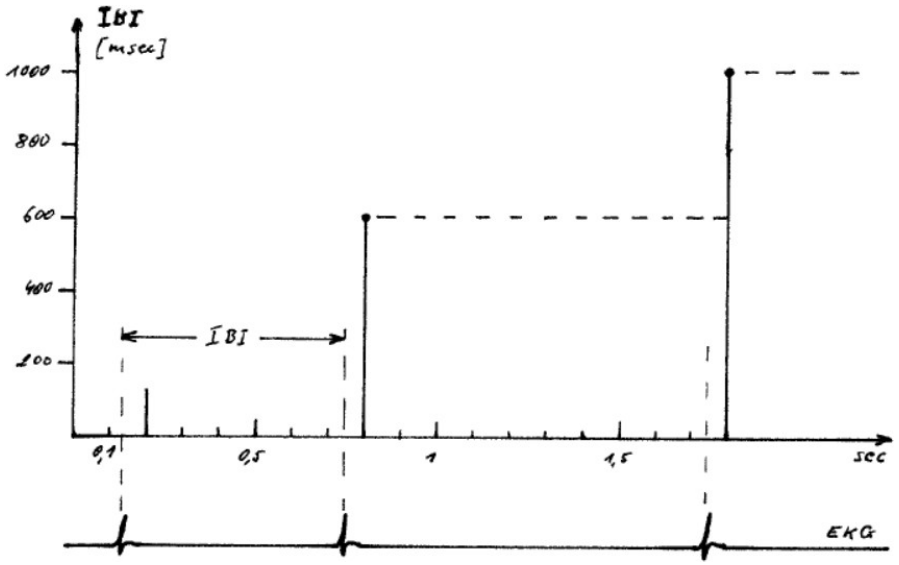

Fig. 4.8: Storing the heart rate

- whether the subjects succeeded in pacing their breathing; in particular, when holding their breath for 20 seconds, the subject at first did not succeed and continued breathing before the end of the section.
- whether data dropouts occur: False triggers or a lack of triggering in the ECG result in unusually short or long interbeat intervals, which show up as discontinuities in the averaged course.

A convenient evaluation programme is available for these purposes, with which the data of individual sections can be printed out or displayed on the screen, or the sections can be output on the screen in quick succession. The drift correction for breathing used in the averaging programme can also be switched on here and its function checked. Fig. 4.9 shows some typical time courses.

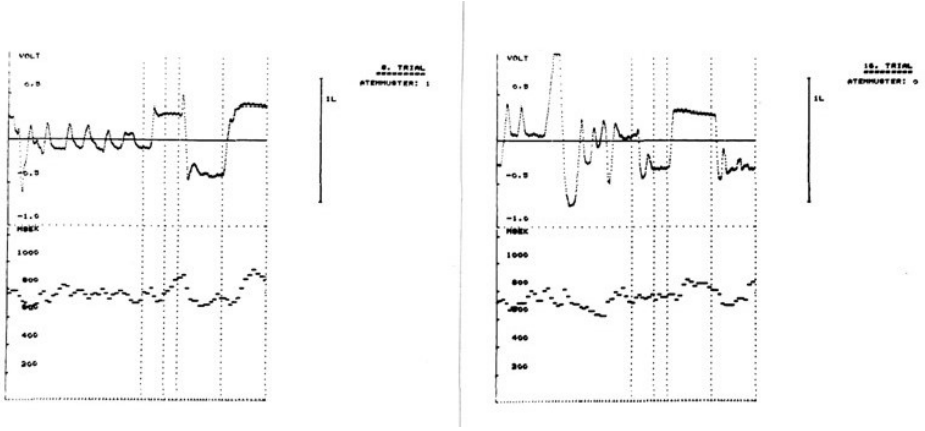

Fig. 4.9: Some typical HR responses to step breathing

4.3.3.3 Calculation of the mean time courses and their confidence interval

After the faulty sections have been sorted out, the successful ones are used for averaging. The averaging programme calculates the mean time course and its standard deviation for HR and breathing, separately for the breathing patterns that occur. From the standard deviation s, the 95% confidence intervals are given by

$$CI = \pm 1.96 \cdot \frac{s}{\sqrt{N}}, \quad N = \text{number of averaged sections}$$

In order to be able to use the same routine for processing breathing and HR data, the latter are reorganised so that a HR value is available at every digitisation time point. When reorganising and processing the HR, there were some difficulties, e.g. when data were missing because only the respiration was to be viewed, or when missing data were to be supplemented by zeros, or else saturation occurred due to missing ECG triggers (at which point the FORTRAN system programs then printed out hundreds of error messages). These difficulties have now been resolved by appropriate error detection. The averaging programme has a somewhat complicated structure overall, as the large real-number arrays do not simultaneously fit into a 4 K word block of the PDP8/E, and the actual processing was therefore relocated to subroutines.

The reorganisation of the HR data and the calculation of the standard deviation takes a relatively long time; the complete programme runs for 20 minutes. To save time, the averaging can therefore be limited to the actual time course of the step (without the breaks).

4.3.4 Results

4.3.4.1 Presentation of the results

Several programmes have been written (by the author) to display the results on the screen and output them to the D/A converters. Following the recent acquisition of a Tektronix plotter in our lab, plotting programmes are in preparation.

The mean courses of respiration and HR with and without the course of the standard deviation can be displayed on the screen (program MITDA1 & 2). The programmes calculate the display size and draw a calibration grid for interpretation. Time markers can be displayed for the exact determination of time points (Fig. 4.10 to 4.14, 4.19 and 4.20).

For a more precise analysis of the mean HR curve, it can be displayed on ts own, with adjustable magnification; the programme (MITDA3) again calculates the corresponding calibration grid (Fig. 4.15, 4.16).

There is further a programme for displaying the logarithms of the HR (with corresponding calibration) is also available (LOGDA1).

In addition to the display on the screen, the data can be output cyclically at D/A outputs (programmes HSZYK & HSZYK1). This allows them to be fed into the analogue computer for further processing or drawn with an X/Y plotter, for example (Fig. 4.17, 4.18).

Figs. 4.10 and 4.11 show the mean total time course of breathing and HR of a subject for the breathing pattern Ø without and with standard deviation, Fig. 4.12 shows the same for 20/20 sec steps. The breath signal is inverted here compared to the other images, with inspiration pointing downwards.

The confidence intervals are not shown, otherwise the curves would have been too close together. The averaging in Fig. 4.11 includes N=15 sections, the confidence intervals are therefore 51% of the standard deviation shown. For the confidence intervals of the other images, see Table 4.3.

Data set	DN0903		DN0604	
Step duration [sec]	10/10		20/20	
Breathing pattern	0:	1: 	0: 	1: Pause
Confidence int. in % of the std.dev. marked in the graph	57%	54%	62%	54%
Total std. dev. [msec]	100.3	93.3	53.6	752.3
Total confidence interval	±57.2	±50.4	±32.6	406.25±
Total std. dev.* [bpm]	≈9	≈8 ½	≈5 ½	≈59
Total confidence interval [bpm]	≈5	≈4 ½	≈3 ½	≈32
Fig. No.	4.10 4.11 4.15 4.17	4.12	4.13 4.14 4.16 4.18	4.19 4.20

*At the rest value of 820 msec in DN0903 or 760 msec in DN0604

Table 4.3: Standard deviations and confidence intervals of the heart-rate step response

The table also shows the total standard deviation s_{HR} of the heart-rate step response,

$$s_{HR} = \sqrt{\frac{\sum_{i=1}^{n} s(t_i)^2}{n}},$$

where $s(t_i)$ is the standard deviation at time t_i and n the number of samples per segment (excluding the pause segment), as well as the resulting overall confidence interval,

$$CI = \pm 1.96 \cdot \frac{s_{HR}}{\sqrt{N}}, \quad N = \text{number of averaged sections}$$

Fig. 4.15 shows the HR from Fig. 4.10 and 4.11 enlarged, Fig. 4.16 the HR from Fig. 4.14 enlarged. The Figs.4.17 and 4.18 show the curves from Figs. 4.15 and 4.16 on the X/Y plotter with subsequently drawn-in calibration marks. In difference to Fig. 4.16, a slow ramp has been superimposed on the HR in Fig. 4.18 in order to compensate for a medium acceleration (see Chapters 4.3.4 and 4.4.5). Figs. 4.19 and 4.20 show the mean course of respiration and HR in the pauses between the 20/20-sec stages in Figs. 4.13, 4.14, and 4.18.

Outliers due to false triggers are clearly visible in all images. Minor differences between the curves of the same experiment, e.g. between Fig. 4.10 and 4.15 arise because sections with relatively few outliers were included in the averaging by way of trial.

All the data images shown are from the same subject (female, 25 years old, height 174 cm, weight 63 kg). The 20/20-sec experiment was carried out approximately one month after the 10/10-sec experiment.

4.3.4.2 Interpretation and discussion

Even though the results of only one test subject are available so far, interesting conclusions can already be drawn. In particular, a comparison with the results of the study by DAVIES & NEILSON is revealing.

Time course:

First and most important result: the heart rate step response shows the expected biphasic course (acceleration - deceleration), and shows it in the same direction for inhalation and exhalation, with comparable amplitudes, but larger time constants for the exhalation response. CLYNES' "unidirectional rate sensitivity" is thus confirmed for this subject.

Table 4.4 provides a summary of the minima and maxima of the HR response; the HR values are also given in bpm to enable comparison

with the curves given by DAVIES & NEILSON. One second after the start of the inhalation stage – which itself lasts 1 sec – the HR has already reached its acceleration maximum (-70 msec); after 5 sec it is counter-regulated to a deceleration minimum of + 80 msec. At the exhalation stage, the acceleration maximum (–80 msec) is reached after approx. 3.6 sec; the deceleration minimum does not appear to have been reached after 9.5 sec, at the end of the phase (see Figs. 4.10, 4.11, 4.15, & 4.17).

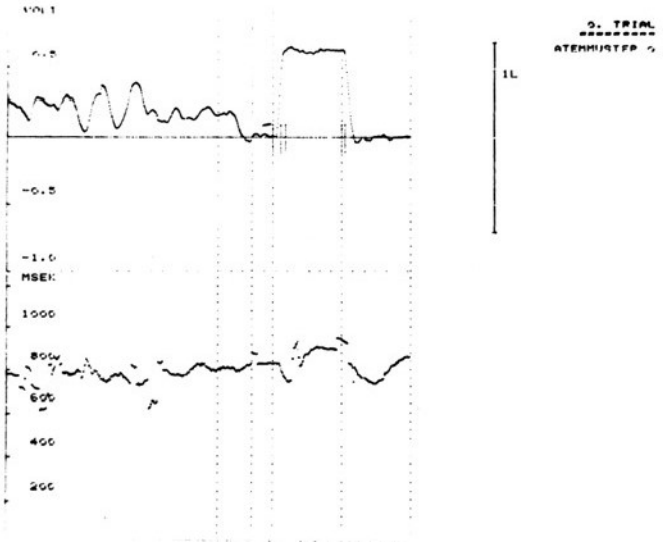

Fig. 4.10: Mean course of breathing and heart rate; breath holding time 10 + 10 sec (breathing pattern Ø)

A comparison with the confidence intervals given in Table 4.3 shows that all minima and maxima are significant.

After 10 seconds, the inhalation response has obviously not yet subsided. The interpretation of the exhalation response is therefore difficult with 10/10 sec steps. For this reason, the experiment shown was carried out again, but now with 20 sec breath holding in the inspiratory position and 20 sec breath holding in the expiratory position. After 13.3 sec, the inhalation response seems to have subsided; the exhalation response takes 15.6 sec (Figs. 4.13, 4.14, 4.16 & 4.18).

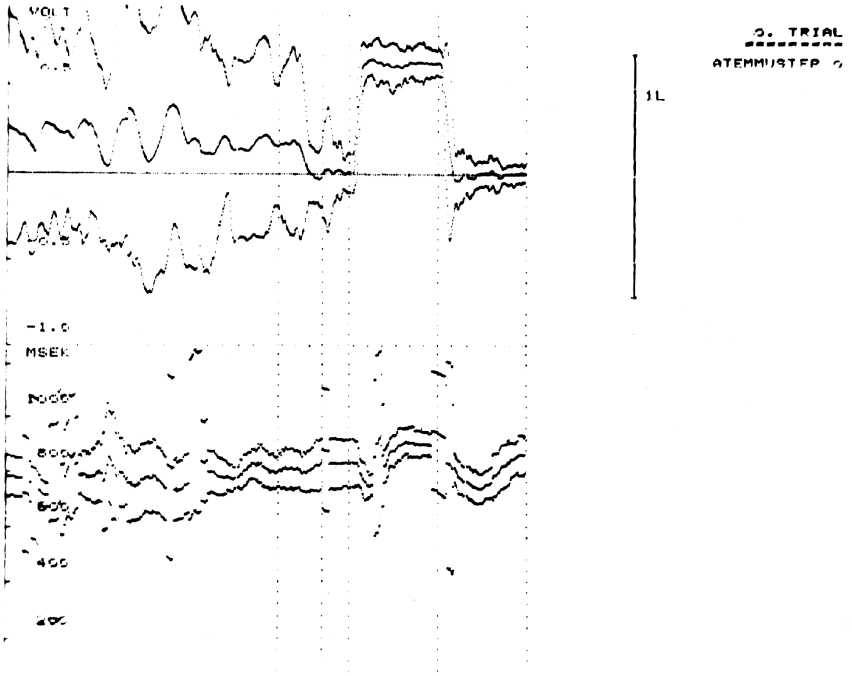

Fig. 4.11: Mean course of breathing and heart rate and time course of the standard deviation; breath holding time 10 + 10 sec (breathing pattern Ø)

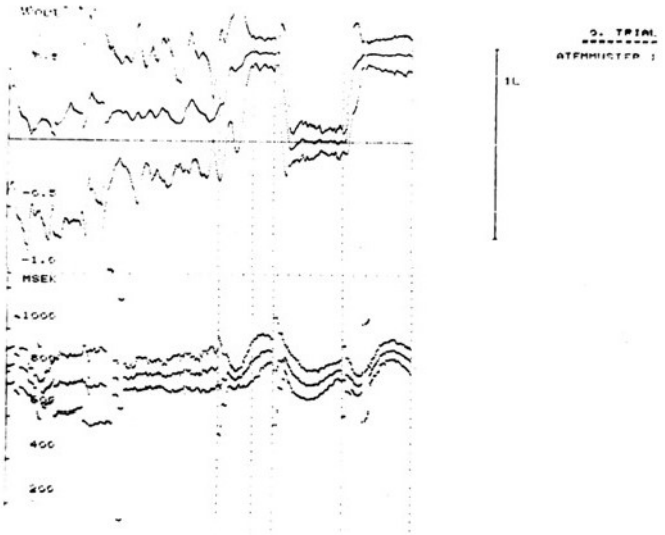

Fig. 4.12: Mean course of respiration and heart rate and time course of the standard deviation; breath holding time 10 + 10 sec (breathing pattern 1)

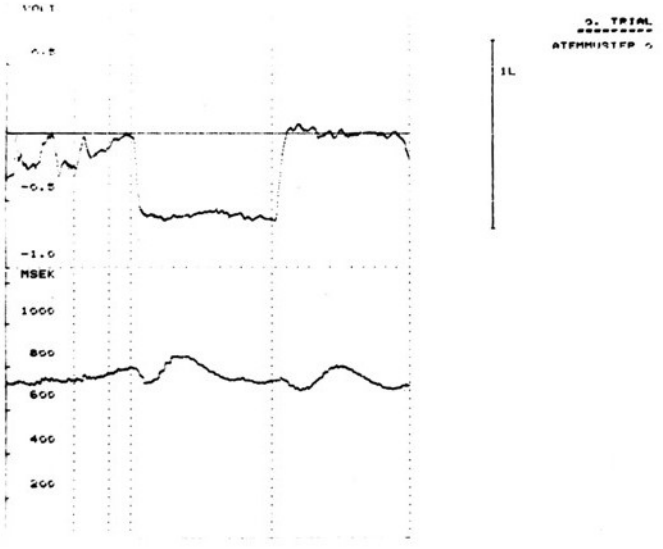

Fig. 4.13: Mean course of respiration and heart rate; breath holding time 20 + 20 sec (inspiration pointing downwards)

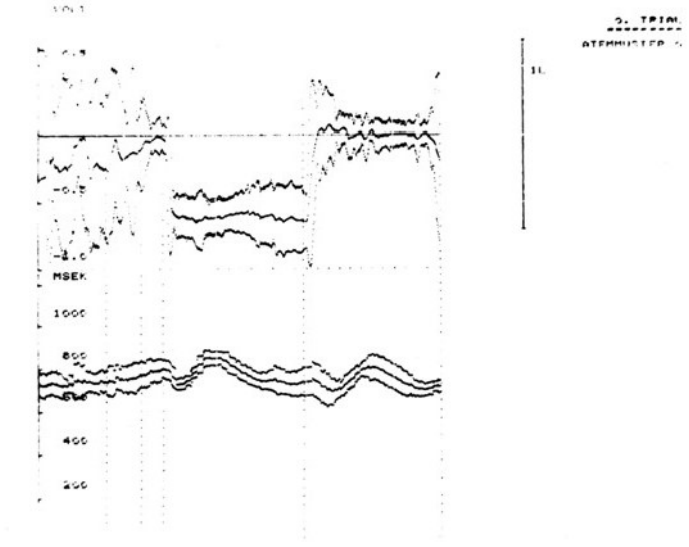

Fig. 4.14: Mean course of respiration and heart rate and course of the standard deviation; breath holding time 20+ 20 sec (inspiration downwards)

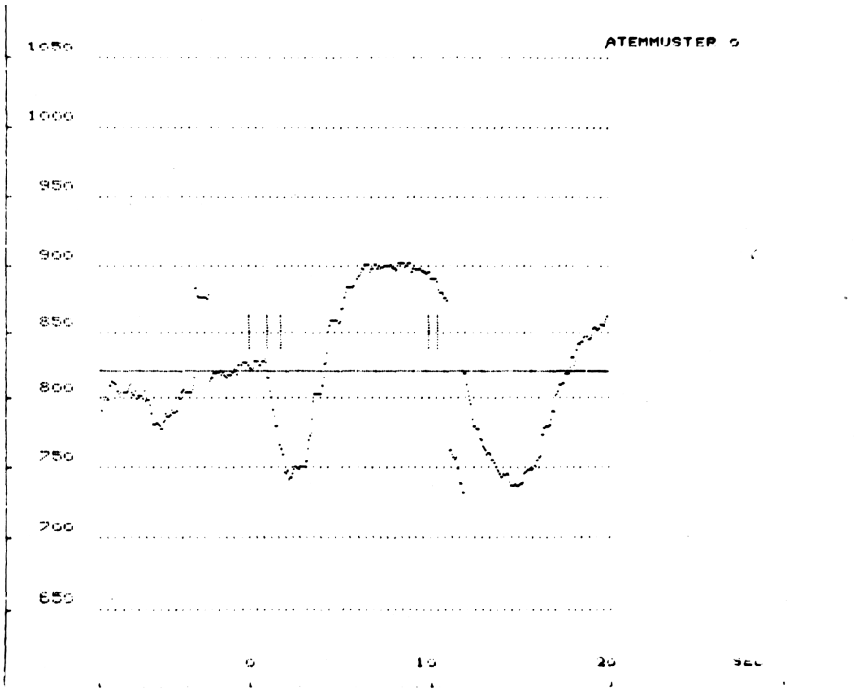

Fig. 4.15: Mean step response of the heart rate; breath holding time 10+ 10 sec

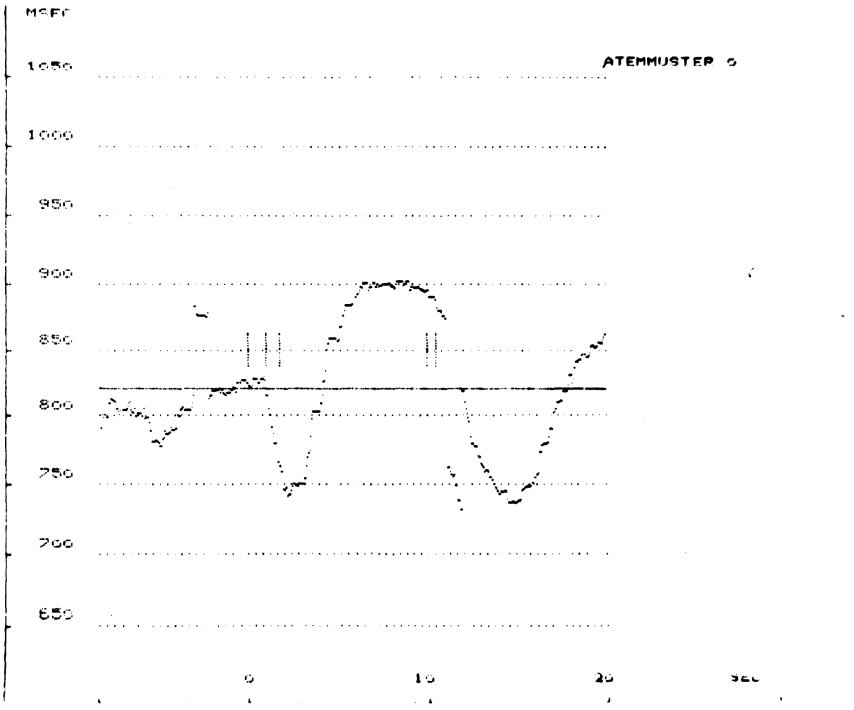

Fig. 4.16: Mean step response of the heart rate; breath holding time 20 + 20 sec

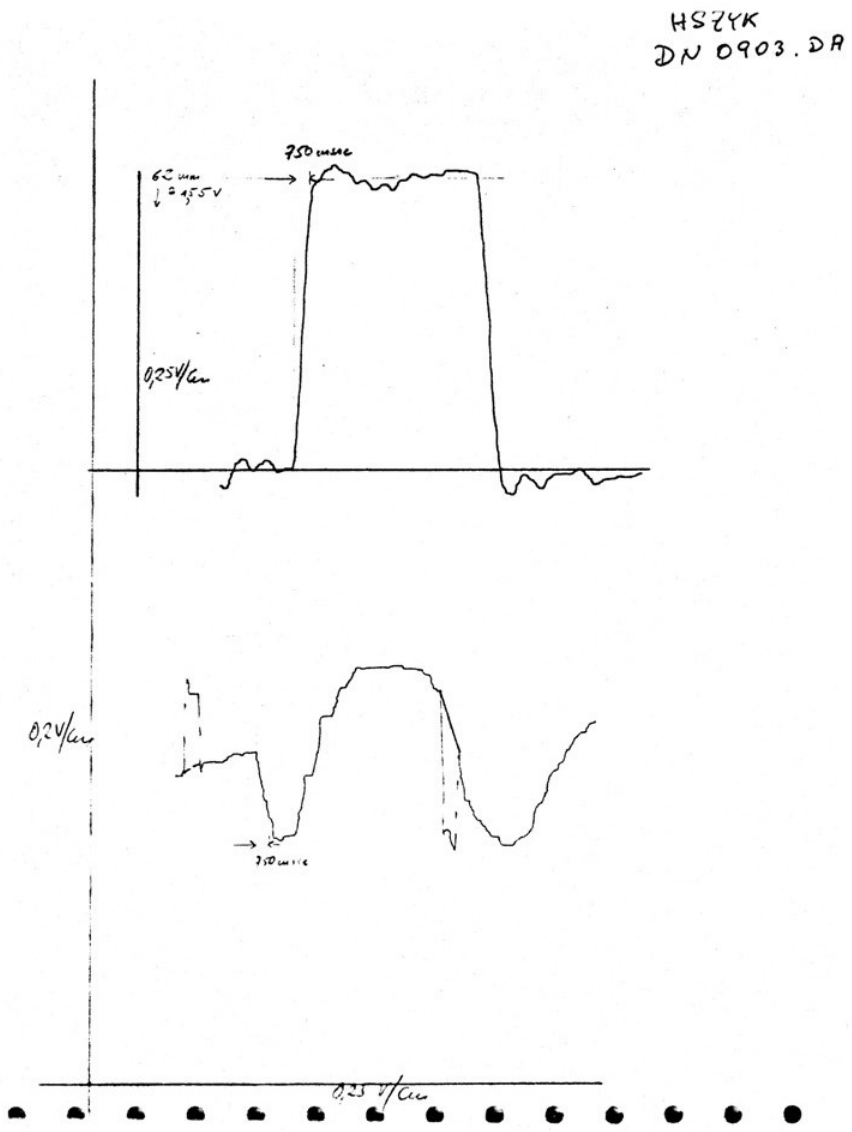

Fig. 4.17: As Fig. 4.15; representation on an X/Y recorder

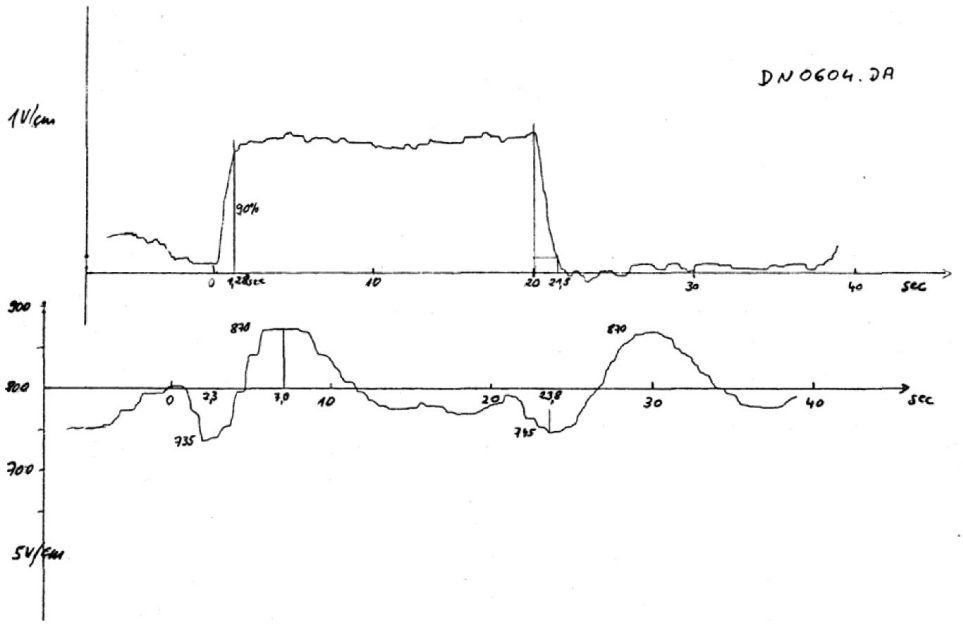

Fig. 4.18: Smaller step response of the heart rate with drift correction; breath holding time 20 + 20 sec

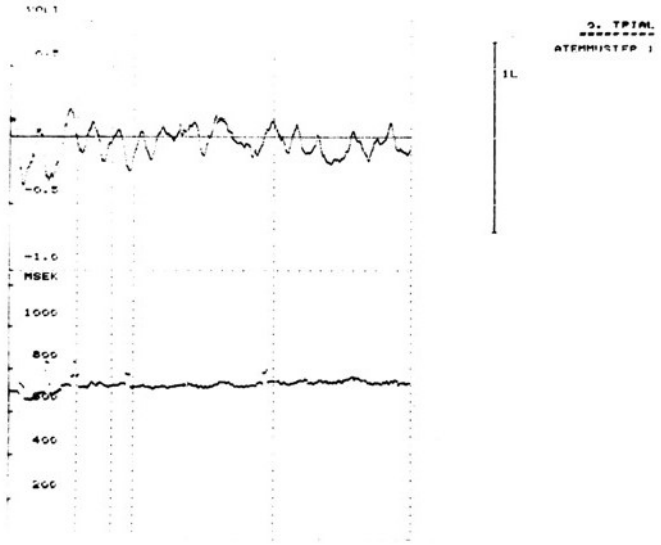

Fig. 4.19: Mean course of respiration and heart rate in the 58-second pauses between responses according to Fig. 4. 16

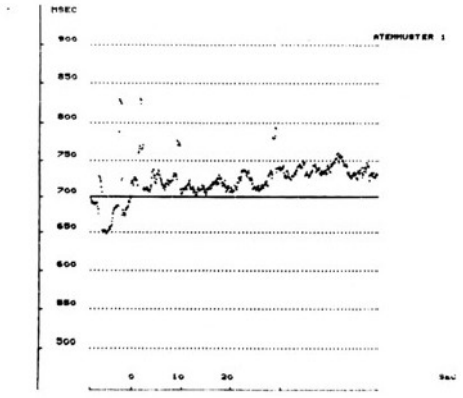

Fig. 4.20: As Fig. 4.19; enlarged

Data set	DN0903, Breathing Pattern 0							
Cf. Fig. No.	4.10, 4.11, 4,15, 4,17							
Breath flank	Inspriation				Expiration			
Accel./decel.	Accel. Max.		Decel. Min.		Accel. Max.		Decel. Min.	
Msec/bpm	msec	bpm	msec	bpm	msec	bpm	msec	bpm
Value	750	80	900	66.7	740	81.1	860	69.8
In relation to resting value	820	73.2	820	73.2	820	73.2	820	73.2
Diff. to Rest Value	–70	6.8	+80	–6.5	–80*	+7.9	+40	–3.4
Time point**	1.0 sec		5.0 sec		≈ 3.6 sec		After 9.5 sec min. not reached	

* Difficult to interpret

** Time point at which first max/min occurred, calculated from start of step

Table 4.4: Maxima and minima of the HR step response

Data set	DN0604, Breathing Pattern, no drift correction							
Cf. Fig. No.	4.13, 4.14, 4,16							
Breath flank	Inspriation				Expiration			
Accel./decel.	Accel. Max.		Decel. Min.		Accel. Max.		Decel. Min.	
Msec/bpm	msec	bpm	msec	bpm	msec	bpm	msec	bpm
Value	720	83.3	850	70.6	680	88.2	800	75.0
In relation to resting value	790	75.9	790	75.9	730	82.2	730	82.2
Diff. to Rest Value	–70	+7.4	+60	+5.4	–50*	+6.0	+70	–7.2
Time point**	1.3 sec		5.0 sec		2.5 sec		7.3 sec	

Continuation of Table 4.4

Data set	DN0604, Breathing Pattern, with drift correction							
Cf. Fig. No.	4.18							
Breath flank	Inspriation				Expiration			
Accel./decel.	Accel. Max.		Decel. Min.		Accel. Max.		Decel. Min.	
msec/bpm	msec	bpm	msec	bpm	msec	bpm	msec	bpm
Value	735	81.6	870	69.0	745	80.5	870	69.0
In relation to resting value	800	75.0	800	75.0	790	75.9	790	75.9
Diff. to Rest Value	–65	+6.6	+70	–6.0	–45	+4.6	+80	–7.0
Time point**	1.5 sec		5.4 sec		3.3 sec		8.7 sec	

Continuation of Table 4.4

Reliability:

This repeat experiment with longer breath holding is, at the same time, proof of the extremely high repeatability of the time courses found: despite the intervening time, changed test conditions (twice the duration) and breath calibration to be carried out again, the time courses are not only similar in principle, but also agree well in the size and position of the extreme values (Table 4.4). The confidence intervals shown in Table 4.3 are proof of the good reliability within a test session. They are between 30 and 60 msec. For comparison: with free breathing, the confidence interval was 400 msec, i.e. a multiple of that in the paced condition. The clearly visible decrease in variance at the beginning of the stimulus in Figs. 4.11, 4.12 and 4.14 is striking.

Acceleration correction

With 40 seconds of effective breath holding, it is to be expected that other mechanisms besides RSA also affect HR. The decrease in blood oxygen concentration, for example, can lead to an increase in HR to keep the oxygen supply constant. . The time course shown in Fig. 4.16 can be explained as a superimposition of the bi-phasic acceleration-deceleration-regulation back to the baseline level, with a slow linear mean acceleration of approx. 790 msec to 700 msec. In Fig. 4.18, this average acceleration was compensated for by superimposing a corresponding ramp function in the opposite direction. A further indication that the assumption of linear acceleration is reasonable is provided by the mean progression in the pauses between the breathing stages: Figures 4.19 and 4.20 show how the HR, on average, returns linearly to the initial value.

Sequence of breathing stages

The design of the first experiment included the question of how the sequence of inhalation and exhalation stages affects the course of the HRR. This was the reason why the breathing patterns Ø and 1 (Fig. 4.5) were alternated in a pseudo- random order. When looking at the results (Fig. 4.12), however, it is noticeable that the courses for breathing pattern 1 (exhalation/inhalation) cannot be interpreted without further ado: Even before the beginning of the first stage, the HR already shows a pronounced deceleration/acceleration. The course of the corresponding breathing curve provides the explanation: Since the inspiratory position (1/2 l) specified by the pacing is significantly higher than the normal inspiratory stroke, an inhalation is necessary on average during the preparatory interval. This preparatory inhalation triggers the described responses. Otherwise, the HR responses show the expected course.

Definition of the exhalation stage:

The observation described in the preceding leads to the question of the starting level from which an exhalation step should take place. The exhalation can go from the normal inspiratory position to the relaxed expiratory position, in which case the breath stroke would be smaller than the one used here so far. However, it can also take place from a higher level, or it can begin in the relaxed expiratory position and continue below it by tensing various expiratory muscles. Breathing out below the relaxed expiratory position does not occur under normal physiological conditions (but happens, e.g., when inflating an air mattress), so only the first two possibilities are of interest in our context.

Slope of the breathing steps

According to CLYNES, the HRR depends essentially on the first derivative of respiration. For the following comparison with the results of DAVIES & NEILSON, quantitative data on the achieved edge slopes of the respiratory steps are therefore necessary. Table 4.5 shows the results.

To ensure that rounding at the beginning and end of the edge has no influence on the measurement accuracy, rise and fall times are usually defined from 10% to 90% of the amplitude. Since the roundings at the beginning of the flanks are very small, the times from 0% to 90% and 100% to 10% were used for the sake of simplicity.(Fig. 4.21).

Data set	Flank	Mean rise time for ½ l	Std. dev.	Corresp. slope	Rise time after averaging	Corresp. slope
D*0903	Inhalation	875 msec	208 msec	1.75 sec/l	750 msec	1.5 sec/l
	Exhalation	846 msec	356 msec	1.69 sec/l	1.0 sec	2.0 sec/l
D*0604	Inhalation	810 msec	260 msec	1.62 sec/l	1.0 sec	2.0 sec/l
	Exhalation	890 msec	292 msec	1.78 sec/l	1.4 sec	2.8 sec/l
	Mean Std. dev.	855 msec 35.3 msec		1.71 sec/l	1.04 sec	2.08 sec/l

Mean difference of the flank's slope before and after averaging:
0.37 sec/l = 18% (of 2.08 sec/l)

Table 4.5: Rise times and slope of the breathing steps (increase from 0 to 90%; decrease from 100% to 10%; target amplitude ½ litre)

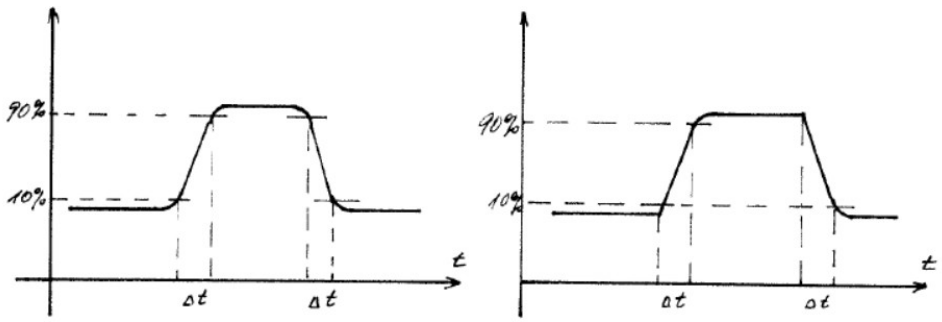

Usual definition Definition used in Table 4.1

Fig. 4.21: Definition of the rise and fall time of a step function

The rise/fall times of the mean breathing patterns determined in this way are 1.04 sec on average, which corresponds to an edge steepness of 2.08 sec/l. The breathing edges of the raw data do not occur simultaneously in relation to the segment boundaries. When the segment boundaries are used as a coherence marker for the averaging, flatter flanks are to be expected in the mean (illustrated in Fig. 4.22). This could have been corrected in the averaging by shifting the sections against each other so that the flanks coincide exactly. In the images shown, this has not been done, however. To estimate how large the gain of such a correction would be, the mean rise/fall time values were calculated from the raw data and included in Table 4.5. As expected, the slopes are somewhat steeper, but the difference is only 18%. Fig. 4.23 shows two examples for the procedure.

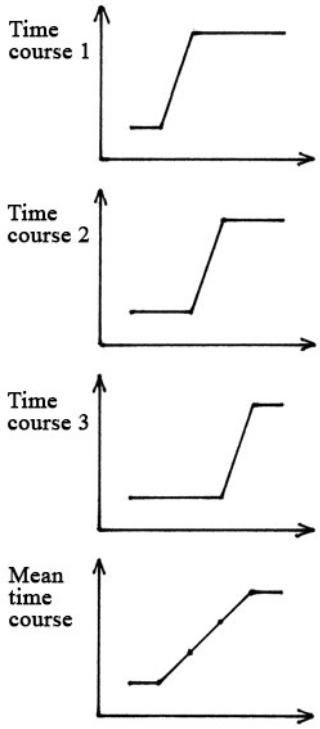

Fig. 4.22: Flanks become flatter with not exactly coherent averaging

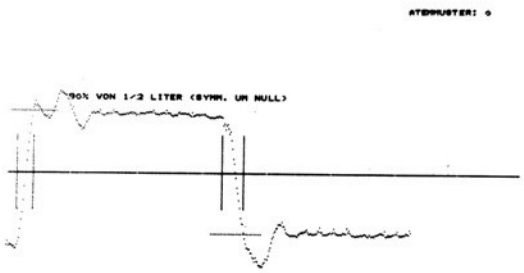

Fig. 4.23: Determining the flank steepness of the breathing step

4.3.4.3 Comparison with the work of DAVIES & NEILSON

The study by DAVIES & NEILSON (1967) is one of the few physiological investigations of the RSA with systems theory approach. Its methodology shows some improvements over that of CLYNES:

1) Parameters of the step responses are not taken from individual responses, but from average responses.

2) A calibrated breath control is used.

3) During breath holding, care is taken to ensure that the glottis remains open in order to avoid unwanted effects of pressure in the thoracic cavity.

4) The effect of body posture on the RSA is also recorded.

Due to the similarity of their approach to that of the present work, a direct comparison of the results is possible. Apparent differences in the course of the inspiratory responses can be explained by different parameters and boundary conditions. However, the study's finding that

exhalation has no effect is not supported by the results of the present study.

Inspiration responses

Fig. 4.24 shows the mean HR response to step-shaped inhalation found by DAVIES & NEILSON (1967). It is the mean of 97 responses of 10 subjects. Table 4.6 shows the corresponding range of amplitudes.

It is not clear from the table whether this relatively large range can be explained by variance within a subject or primarily by variance between subjects. However, the high reliability found in the present study for responses of the same subject suggests that differences between subjects were the main reason.

TABLE 2. *Response of the heart rate to inspiration*

	No. of Observ	Heart Rate, beats/min		
		Range	Mean	SD
Amplitude	97	4 to 33	15.90	6.68
Overshoot	97	−14 to +13	−1.40	3.74

Table 4.6 (from DAVIES & NEILSON 1967)

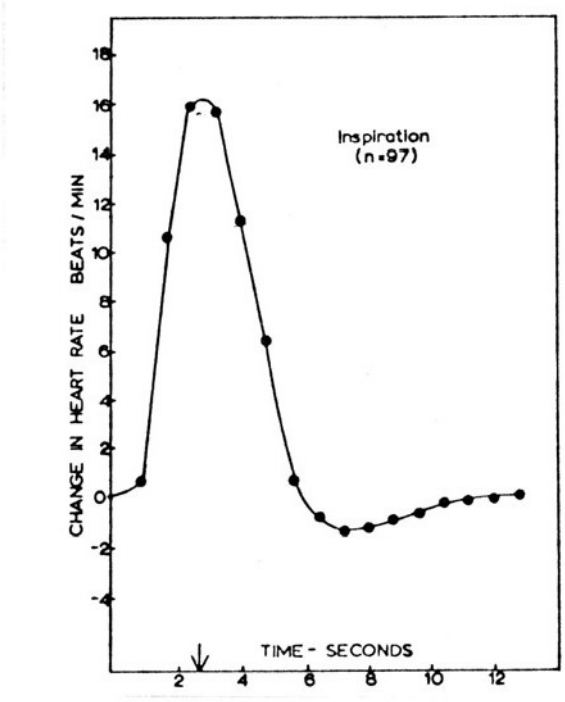

Fig. 4.24: Mean HR response to step-shaped inhalation (from DAVIES & NEILSON 1967)

Compared to that time course, the acceleration maximum in the present paper is weaker and the deceleration minimum more pronounced, and both are earlier in time (see Table 4.4). However, the amplitudes are within the specified scatter range.

About the scattering of the points of time of the extremes, DAVIES & NEILSON did not provide any data. However, their study on the influence of posture showed that a change in posture from sitting upright to supine shifted the extremes forward in time. Figure 4.24 applies to sitting upright, whereas the curves in the present study were recorded in the supine position. The results for inspiration are thus also consistent with regard to the response latencies.

Breathing pattern

A prerequisite for the comparability of the HR responses is the comparability of the breathing patterns used. For the mean curves (Figs. 4.24 and 4.25), DAVIES & NEILSON do not provide information on the amplitude and shape of the respiratory steps used. This is surprising since they themselves criticised that a comparison with the work of CLYNES was not possible because he did not use calibrated breath measurements.

From later illustrations of individual responses, however, it can be assumed that their breathing amplitudes are approx. 1.6 litres and the edge rise times approx. 1 sec (rise from 0% to 90%), which corresponds to slopes of approx. 0.6 sec/litre.

In the experiment in the present study, significantly smaller breathing amplitudes were used in order to come closer to the conditions during normal breathing. As Fig. 4.12 shows, even the setpoint value of 1/2 l used was still above the normal inspiratory stroke. The required rise times (approx. 0.8 sec) are comparable to those in DAVIES & NEILSON's study (1.0 sec). This means that both breath amplitudes and edge slopes of the present work were approx. 1/3 of their values. Correspondingly smaller RSA responses were therefore to be expected.

The subject was instructed to breathe inor out as quickly as possible. The fact that the slopes were nevertheless much smaller than DAVIES & NEILSON's study can be explained by two hypotheses:

1) Presumably, rise times do not increase proportionally with larger breathing amplitudes.

2) During paced breathing, the subject must stop exactly at the target value and for that reduce their breathing speed a little earlier.

Expiration response

A central finding of the work by DAVIES & NEILSON was that exhalation has essentially no effect on HR. This finding is in clear contradiction to the present results. How can this discrepancy be explained?

Fig. 4.25 shows the mean HR response to exhalation levels found by DAVIES & NEILSON. It represents the mean of responses from different subjects (10 subjects). Now, when forming a group mean, it is possible that person-specific responses cancel each other out, e.g. due to differing latency times.

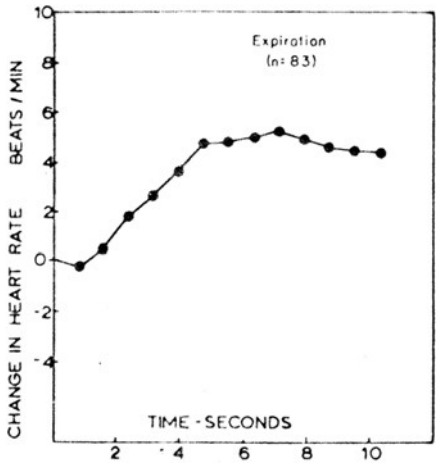

Fig. 4.25: Mean HR response to stepped exhalation (from DAVIES & NEILSON, 1967)

Furthermore, the exhalation stages used differ (see Section 4.3.4.2); in the curve shown in Fig. 4.25, they begin in the expiratory position. Exhalation stages from the inspiratory position are only marginally treated by DAVIES & NEILSON.

There is further no information on how long the subjects held their breath before exhaling in order to assess whether the inhalation response had really subsided. According to the results reported above, this can be up to 12 sec.

The group means shown are therefore not sufficient to support the proposition that exhalation has no effect; let us therefore consider the individual responses shown in their report. In fact, no pronounced exhalation response can be seen in one of them (Fig. 4.26), but the breath holding time of 7 sec would be too short in any case for a complete response. After 7 sec, a clear acceleration of approx. 7 bpm shows up. The exhalation acceleration maximum of the present study

occurred after 3 1/2 sec, but the subsequent deceleration occurred only after 9 – 12 sec.

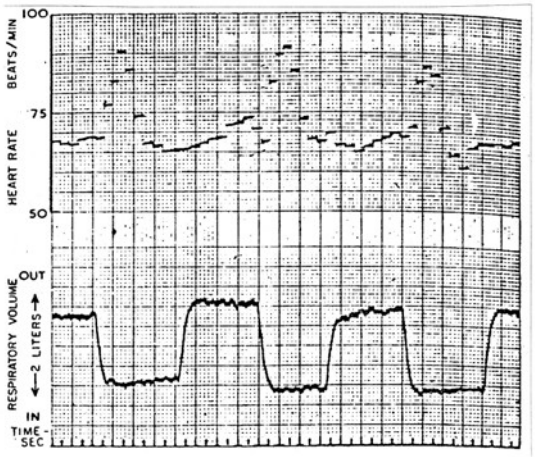

Fig. 4.26: HR response to rectangular breathing (from DAVIES & NEILSON, 1967)

There are therefore two possible explanations for this specific time course: Either there is actually no biphasic response to exhalation in the subject shown by DAVIES & NEILSON, or the latency times are longer, so that the response was not visible. Since many biological systems react more slowly after a state of saturation, the longer latency could also be the result of the higher breathing amplitudes used.

As further evidence for the lack of an exhalation response, DAVIES & NEILSON cite the similarity of the responses to positive and negative impulse breathing with the inhalation step response (see Fig. 4.27). However, the impulse responses can be explained equally well by the superposition of similar inhalation and exhalation responses. The response to free, sinus-like breathing can also be explained in this way (see Fig. 4.28 with the model responses to sine breathing illustrated in Section 4.4.5).

To summarise: It can be assumed that exhalation responses are either very differently pronounced in different people and may be completely absent in some subjects, or that they vary greatly from person to person. Even if, under certain conditions, the RSA can be described with sufficient accuracy using inspiratory responses alone, the proposition that exhalation has a negligible effect, cannot be maintained in this general form.

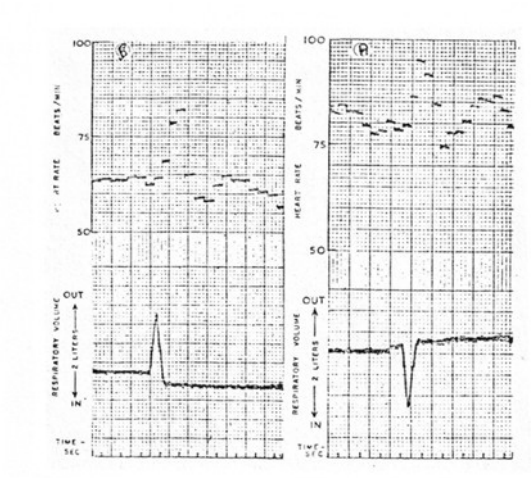

Fig. 4.27: HR response to impulse breathing (from DAVIES & NEILSON, 1967)

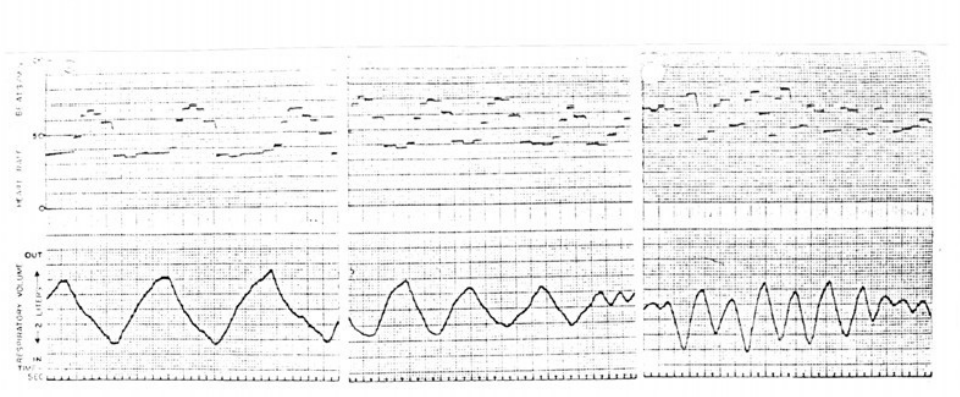

Fig. 4.28: HR response to free breathing with different frequencies (from DAVIES & NEILSON, 1967)

4.4 Determining the structure of the model

4.4.1 Introduction

To build a suitable analogue computer model, the transfer function must be determined from the step responses. In principle, analytical, graphical and simulation methods are available for this purpose. (A somewhat outdated but very detailed presentation can be found in STROBEL 1968).

A linear dynamic system with a fractional transfer function of the nth order,

(i) $$G(s) = \frac{(s+a_1)(s+a_2)\ldots(s+a_n)}{(1+T_1 s)(1+T_2 s)\ldots(1+T_n s)},$$

has a step response function composed of exponential functions,

(ii) $h(t) = A_0 + A_1 e^{-t/T_1} + \ldots + A_n e^{-t/T_n}$.

The exponents contain the zeros $-1/T_i$ of the denominator polynomial, these are called poles. The coefficients A_i can be determined by partial fractional decomposition of G(s), whereby unwieldy expressions occur at higher orders; Table 7.2 in the appendix therefore provides a compilation up to the third order.

I gained a first impression of the transfer function by the graphical method of pole compensation (STROBEL, p. 38, 39, OPPELT 1960, p. 172). With this, the exponential functions are “stretched” into straight lines by plotting them on semi-logarithmic paper (Section 4.4.2).

Drawing by hand was then replaced by a display programme on the PDP8/E, which draws the exponential function sums (ii) on the screen with parameters that are entered beforehand (Section 4.4.3). This gives you the opportunity to experiment with parameters in order to obtain an overview of achievable ideal step responses. From the parameters used in this, you can calculate the corresponding transfer function parameters by the formulae in Table 7.2; this gives an initial reference point for for the settings on the analogue computer (Section 4.4.4). Since the possibilities of our analogue computer are quite limited, we tried to get by with 2nd-order transfer functions, but it turned out that 3rd-order functions are more suitable. The digital simulation programme was therefore extended and a model of 3rd order was created on the analogue computer (Section 4.4.5).

The reference values of the digital programme were a good help in setting the parameters (Section 4.4.6). Section 4.4.5 shows the result, the simulation of the step response, as well as the response of the model to sinusoidal breathing and the frequency response. Finally, the differences to other models and the applicability of RSA extraction are discussed.

4.4.2 Graphical analysis

The 2nd-order transfer function corresponds to a step response function

(i) $h(t) = A + Be^{-t/T_1} + Ce^{-t/T_2}, \quad T_2 \geq T_1$

Four basic time courses are possible (Fig. 4.29).

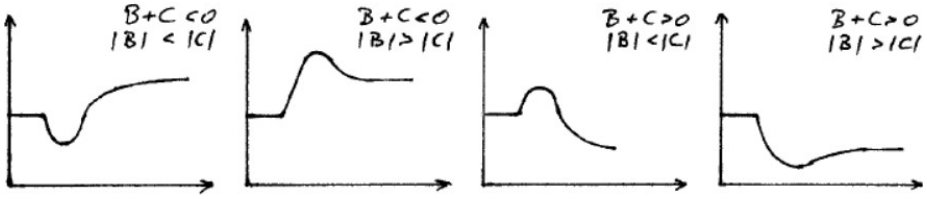

Fig. 4.29: Possible time courses of a step-response function of 2nd order

Fig. 4.30 shows once again the heart rate response during inspiration, which is to be approximated by such a 2nd order step response function.

For large t, the exponential functions vanish and it is thus

$$\lim_{t\to\infty} h(t) = A$$

First, the asymptote of the empirical curve is determined for large t; in the example, this is 900 msec:

A = 900 msec

The difference curve $h_1(t) = A - h(t)$ of the asymptote A and the step response function is now drawn on semi-logarithmic paper (Fig. 4.31). From the ansatz, it follows

$$h_1(t) = A - h(t) = -Be^{-t/T_1} - Ce^{-t/T_2}$$

When it is assumed that T_2 is sufficiently larger than T_1, then, for large t, the asymptotic curve is mainly determined by

$$\hat{h}_1(t) = -Ce^{-t/T_2}$$

The semi-logarithmic representation turns this exponential curve into a straight line whose gradient can be used to determine T_2. The intercept on the y-axis gives –C. Thus, from Fig. 4.31 we take T_2 = 1.15 sec and C = 1200. We then calculate and plot the difference h_2 (t) between the asymptotic curve of $h_1(t)$, and $h_1(t)$, shown in Fig. 4.32 . It is

$$\begin{aligned} h_2(t) &= \hat{h}_1(t) - h_1(t) \\ &= Be^{-t/T_1} \end{aligned},$$

and from the semi-logarithmic representation we can read-off T_1 = 0.75 sec and could read-off B as well. However, determined that way the intercept B will be no longer particularly accurate due to taking a double difference; it is better determined from the initial value of the transition function:

$$h(0) = A + B + C$$
$$B = h(0) - A - C$$

In the example, C = –1200, A = 900, h (0) = 820, and thus B = 1120.

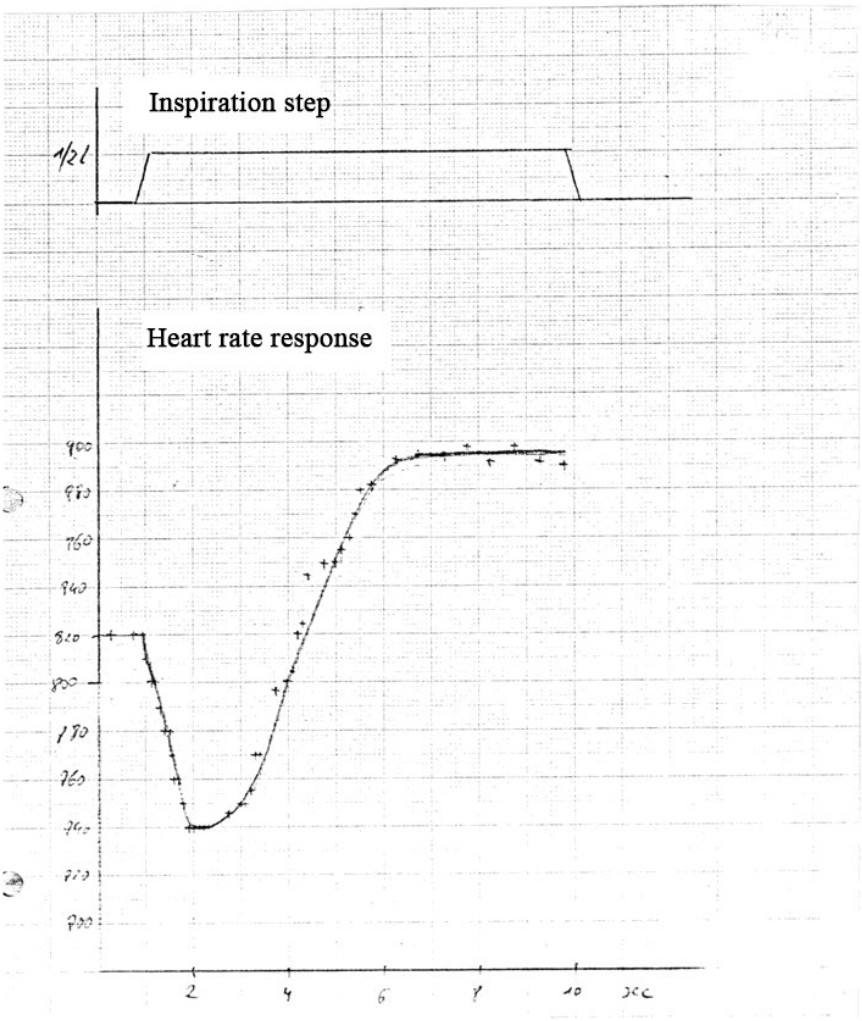

Fig. 4.30: HR response at inhalation level (data set as in Fig. 4.11).

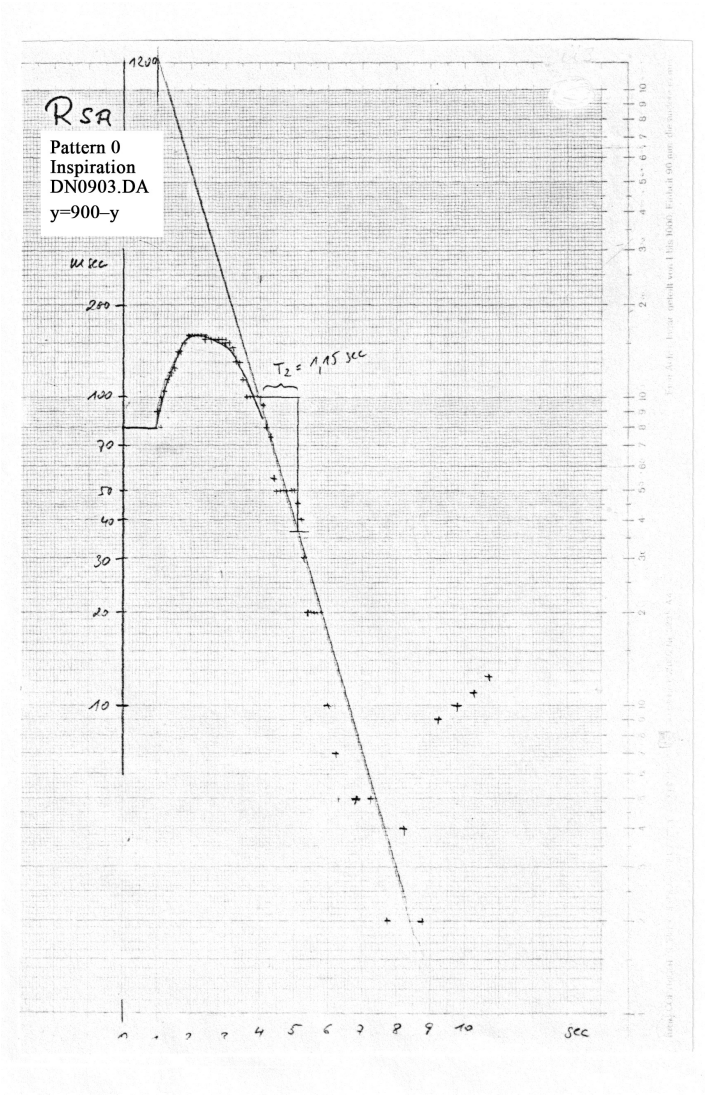

Fig. 4.31: Difference to the asymptote, drawn semilogarithmically

The method is called "pole compensation" because the asymptotes

$$h_i = K_i e^{-t/T},$$

which are "compensated", are determined by the poles –1/T of the transfer function. It can obviously also be used for step response functions of higher order as long as all poles are different and sufficiently far apart. However, the results become increasingly imprecise due to repeatedly taking differences.

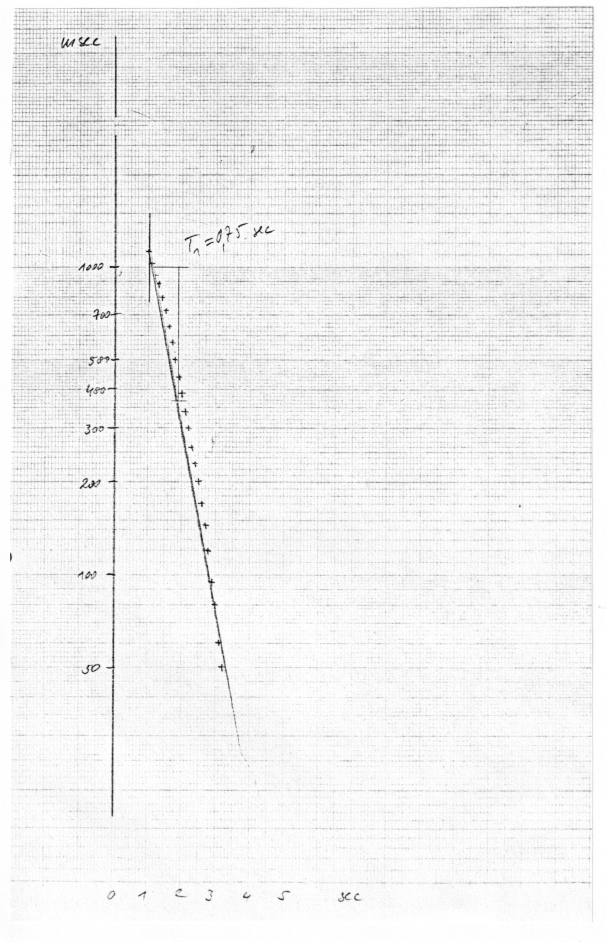

Fig. 4.32: Repeated difference to the asymptote, drawn semi-logarithmically

The condition that T_1 and T_2 are sufficiently different is not quite fulfilled in the example, so the reconstructed curve in Fig. 4.33 does not match the empirical curve exactly; the minimum of the simulated curve is more pronounced and occurs earlier.

4.4.3 2nd order model

4.4.3.1 Examination of the step responses on the digital computer

In order to improve the approximation and simplify the parameter determination, I wrote a computer programme which calculates the step response functions for any parameter combinations and displays them on the terminal. A subroutine (SIMUL), written for the MITDA3 programme mentioned in Chapter 4.3.4.1 for displaying the mean HR curves, calculates such sums of two exponential functions and draws them at the right scale and in the right place in the display of the empirical curve. This allows parameters to be determined quickly and

easily; Fig. 4.34 shows the result and once again the simulation with the parameters from the previous section.

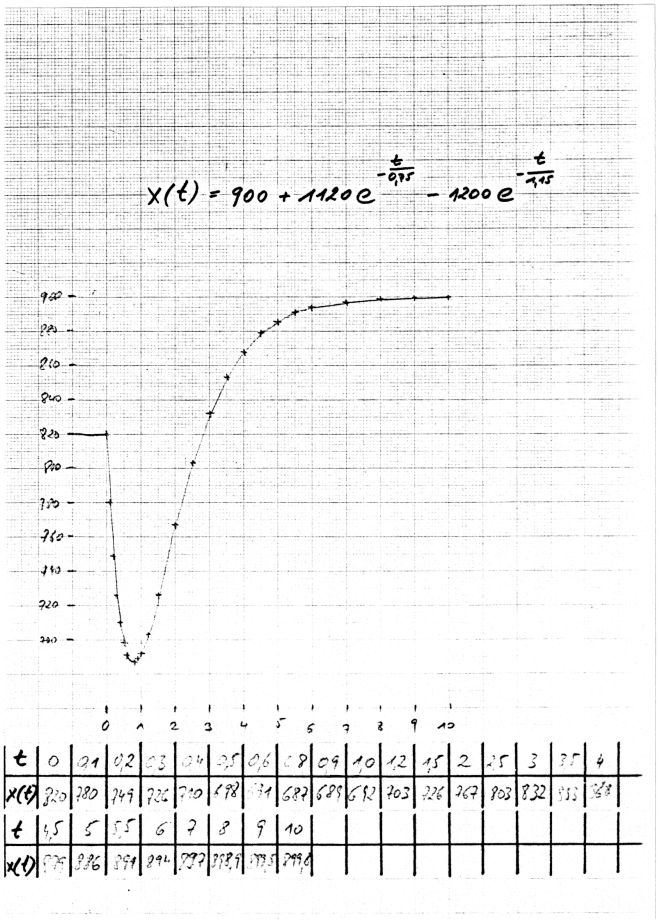

Fig. 4.33: Reconstructed 2nd order response

Even with the improved parameters, the minimum of the simulated inhalation response curve always occurs approx. 0.7 seconds before that of the original; shifting the minimum to a later point in time also delays the subsequent increase. However, the small time difference is of no significance; overall, both curves are in good agreement.

However, there were difficulties with the simulation of the exhalation stage: A sufficiently slow acceleration (course of h(t) going downwards) results in a much too slow deceleration (Fig. 4.35 a), or, vice versa: If the speed of the deceleration is to be comparable to that of the original, the maximum acceleration occurs too early (Fig. 4.35 b).

4.4.3.2 Realisation on the analogue computer

Nevertheless, the realisation of the preceding on the analogue computer was tried out.

In this first attempt, the breathing signal – depending on the direction of breathing – is processed in two different second- order systems ("delay line elements", "DT_2 elements"). The question arises as to how the two systems are to be combined for an overall model.

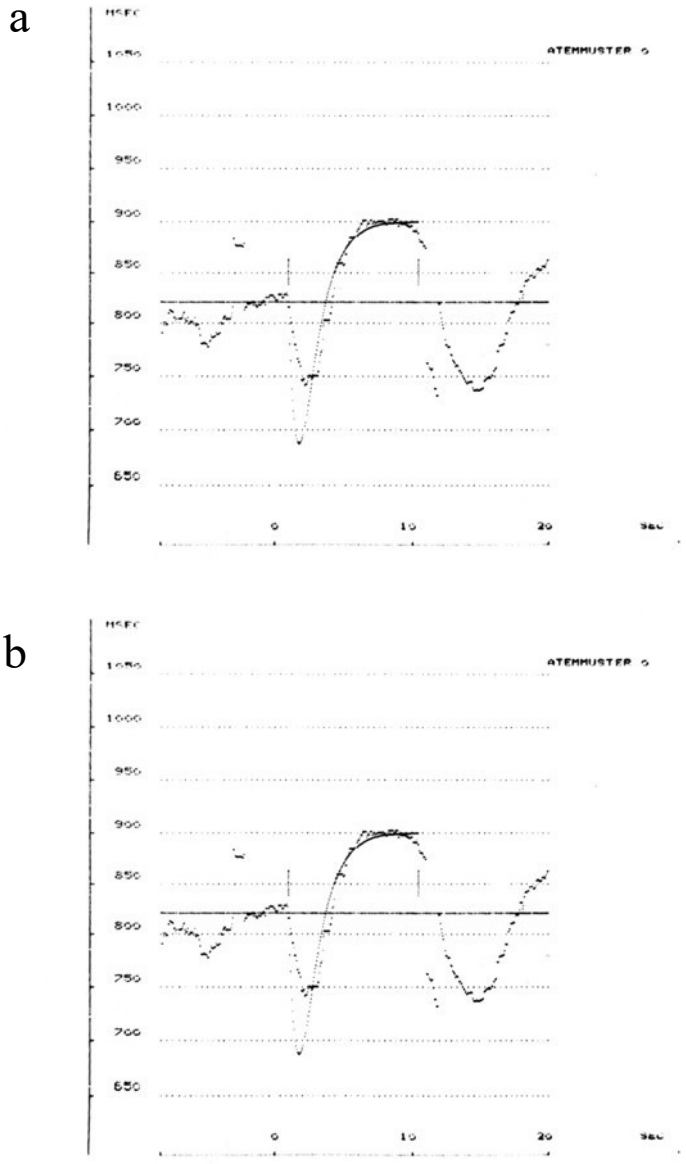

Fig. 4.34: Simulation of the inspiratory response of the HR on the digital computer with two 2nd-order systems
a) h(t) = 900 + 1120 exp(-t/0.75) - 1200 exp(-t/1.15)
b) h(t) = 900 + 1300 exp(-t/1.0) - 1380 exp(-t/1.3)

a

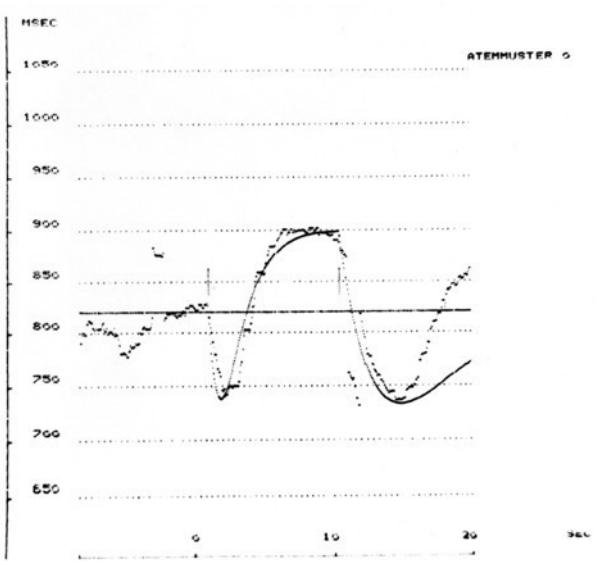

b

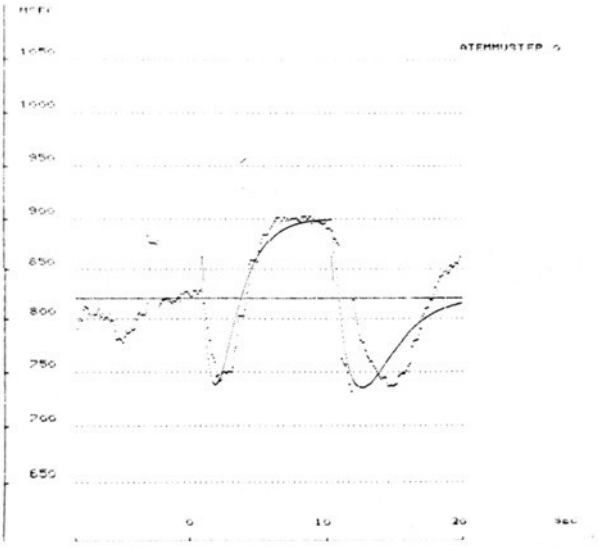

Fig. 4.35: Simulation of inspiration and expiration response of HR

a) Inhalation response: Same as in Fig. 4.34b
Exhalation response:
h(t) 820 + 2650 exp(–t/3.2) – 2570 exp(–t/3.6)

b) Exhalation response:
h(t) = 820 + 1700 exp(–t/1.5) – 1620 exp(–t/1.8)

Firstly, an attempt was made to switch the respiratory signal between the systems depending on its direction. Since the overall course of the HRR is to be explained by superposition of inspiratory and expiratory

responses, the output signals are summed-up in a subsequent amplifier. To determine the direction of respiration, the respiratory signal was differentiated using a bandpass filter with a high cut-off frequency and the sign was determined using a Schmitt trigger with adjustable hysteresis. The output signal of the Schmitt trigger was used to switch the breathing signal. Fig. 4.36 shows the block diagram.

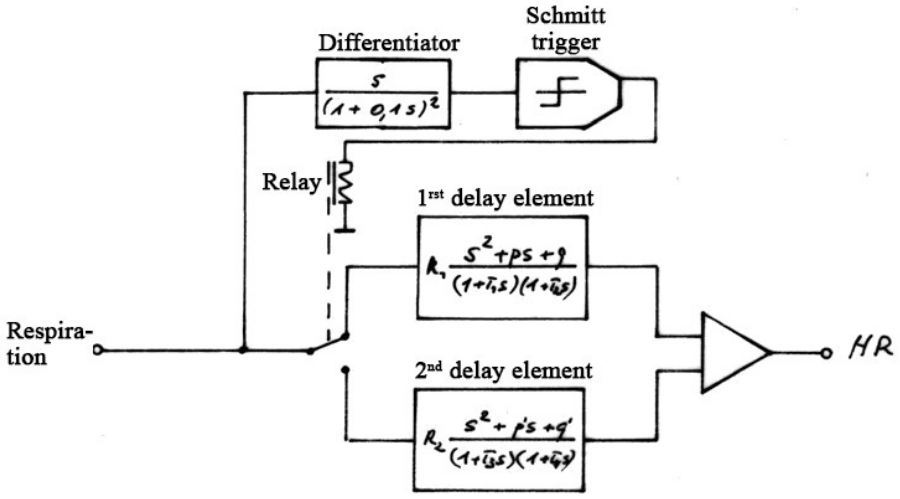

Fig. 4.36: First simulation test on the analogue computer

However, the circuitry contains a fundamental error: During the pauses also, a signal must be defined at the inputs of the delay elements. Since the input signals must not make any jumps at the switchover time (which would lead to a system response), the signal values must further be identical at the switchover times. This will generally not be the case: The momentary amplitude of a signal (here of breathing), at a given time, is not related to its derivation at the same point in time. See Fig. 4.37 for an illustration.

Switching must therefore take place at another point in the circuit where this condition is fulfilled. Since the breathing direction is the switching criterion, only it will fulfil this condition. The differentiator element for respiration must therefore be placed before the switching point (Fig. 4.38). This essentially brings us to CLYNES' model.

Since the ideal differentiator amplifies high- frequency noise to an infinitely high level, the bandwidth of a real differentiator must be limited at a sensible point. Fig. 4.39 shows the Bode diagram (i.e. the schematised logarithmic frequency response). of the differentiator used.

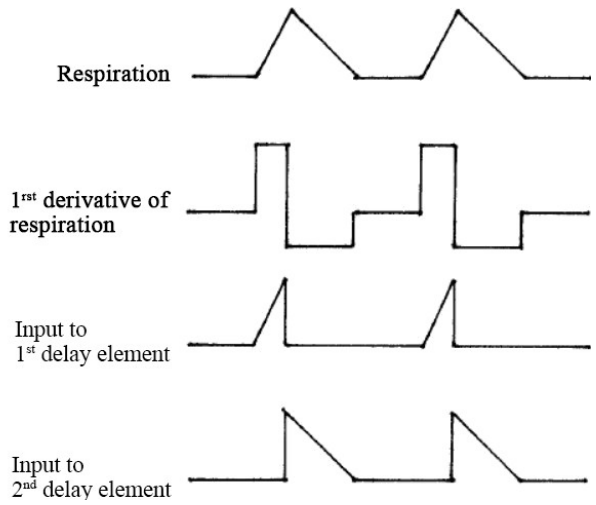

Fig. 4.37: Input signals of the delay elements in Fig. 4.36

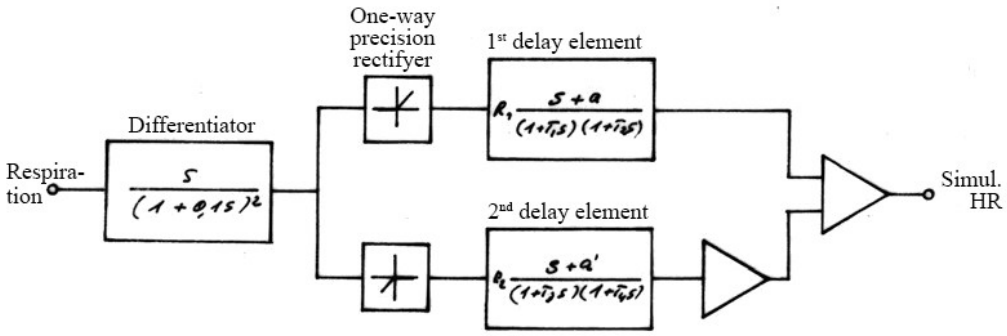

Fig. 4.38: Modified model: Differentiator positioned before the switching point

The additionally introduced low-pass behaviour

$$\frac{1}{(1+0.1s)^2}$$

changes the model behaviour at high frequencies – above

$$f = \frac{1}{2T} = 1.6\,\text{Hz}\,.$$

This is irrelevant for real breathing frequencies, but changes the early) parts of the step response (below 0.1 sec). These must therefore not be interpreted.

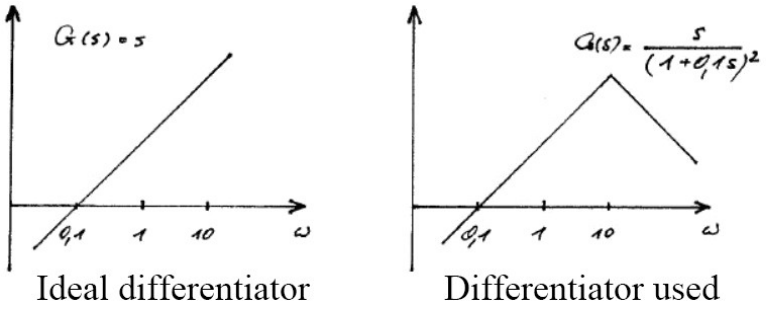

Fig. 4.39: Bode diagram of the ideal and real differentiator

Since a high-pass filter has now been factored out, the counters of the delay filters are only of 1rst order. As a result, the transfer function is now

$$G(s) = k \cdot \frac{s(s+a)}{(1+T_1 s)(1+T_2 s)},$$

with parameters being different for inhalation and exhalation. The corresponding step response is

$$h(t) = k \cdot \frac{T_2(1-aT_1)}{T_1 T_2 (T_2 - T_1)} e^{-t/T_1} - k \cdot \frac{T_1(1-aT_2)}{T_1 T_2 (T_2 - T_1)} e^{-t/T_2};$$

it has the start and end values

$$h(0) = \frac{k}{T_1 T_2}, \quad \lim_{t \to \infty} h(t) = 0.$$

This is no longer the general form of the second-order transfer function or step response (see Section 7.2). If the final value is to be higher than the initial value (Fig. 4.29 a), a proportional element must be added. A constant is therefore added for fixing the heart rate at rest. The complete block diagram is shown in Fig. 4.40.

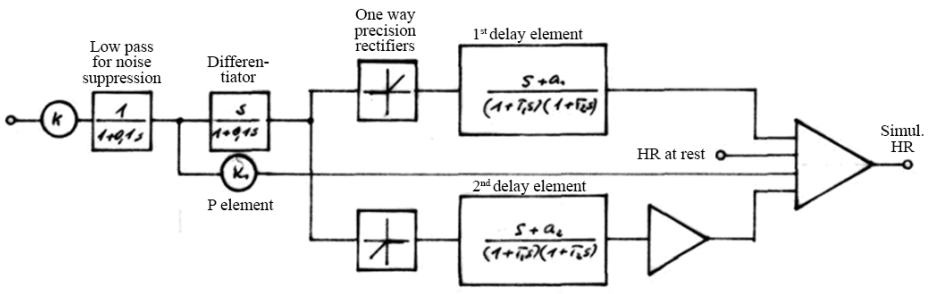

Fig. 4.40: Complete RSA model with second-order transfer functions

The transfer function's equation is now:

$$Y(s) = \begin{cases} \left[k \cdot \dfrac{s(s+a)}{(1+T_1 s)(1+T_2 s)} + k_1 \right] \cdot X(s) + \text{Rest value for inspiration} \\ \left[-k \cdot \dfrac{s(s+a)}{(1+T_3 s)(1+T_4 s)} + k_1 \right] \cdot X(s) + \text{Rest value for expiration} \end{cases}$$

Its realisation on the analogue computer is shown in Fig. 4.41 below.

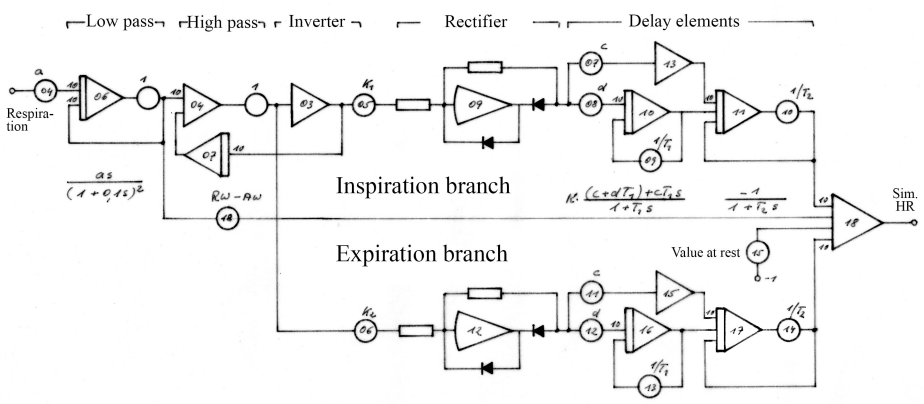

Fig. 4.41: Analogue computer model of the RSA with transfer functions of 3rd order

A function generator (Wavetek model 164) was used to simulate a breathing stage, whose amplitude and slope match that of the mean breathing time courses in the identification experiment. The inspiratory response of the model corresponds to the principle response shown as a) in Fig. 4.29, the expiration response follows the course shown as d) in Fig. 4.4b).

Fig. 4.42: Response of the model (lower curve) according to Fig. 4.40/4.41 to simulated breathing stages (upper curve)

Due to the superposition of the proportional element $k_1 \cdot X(s)$, the course of the exhalation response, even when the same parameters are used, is no longer the same as that of the inhalation response. This is because the proportional element, in contrast to the delay element, retains its sign when the direction of breathing is reversed, , so that the two

interact differently.

In principle, the course of the second-order step responses is monophasic: acceleration (or deceleration) and then decline to a resting value. The deceleration of the inspiratory response was achieved by the proportional element, which shifts this resting value. However, this deceleration following the acceleration cannot be used in this way for both inhalation and exhalation together.

When we compare the model behaviour with the result of the identification experiment (Fig. 4.15), we find a high degree of similarity in the course of the inspiration response; in the course of the expiration response, however, the deceleration is too slow and there is no deceleration minimum.

4.4.4 3rd order model

4.4.4.1 Introduction

In the simulation with 2nd order delay elements, the question arose as to whether the deceleration during inspiration should be interpreted as a shift in the resting heart rate during inspiration or as part of a biphasic course. This was the reason for the described identification experiment with 20 sec breath holding, from which it emerged that both inspiration and expiration responses have a biphasic time course.

To simulate a biphasic process, a 3rd order system is required. Compared to a 2nd order system, it allows, on the one hand, simulating the inspiration response beyond 10 sec, and, on the other hand to simulate the deceleration of the expiratory response following its acceleration.

The higher cost of the circuitry is justified by the greater fidelity of the simulation and the greater flexibility in the choice of progression shapes. The larger number of parameters to be set turned out to be a simplification during testing.

4.4.4.2 Investigation of the step responses on the digital computer

The general form of a transfer function of 3rd order is

(i) $$G(s) = k \cdot \frac{s^3 + ps^2 + qs + r}{(1 + T_1 s)(1 + T_2 s)(1 + T_3 s)}$$

As before, a differentiator is factored out, resulting in the more specific form

(ii) $$G(s) = k \cdot \frac{s(s^2 + ps + q)}{(1 + T_1 s)(1 + T_2 s)(1 + T_3 s)} + RV$$

RV: value at rest

Formula 12 in Appendix 7.2 of the German version describes the corresponding step response function h(t) (a sum of three exponential functions with time constants T_1, T_2, T_3).

The influence of the parameters p, q, T_1, T_2, T_3 on its time course is difficult to assess at first glance, so the programme described in 4.4.3.1 for displaying step response functions on the screen was extended to 3rd order systems. A transfer function with a lower-order numerator was also taken into account:

(iii) $$G(s) = k \cdot \frac{s(s + p)}{(1 + T_1 s)(1 + T_2 s)(1 + T_3 s)},$$

as this is the form used by CLYNES to simulate the exhalation response.

The parameters p, q, T_1, T_2 and T_3 are entered into the programme, as well as the initial value h(0) and rest value h(∞); the programme calculates the factor k and the coefficients of the exponential functions. Sets of curves with different parameter combinations were then drawn (Fig. 4.43). To summarise, the effect of the parameters can be described as follows:

1) The amplitude of the response is proportional to the difference between the initial and resting values (Fig. 4.43 a). When the initial value and value at rest are equal, the response is zero.

2) Parameter p determines the initial slope: p>0: increasing, p<0: decreasing slope (Fig. 4.43 b).

3) Parameter q determines the further behaviour: q>0: increasing, q<0: decreasing response (Fig. 4.43 c).

4) Parameters p and q together influence the amplitude (Fig. 4.43 d).

5) The time constants T_1, T_2, and T_3 of the denominator determine when and how the time course declines to the rest value. They have no influence on the initial slope nor the first extremum (Fig. 4.43 c).

6) Stretching in the time domain by a factor a is achieved by the transformation

$t \rightarrow t/a$ $\quad k \rightarrow ka^3$
$T_1 \rightarrow aT_1$ $\quad p \rightarrow p/a$

$T_2 \rightarrow aT_2$ $\quad q \rightarrow q/a^2$
$T_3 \rightarrow aT_3$ $\quad$ (Fig. 4.43 f).

The curves are biphasic; their shape can be changed within wide limits by the parameters.

a) Influence of initial and rest value AW RV 790 770 750 770	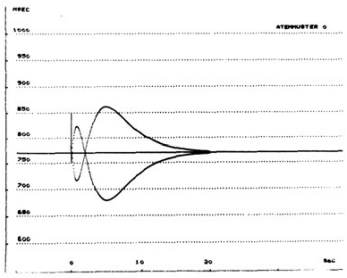
b) Effect of p p 5 0 –5 –10 –15	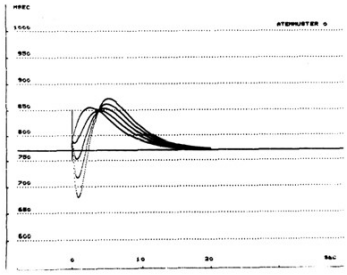
b) Effect of q q 12 6 0 –6 –12	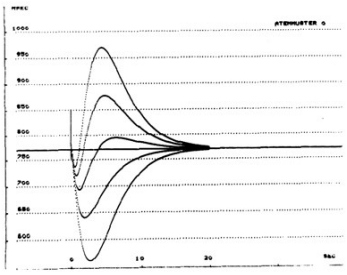

Fig. 4.43: Step response functions to the transfer function

$$G(s) = k \cdot \frac{s(s^2 + ps + q)}{(1+T_1 s)(1+T_2 s)(1+T_3 s)} + RV$$

For parameter k, we have $k = T_1 T_2 T_3 \cdot$ (initial value – rest value)

d) Influence of p and q together

p	q
–2	1
–6	3
–10	5
14	7

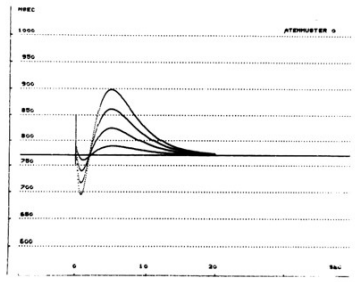

e) Influence of the time constants of the denominator

T_1	T_2	T_3
1	2	3
1	3	5
1	4	7
2.5	3	3.5
3	3.1	3.2

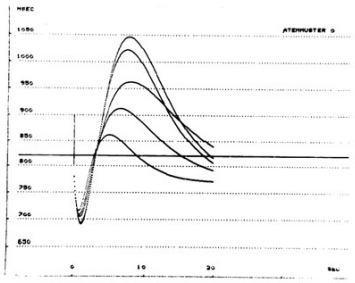

f) Stretching in the time domain

T_1	T_2	T_3	p	q
1	2	3	–10	5
2	4	6	–5	1.25
3	6	9	–3.33	0.56

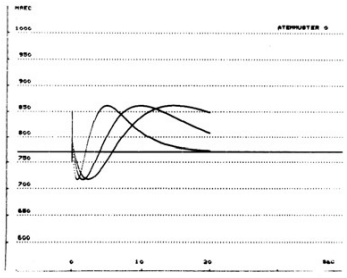

Fig. 4.43. Step response functions, continued. Unless otherwise specified, the parameters have the following values:

T1	T2	T3	p	q	AW	RW
1	2	3	–10	5	790	770

4.4.4.3 Realisation of the model on the analogue computer

Setting up the associated analogue computer model (Fig. 4.44) did not present any fundamentally new problems compared to the 2nd order model. However, difficulties arose due to the limited capacity of the available EAI 380. Various measures had therefore to be taken to limit the circuitry's complexity:

1) A low-pass filter of the differentiator has been omitted. This now has the transfer function of a high-pass filter (see Fig. 4.45):

$$G(s) = \frac{T_D s}{1 + T_D s}$$

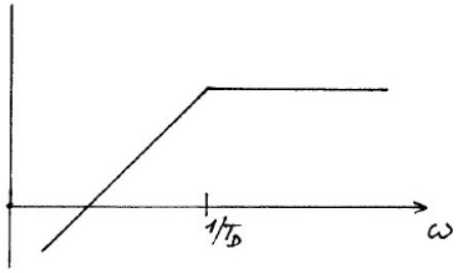

Fig. 4.45: Bode diagram of the differentiator

2) The third low-pass filter ($1/(1+T_3 s)$) of the delay elements is used jointly by both; this is possible because, by factoring out the differentiator, the numerator of their transfer functions is now only of 2nd order (see equation (ii)).

3) A circuit was sought for the delay elements in which all parameters are independent of each other and which uses as few summators and inverters as possible. The circuit shown has the transfer function

$$G(s) = \frac{s^2 + ps + q}{1 + us + vs^2}.$$

For parameters u and v we have

$u = T_1 + T_2$
$v = T_1 - T_2$

The form of the denominator in this transfer function does not prevent realising complex time constants T_1 and T_2. This happens when the discriminant $D = u^2-4v$ becomes negative. The system then performs damped oscillations; the damping is determined by the magnitude of u. A slightly sub-critically damped system is suitable for accelerating the decrease in the response to the rest value.

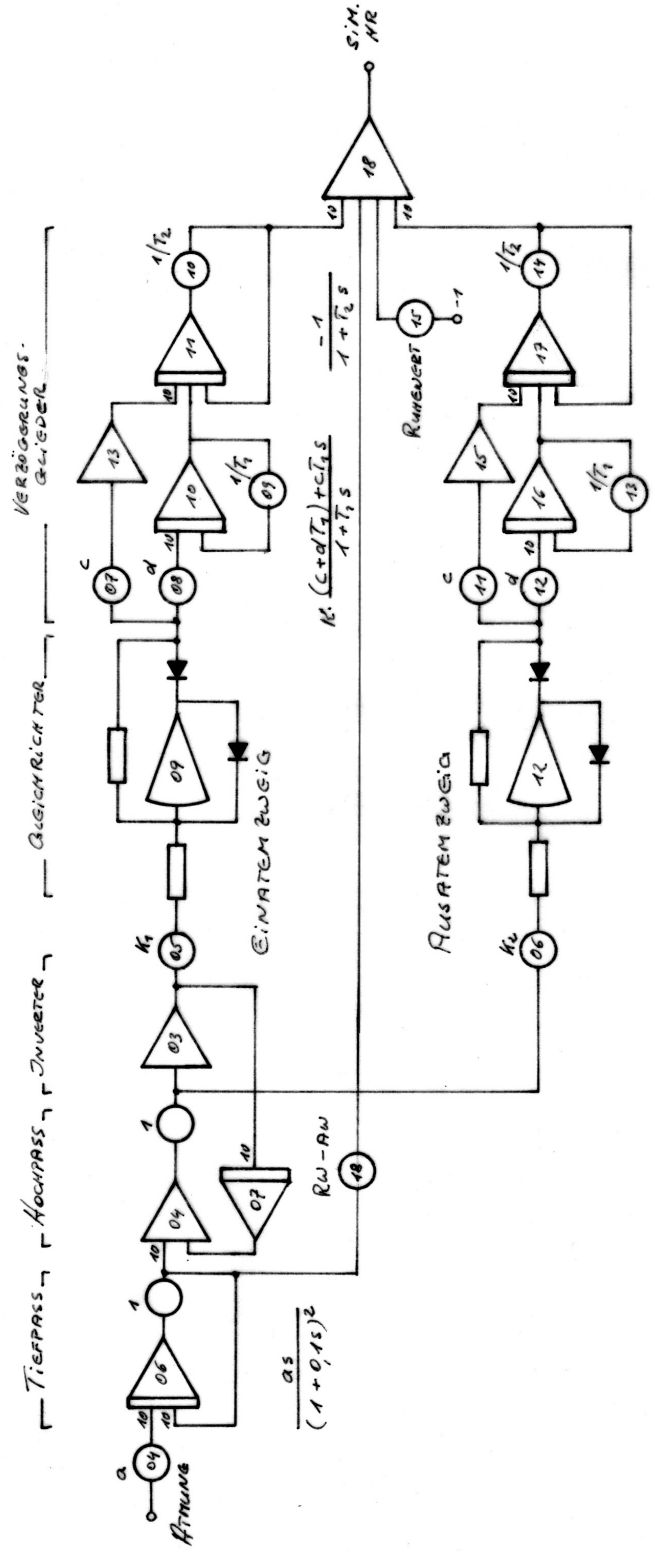

Fig. 4.44: Analogue computer model of the RSA with 3rd order transfer functions

4.4.4.4 Scaling of the model

As expected, there were difficulties with the scaling[13] due to factoring out the differentiator. First, the model was analysed with ideal step functions (i.e. those with a steep slope at the edge). It was found that the cut-off frequency of the differentiator/high-pass filter was set too low at $\tau = 10$ sec (corresponding to $T_D = 0.1$ sec). While this prevents overdriving even with steep input edges, the low energy content of the output signal with now flatter edges is no longer sufficient to excite the subsequent system stage (see Table 4.7 b).

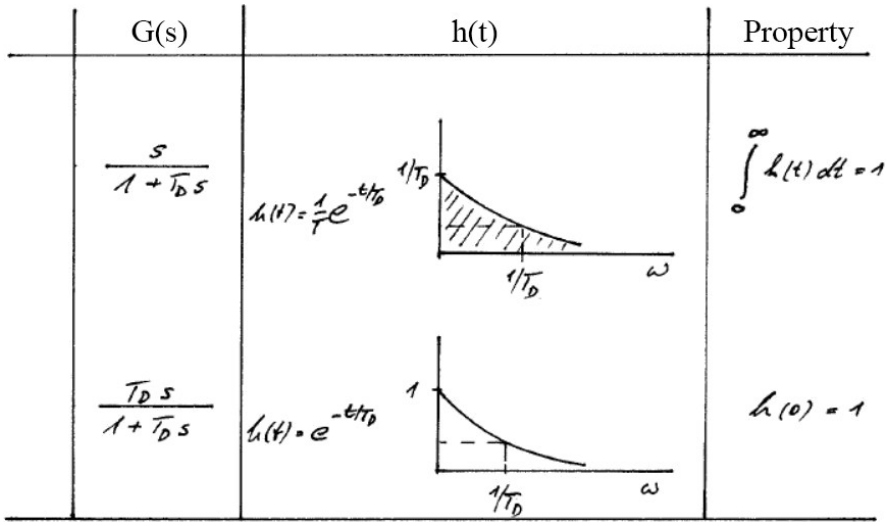

Table 4.7: Transition function h(t) of a high-pass filter

The scaling must therefore be carried out for the expected real edge slopes of the respiratory signal; when testing with ideal step functions, their amplitude must be selected correspondingly smaller.

The maximum breathing amplitude was again assumed to be approx. 1.5 litres. The scaling of the identification experiment was used as a basis (Table 4.1) and and the input signal was set to 1 litre breathing volume, corresponding to 7.24 V, at the EAI. The average HR values are around 800 msec. Since no negative values can occur, I chose 1000

[13] **Scaling:** When modelling a natural system, the units of measurement of its physical variables must be set in relation to those of the model. This is called scaling. A distinction is made between time and amplitude scaling. When you are interested in a simulation only, the machine time is chosen so that the model behaviour can be easily observed and recorded. If the model is to be used in real time, machine time is set equal to natural time. With amplitude scaling, care must be taken to ensure that no computing element is overdriven at any time and that at the same time the signal level is always sufficiently far above the noise level.

msec IBI to correspond to 0V output signal of the EAI. A sampling resolution of 1 msec was selected for the PDP8/E. The maximum IBI occurring due to the PDP8/E's limited integer range is therefore 2048 msec, and I set

2000 msec = 10 V.

The maximum value of 2000 msec = 30 bpm will be sufficient in any case. The required conversions were included in the programmes generating the output at the D/A converters (HSZYK & HSZYK1). The amplification factors of the integrators and summators are shown in Fig. 4.44.

4.4.4.5 Parameter settings

For setting the parameters of the delay elements, the mean respiratory signal is repetatively fed to the model again, and the model responses are compared with the stored mean HR responses on the oscilloscope.

Optimising the approximation in real time is too time-consuming. A single saved process (Fig. 4.16) takes 58 seconds, i.e. after each parameter adjustment it would be necessary to wait until the result is visible. A repetition rate at which stationary images are obtained on the oscilloscope would be desirable; this would correspond to approx. 20 sequences/sec. However, the software-controlled output at the D/A converters is too slow for this, achieving a rate of only about. 0.3/sec (with 1000 values per cycle). A fast digital buffer that would allow high rates will be at our disposal only in the near future, so for the time being the following compromise was chosen:

The comparison with the original takes place at 10x speed. For each parameter adjustment, the system switches to 5000x speed, whereby a test signal from the function generator is used. The success of the corrected settings is checked again at 10x speed (see Fig. 4.46 for an overview).

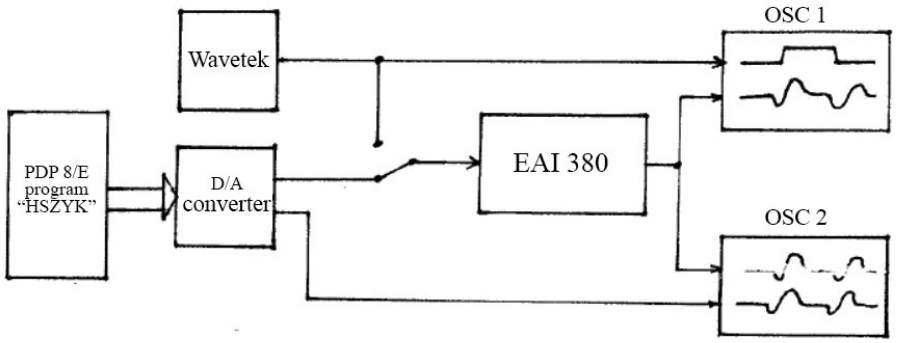

Fig. 4.46: Arrangement for setting the model parameters

4.4.5 Result of the simulation, properties of the model

The described procedure was used to simulate the HRR shown in Fig. 4.16. The result was recorded with an X/Y recorder (manufacturer: BRYANS); it is shown in Fig. 4.47. The upper curve shows the repetitive respiratory stage output twice, followed by the stored average HRR and the output signal of the model. Simulated and averaged step response of the HR show an excellent match.

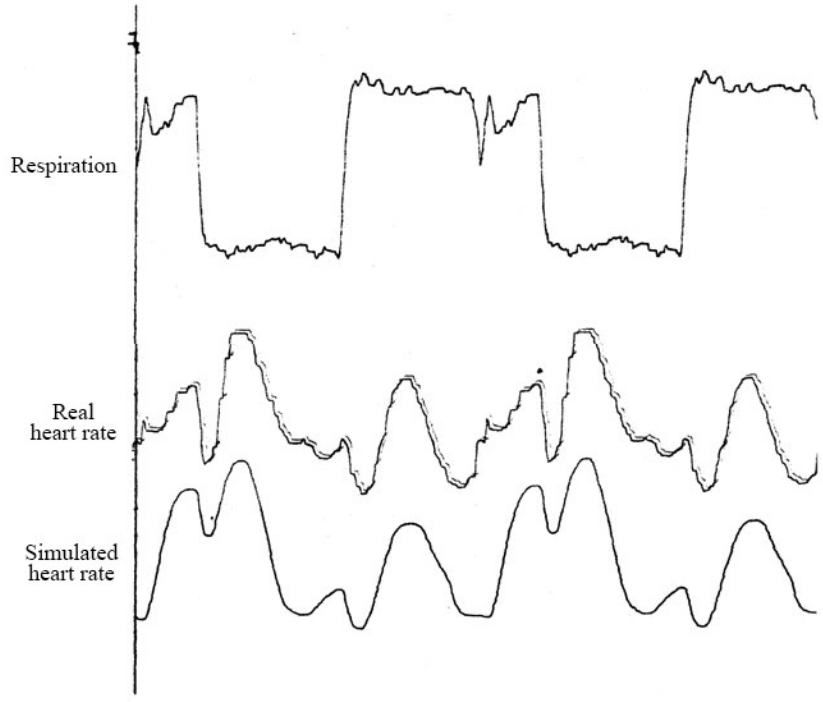

Fig. 4.47: Simulation of the heart rate response during stepped breathing with a 3rd order analogue computer model.

The corresponding potentiometer settings are summarised in Table 4.8.

Potentiometer #	Setting	Parameter	Functional stage
P02	0.60	1/100 T_D	Differentiator
P04	0.22	k	Total amplification factor
P05	0.9	k	Delay element for inspiration
P09	0.65	–p/10	
P10	0.39	q/10	
P11	0.25	u/10	
P12	0.11	1/v	
P06	0.73	k	Delay element for expiration
P13	0.99	–p/10	

P14	0.18	q/10	
P15	0.31	u/10	
P18	0.070	1/v	
P19	0.36	$1/T_3$	3rd low pass

Table 4.8: Potentiometer settings for simulating the course of Fig. 4.16

The following transfer function can be taken from the potentiometer settings:

$$G(s) = \begin{cases} \dfrac{0.167s}{1+0.017s} \cdot 0.9 \dfrac{s^2 - 6.5s + 3.9}{1+2.5s+9s^2} \cdot \dfrac{27.8}{1+2.78s} \cdot 2.2 & \text{inspiration} \\ \dfrac{0.167s}{1+0.017s} \cdot 0.73 \dfrac{s^2 - 9.9s + 1.8}{1+3.1s+14.3s^2} \cdot \dfrac{27.8}{1+2.78s} \cdot 2.2 & \text{expiration} \end{cases}$$

or, after summarizing the equations

$$G(s) = \begin{cases} 1.02 \cdot \dfrac{s}{1+0.17s} \cdot \dfrac{s^2 - 6.5s + 3.9}{(s^2 + 0.28s + 0.11)(1+2.78s)} & \text{inspiration} \\ -0.52 \cdot \dfrac{s}{1+0.17s} \cdot \dfrac{s^2 - 9.9s + 1.8}{(s^2 + 0.22s + 0.07)(1+2.78s)} & \text{expiration} \end{cases}$$

Poles and zeros for this are:

For inspiration

Poles	Zeros
$P_{1/2} = -0.14 + 0.30i$	$N_1 = 0$
$P_3 = -0.36$	$N_2 = +0.67$
$P_D = -60$	$N_3 = +5.83$

For expiration

$P_{4/5} = -0.11 + 0.24i$	$N_4 = 0$
$P_6 = -0.36$	$N_5 = +0.19$
$P_D = -60$	$N_6 = +9.71$

It is therefore a maximum-phase system. We can illustrate the behaviour of the individual systems by their corresponding pole/zero and Bode diagrams, for inhalation and exhalation (Figs. 4.48 and 4.49).

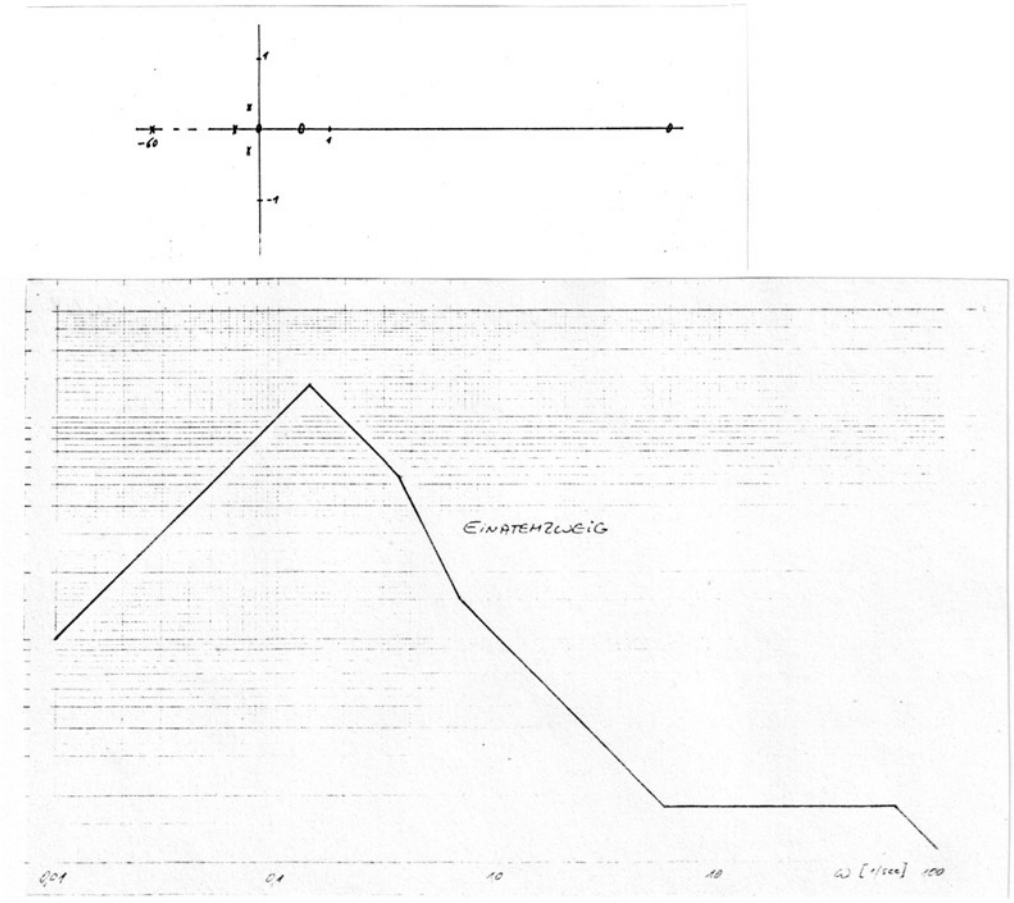

Fig. 4.48: Pole/zero and Bode diagram for inhalation

The frequency response of the total system was measured point by point with sinusoidal excitation (1 V_{pp} corresponding to 140 ml breathing volume) (Fig. 4.50). The maximum is at 50 mHz, about one fifth of the subject's normal breathing frequency (250 mHz). It is 500 mV_{pp}; converted to 1 litre of respiratory volume this results in 3.62 V_{pp} = 362 msec = 36 bpm (based on a resting heart rate of 800 msec). To the left and right of the maximum, the RSA amplitude drops by 6 dB/octave; at normal respiratory rate it is still approx. 30% of the maximum value.

For comparison: The RSA curves with sinus-like breathing shown in DAVIES & NEILSON (1967) (see Fig. 4.28) were analysed with breathing frequencies of 74 mHz (approx. 4/min), 115 mHz (approx. 8/min), and 240 mHz (approx. 16/min). Compare the HR curve with the model output signals with sinusoidal excitation at comparable frequencies (Fig. 4.51).

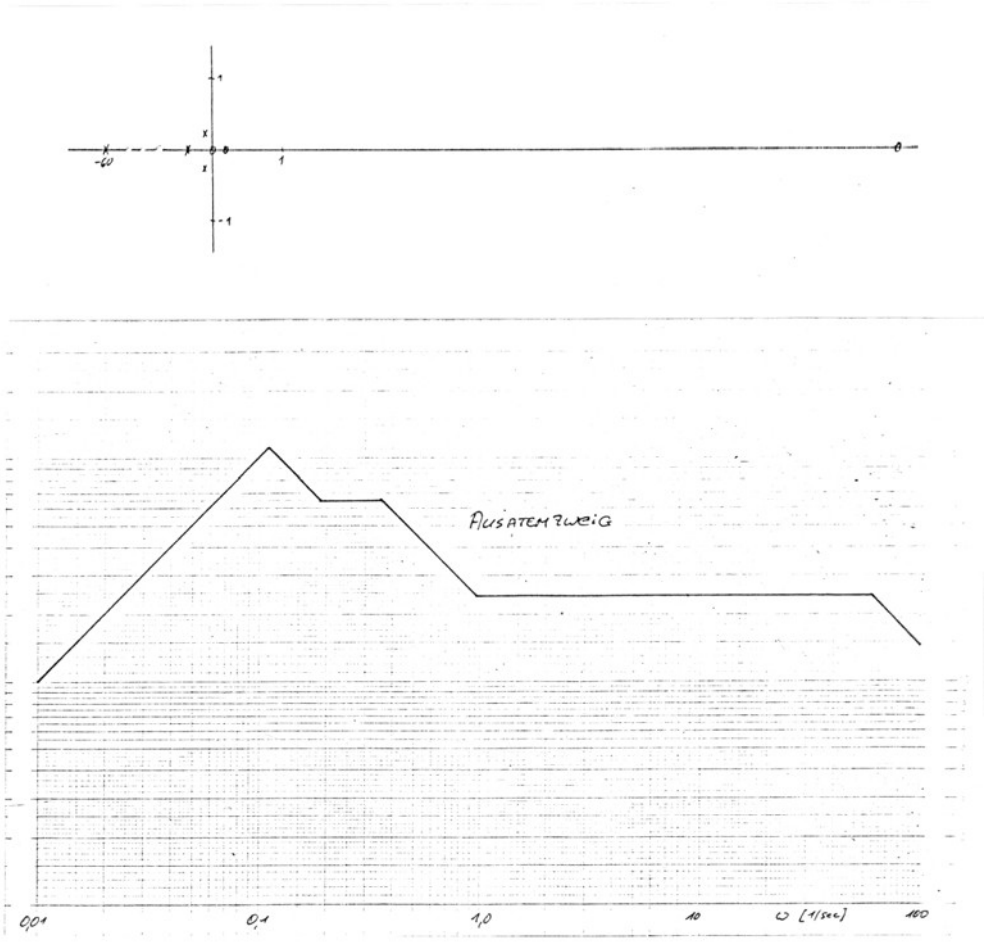

Fig. 4.49: Pole/zero and Bode diagram for exhalation

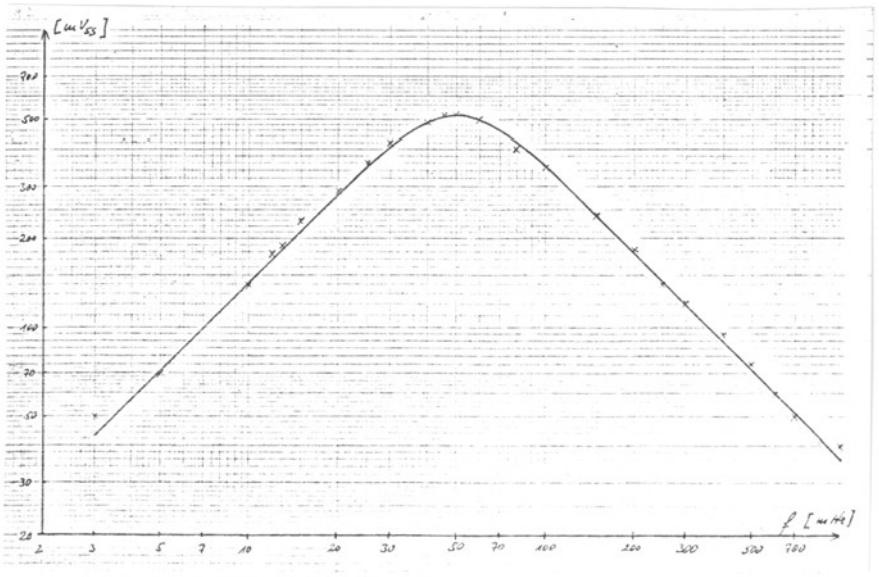

Fig. 4.50: Frequency response of the RSA model

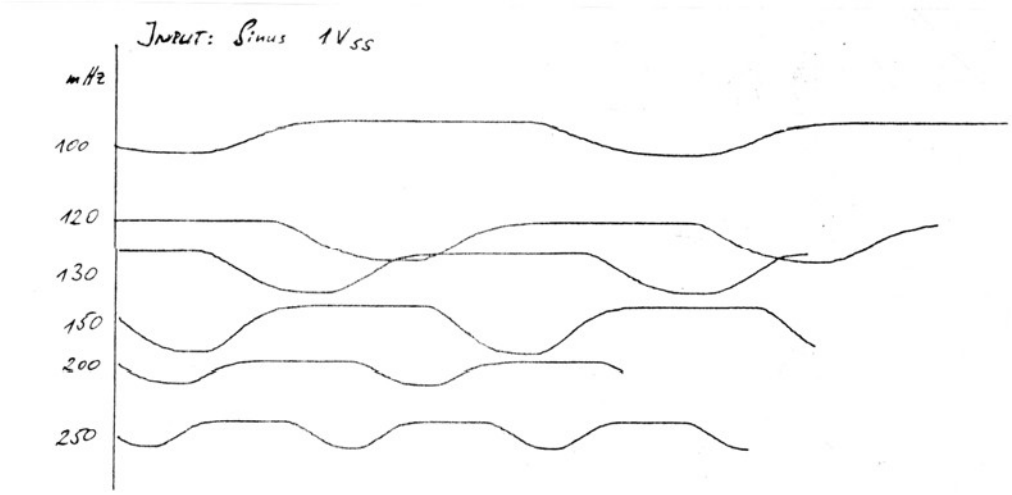

Fig. 4.51: Model response with sinusoidal excitation

4.5 Discussion of the RSA model

The model described is not the first attempt to simulate respiratory arrhythmia. It differs from its predecessors in that the aim was to use it for RSA extraction in psycho-physiological investigations.

While CLYNES, for example, was interested in simulating the ECG pulse sequence, the tachogram of the HR was used here. The omission of the non-linear oscillator, which was used to generate this pulse sequence and had now become unnecessary, had consequences for the structural details of the model.

The control-theoretical blood circulation models presented above, such as that of LUCZAK & RASCHKE, are too complex to be useful at this point in time. Compared to the model in this paper, they have the advantage that they can also be used to predict the behaviour of HR under physical stress. There is still little information available, however, at which point such an extension becomes necessary. Perhaps an amplitude control, controlled by the mean HR, is sufficient to adapt the present model to stressful situations.

The first priority should probably be to test the model under resting conditions. Is it capable of capturing the entire range of typical RSA curves? CLYNES (1960, 1961, 1969), LUCZAK & RASCHKE (1975), FÖRSTER et al. (1978) are content with specifying average parameters with which the simulation should be possible for a wide range of people with little loss of accuracy. On the other hand, all authors agree that the extent of the RSA varies greatly from person to person and the arrhythmia is often even completely absent.

An average RSA model may therefore be sufficient for responses averaged over groups. As soon, however, as information about individuals is of interest, person-specific parameters become necessary. One example would be the investigation of the habituation of the HR-OR for diagnostic purposes. The standardised identification experiment described above is justified here.

Regarding the choice of the analogue computer as a simulation instrument, real-time applications were the main consideration. For off-line analyses, digital extraction might be considered instead. However, the alternative put in this way does not quite meet the core of the question. Namely, the knowledge of the transfer function required for the analogue simulation allows the construction of a digital recursive filter that works so rapidlythat it does not overload the digital computer during data recording. Only when the computer is operated at the limits of its capacity in the application situation, outsourcing of the preprocessing of data must be considered.

Since an analogue computer will only be available in rare cases, circuitry with integrated analogue components or a microprocessor system can be considered. The analogue computer circuitry described here can be replicated compactly and cheaply with an integrated multiple operational amplifier. For a digital realisation, the newly available single-chip processors with integrated A/D and D/A converters offer a particularly elegant option for miniaturisation. However, the high price of these components currently stands in the way of routine use.

The experimental effort and cost of implementing the procedure are still relatively high. Calibration of the breath measurement, identification experiment, evaluation and adjustment of the parameters together required approx. 4 hours per person. The time could be reduced by automating the calibration of the breath measurement belt and getting more routine in carrying out the experiment.

In retrospect, the question arises as to whether respiratory volume is the appropriate input variable for an RSA model. Through the choice of the criterion variable in the regression, a preliminary decision was made for this variable. The common differentiator for the inhalation and exhalation branches in the model in effect first calculates respiratory flow velocity from the respiratory volume. By recording respiratory flow velocity directly, the differentiator stage, which turned out to be problematic with respect to scaling, could be omitted.

However, when considering the physiological mechanisms underlying

the RSA, the question arose as to whether the intrathoracic pressure, which is responsible for the magnitude of the flow velocity, might not be the actually effective variable. A suitable indirect method of pressure measurement could therefore perhaps allow for an even more reliable prediction of the RSA.

5. SUMMARY

Respiratory arrhythmia (RSA) is a confounding factor in the recording of short-term heart rate changes. An analogue computer simulation of the RSA was developed, which is suitable for real-time correction of the heart rate measurement in psychophysiological experiments. Special emphasis was placed on an exact indirect respiratory volume measurement, through which the subject is particularly little impeded. The theoretical principles of RSA extraction are discussed in detail.

6. LITERATURE

ANGELONE, A. & COULTER, N. A. (1964). Respiratory sinus arrhythmia: a frequency dependent phenomenon. J. Appl. Physiol. 19, 479 - 482.

BELMAKER, R., PROCTOR, E. & FEATHER, B. W. (1972). Muscle tension in human operant heart rate conditioning. Conditioned Reflex 7, 97-106.

BROWN, C. C. (1967). Methods in Psychophysiology. Williams & Wilkins, Baltimore.

CLYNES, M. (1960). Respiratory control of heart rate. Laws derived from analogue computer simulation. IRE Trans. Med. Electr. ME-7, 2-14.

CLYNES, M. (1961). Unidirectional rate sensitivity: A biocybernetic law of reflex and humoral systems as physiologic channels of control and communication. Ann. N. Y. Acad. Sci. 92, 946-969.

CLYNES, M. (1969). Cybernetic implications of rein control in perceptual and conceptual organisation. Ann. N. Y. Acad. Sci. 156(2), 629-670.

CHESS, G.F., TAM, R. M. & CALARESU, F. R. (1975). Influence of cardiac neural inputs on rhythmic variations of heart period in the cat. Am. J. Physiol. 228, 775-780.

DALY, I. de B. (1930). The resistance of the pulmonary vascular bed. J.

Physiol. 69, 238-253.

DAVIES, C. T. M. & NEILSON, J. M. M. (1967). Sine arrhythmia in man at rest. J. Appl. Physiol. 22, 947-955.

EAI, ELECTRONIC ASSOCIATES, INC (1975). 380 Analogue/ hybrid computing system reference handbook. New Jersey.

FERSTL, R. & HÖLZL, R. (1979). Evoked heart rate response as a function of stimulus parameters, respiration phase, and averaging procedure. Psychophysiology 16, p. 194.

FISCHER, F. A. (1969). Einführung in die statistische Übertragungstheorie [Introduction to statistical transmission theory]. BI, Mannheim.

FÖRSTER, F. (1978). Zur psychophysiologischen Methodik: Phasische Herzfrequenz-Reaktion unter Berücksichtigung der respiratorischen Arrhythmie [On psychophysiological methodology: phasic heart rate reaction taking into account respiratory arrhythmia]. Z. Psychol. 186,4 518 528.

FREYSCHUSS, U. & MELCHER, A. (1976). Respiratory sinus arrhythmia in man: Relation to cardiovascular pressures. Scand. J. Clin. Lab. Invest. 36, 221-229.

GALLOWAY, D. G. & WOMACK, B. F. (1969). An application of spectral analysis and digital filtering to the study of respiratory sinus arrhythmia. Electron. Res. Ctr, Univ. of Texas, Austin, Tech. Rep. 71, Aug. 7.

GANONG, W. F. (1972). Medizinische Physiologie [Medical Physiology]. Springer, Berlin.

HAMILTON, L. H. & RIEKE, R. J. (1972). Ventilation monitor based on transthoracic impedance changes. Med Res. Eng. May/June, 20-24.

HART, J. D. (1975). Cardiac response to simple stimuli as a function of phase of the respiratory cycle. Psychophysiology 12, 634-636.

HÖLZL, R. (1976). Methodische Probleme beim Biofeedback der Herzfrequenz: Meßtechnik, Verstärkungspläne, Mediatoren [Methodological problems in heart rate biofeedback: measurement technique, amplification schedules, mediators]. Unpublished Phil. Diss. Munich.

HOLBROOK, J.G. (1970). Laplace-Transformationen. Vieweg, Braunschweig.

ISERMANN, R. (1971). Experimentelle Analyse der Dynamik von

Regelsystemen. Identifikation I. [Experimental analysis of the dynamics of control systems. Identification I]. BI, Mannheim, Vol. 515/ 515 a.

JENNINGS, J. R., STRINGFELLOW, J. C. & GRAHAM, M. (1974). A comparison of the statistical distributions of beat-by-beat heart rate and heart period. Psychophysiology 11, 207-210.

KATONA, P. G. & BARNETT, G. O. (1969). Central origin of asymmetry in the carotid sinus reflex. Ann. N. Y. Acad. Sci. 779 – 786.

KATONA, P. G. & JIH, F. (1975). Respiratory sinus arrhythmia: Noninvasive measure of parasympathetic cardiac control. J. Appl. Physiol. 39, 801-805.

KHACHATURIAN, Z. S., KERR, J., KRUGER, R. & SCHACHTER, J. (1972). A methodological note: Comparison between period and rate data in studies of cardiac function. Psychophysiology 9, 539-545.

KOEPCHEN, H.-P. & THURAU, K. (1958). Studies on the relationship between blood pressure waves and respiratory internalisation. Pflügers Archiv 267, 10-26.

KOEPCHEN, H.-P. & THURAU, K. (1959). About the Conditions for the development of respiratory synchronous fluctuations of the vagus tone (respiratory arrhythmia). Pflügers Archiv 269, 10-30.

LANG, P. J. & HNATIOW, M. (9162). Stimulus repetition and the heart rate response. J. Comp. Physiol. Psychol. 55, 781-785.

LAURIG, W., LUCZAK, H. & PHILIPP, U. (1971). Ermittlung der Pulsfrequenzarrhythmie bei körperlicher Arbeit [Investigation of pulse rate arrhythmia during physical labour]. Int. Z. angew. Physiol. 30, 40-51.

LUCZAK, H. & LAURIG, W. (1973). An analysis of heart rate variability. Ergonomics 16, 85-97.

LUCZAK, H. & RASCHKE, F. (1975). Regelungstheoretisches Kreislaufmodell zur Interpretation arbeitsphysiologischer und rhythmologischer Einflüsse auf die Momentanherzfrequenz: Arrhythmie [Control-theoretical circulatory model for the interpretation of work physiological and rhythmological influences on the instantaneous heart rate: Arrhythmia]. Biol. Cybernetics 18, 1-13.

MCFARLAND, D. J. (1971). Feedback Mechanisms in Animal Behaviour. Acad. Press, London.

MILSUM, J. H. (1966). Biological Control Systems Analysis. McGraw

Hill, New York. (1966).

MIYAWAKI, K., TAKAHASHI, T. & TAKEMURA, H. (1966). Analysis and simulation of the periodic heart rate fluctuation. Techn. Rep. Osaka Univ. 16, 315-325.

OPPELT, W. (1960). Kleines Handbuch technischer Regelvorgänge [A Brief Manual of Technical Control Processes]. Weinheim.

PICKERING, W. D., NIKIFORUK, P. N. & MERRIMAN, J. E. E. (1969). Analogue computer model of human cardiovascular control system. Med. Biol. Eng. BME 7, 401-410.

PIIPER & KOEPCHEN, H.-P. (1972). Atmung. Reihe: Gauer, Kramer, Jung: Physiologie des Menschen, Bd. 6 [Respiration. Series: Gauer, Kramer, Jung:Human Physiology, Vol. 6]. München.

ROSENBLUETH, A. & SIMEONE, F. A. & SIMEONE, F. A. (1934). The interrelations of vagal and accelerator effects on the cardiac rate. Am. J. Physiol. 110, 42.

ROSKO, J. S. (1972). Digital Simulation of Physical Systems. Addison-Wesley, Reading.

SCHANDRY, R., LUTZENBERGER, W. & BIRBAUMER, N. (1977). Die phasische Reaktion der Herzrate und deren Habituation auf Töne verschiedener Intensität [The phasic response of the heart rate and its habitat to sounds of different intensities]. Psychol. Beitr. Vol. 19,2; 256-280.

SCS STANDARDS COMMITTEE (1977). Standard Symbols for Analogue and Hybrid Computers. Simulation 29, 211-218.

SHAPIRO, A. & COHEN, H. D. (1965). The use of mercury capillary length gauges for the measurement of the volume of thoracic and diaphragmatic components of human respiration: A theoretical analysis and a practical method. Trans. N. Y. Acad. Sci. Series II, 634-649.

SROUFE, L. A. (1971). Effects of depth and rate of breathing on heart rate and heart rate variability. Psychophysiology 8, 648-655.

STROBEL, H. (1968). Systemanalyse mit determinierten Testsignalen [Systems analysis with determined test signals]. VEB-Technik, Berlin.

UNBEHAUEN, R. (1971). Systemtheorie. Eine Einführung für Ingenieure [Systems theory. An introduction for engineers]. München, Wien.

VALENTINUZZI, E. E. & GEDDES, L. A. (1974). The central component of the respiratory heart-rate response. Cardiocascular Res.

Ctr. Bull. 12, 87-103.

VANBERGEN, F. H., NOVAK, A. L. & CUMMING, J. F. (1970). Analogue computer for on-line determinations of ventilatory power, work, and volume. Med. Res. Eng. Dec. 1970, 7-13.

WOMACK, B. F. (1971). The analysis of respiratory sinus arrhythmia using spectral analysis and digital filtering. IEEE Trans. Bio-Med. Eng. Vol. BME-18, No. 6.

7. Appendix

7.1 Temperature-compensated belt for breathing measurement

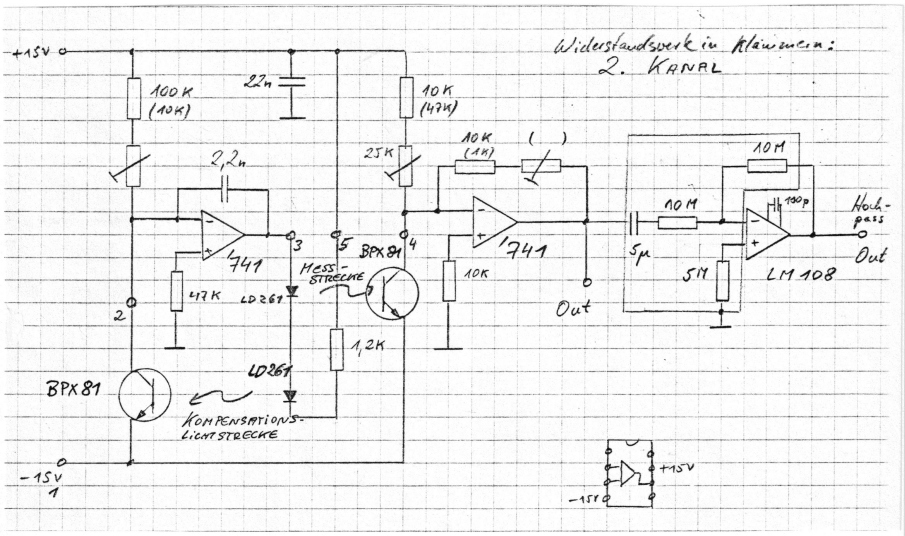

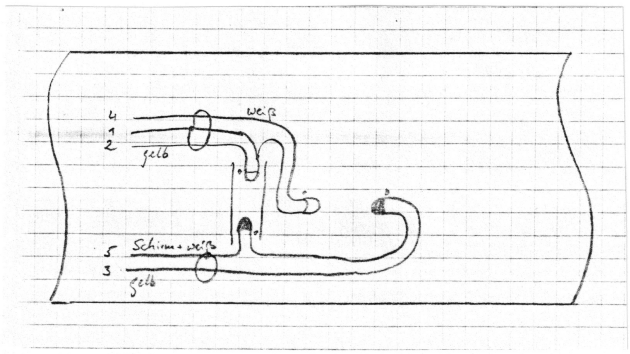

7.2 Transfer functions and step responses

No. (Holb.#)*	Transfer function	h(0)	$\dot{h}(0)$	h(∞)	Step response h(t)
1	$\frac{1}{1+T_1 s}$	0	$\frac{1}{T_1}$	1	$1-e^{-t/T_1}$
2	$\frac{s}{1+T_1 s}$	$\frac{1}{T_1}$	$-\frac{1}{T_1^2}$	0	$\frac{1}{T_1}e^{-t/T_1}$
3 (12)	$\frac{1}{(1+T_1 s)(1+T_2 s)}$	0	0	1	$1+\frac{1}{T_1-T_2}\cdot\left(T_1 e^{-t/T_1}-T_2 e^{-t/T_2}\right)$
4 (11)	$\frac{s}{(1+T_1 s)(1+T_2 s)}$	0	$\frac{1}{T_1 T_2}$	0	$\frac{1}{T_2-T_1}\cdot\left(e^{-t/T_1}-e^{-t/T_2}\right)$
5 (99)	$\frac{s+a}{(1+T_1 s)(1+T_2 s)}$	0	$\frac{1}{T_1 T_2}$	a	$a+\frac{-1+aT_1}{T_2-T_1}\cdot e^{-t/T_1}-\frac{-1+aT_2}{T_1-T_2}\cdot e^{-t/T_2}$
6 (93)	$\frac{s^2}{(1+T_1 s)(1+T_2 s)}$	$\frac{1}{T_1 T_2}$	$\frac{-T_1-T_2}{T_1^2 T_2^2}$	0	$\frac{T_2\cdot e^{-t/T_1}-T_1\cdot e^{-t/T_2}}{T_1 T_2 (T_2-T_1)}$
7 (98)	$\frac{s(s+p)}{(1+T_1 s)(1+T_2 s)}$	$\frac{1}{T_1 T_2}$	$\frac{pT_1 T_2-T_1-T_2}{T_1^2 T_2^2}$	0	$\frac{T_2(1-pT_1)\cdot e^{-t/T_1}-T_1(1-pT_2)\cdot e^{-t/T_2}}{T_1 T_2 (T_2-T_1)}$

* The table was created with the help of the formulary from Holbrook (1970). The names in parentheses correspond to the formula numbering there: HOLBROOK, J.G. (1970). Laplace-Transformationen. Vieweg, Braunschweig, Appendix III, p. 286–316.

2025: Note that Holbrook's table refers to impulse response functions rather than the step response functions shown here in the left column. There is therefore an extra variable "s" in the numerators here (resp. a factor "s" less in the denominator). Note further that there were sign errors in eqs. (3), (4), and (5) in the German original.

No. (Holb.#)*	Transfer function	h(0)	$\dot{h}(0)$	h(∞)	Step response h(t)
8 (156)	$\frac{K(s^2+ps+q)}{(1+T_1s)(1+T_2s)}$	$\frac{K}{T_1T_2}$	$K\cdot\frac{pT_1T_2-T_1-T_2}{T_1^2T_2^2}$	Kq	$Kq+K\frac{qT_1^2-pT_1+1}{T_1(T_2-T_1)}\cdot e^{-t/T_1}-K\frac{qT_2^2-pT_2+1}{T_2(T_2-T_1)}$
	$p=\frac{(A+B)T_1+(A+C)T_2}{(A+B+C)T_1T_2}$ $K=(A+B+C)T_1T_2$ $q=A/K$	$A+B+$	—	A	$A+B\cdot e^{-t/T_1}+C\cdot e^{-t/T_2}$
9 (101)	$\frac{s^2}{(1+T_1s)(1+T_2s)(1+T_3s)}$	0	$\frac{1}{T_1T_2T_3}$	0	$\frac{e^{-t/T_1}}{(T_1-T_3)(T_2-T_1)}+\frac{e^{-t/T_2}}{(T_3-T_2)(T_2-T_1)}+\frac{e^{-t/T_3}}{(T_1-T_3)(T_3-T_2)}$
	Example (time constants taken from Clynes (1960, p. 11) $T_1 = 1.2$ $T_2 = 4.6$ $T_3 = 3.2$ h(0) = 0.02392 h(∞) = 0 $h(t)=\frac{1}{1000}\left(-8.38\cdot e^{-t/1.2}+12.0\cdot e^{-t/4.6}+20.3\cdot e^{-t/3.2}\right)$				
10 (101)	$\frac{s(s+p)}{(1+T_1s)(1+T_2s)(1+T_3s)}$	0	$\frac{1}{T_1T_2T_3}$	0	$\frac{(1-pT_1)e^{-t/T_1}}{(T_1-T_3)(T_3-T_2)}+\frac{(1-pT_2)e^{-t/T_2}}{(T_2-T_1)(T_3-T_2)}+\frac{(1-pT_3)e^{-t/T_3}}{(T_1-T_3)(T_3-T_2)}$

No. (Holb.#)*	Transfer function	h(0)	$\dot{h}(0)$	h(∞)	Step response h(t)
11 (158)	$\frac{s^2(s+p)}{(1+T_1s)(1+T_2s)(1+T_3s)}$	$\frac{1}{T_1T_2T_3}$	∞	0	$\frac{(p-1/T_1)e^{-t/T_1}}{(T_1-T_3)(T_2-T_1)}+\frac{(p-1/T_2)e^{-t/T_2}}{(T_2-T_1)(T_3-T_2)}+\frac{(p-1/T_3)e^{-t/T_3}}{(T_1-T_3)(T_3-T_2)}$
	The coefficients of eq. 10 and 11 are closely related to each other. When we set $h(t)=A_i\cdot e^{-t/T_1}+B_i\cdot e^{-t/T_2}+C_i\cdot e^{-t/T_3},\quad i=10,11,$ we have $A_{10}=-T_1A_{11}\quad B_{10}=-T_2B_{11}\quad C_{10}=-T_3C_{11}$				
12 (158)	$\frac{s(s^2+ps+q)}{(1+T_1s)(1+T_2s)(1+T_3s)}$	$\frac{1}{T_1T_2T_3}$	∞	0	
13	<u>Parallel shift</u>				
	G(s) G(s)+a	G(0) G(0)+a	G(∞) G(∞)+a		h(t) h(t)+a

7.3 Basic analogue-computer circuits

1)	Summator	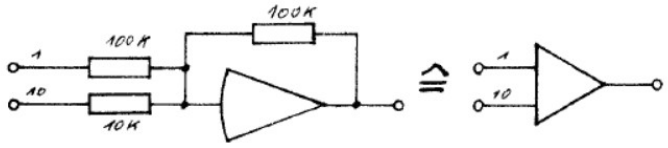	
2)	Integrator	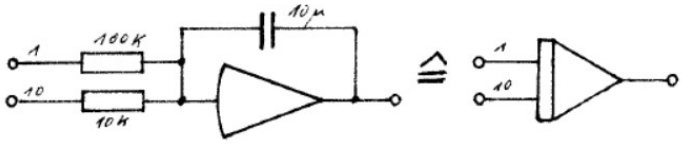	
3)	Low pass	$G(s)=\frac{1}{1+T_1 s}$	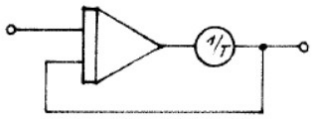
4)	High pass	$G(s)=\frac{s}{1+T_1 s}$	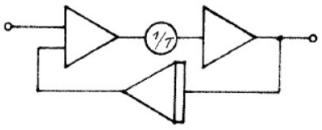
		$G(s)=\frac{cTs}{1+Ts}$	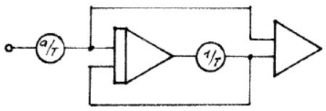
		$G(s)=\frac{as}{1+Ts}$	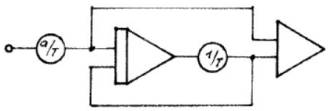
5)	DT_1 element	$G(s)=\frac{(dT-c)-cTs}{1+Ts}$	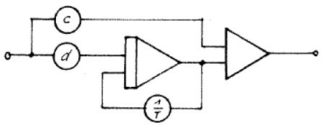
		$G(s)=\frac{(d-c)-cTs}{1+Ts}$	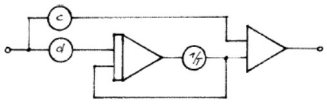
6)	2nd order	$G(s)=\frac{a}{1+Ts^2}$	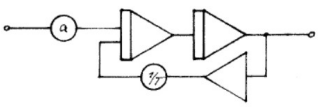
7)	2nd order	$G(s)=\frac{1}{1+s+s^2}$	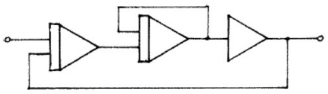
8)	2nd order	$G(s)=\frac{s}{10+10s+s^2}$	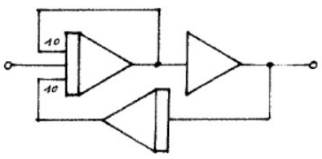

9)	2nd order	$G(s) = \frac{s^2 + ps + q}{1 + us + vs^2}$ 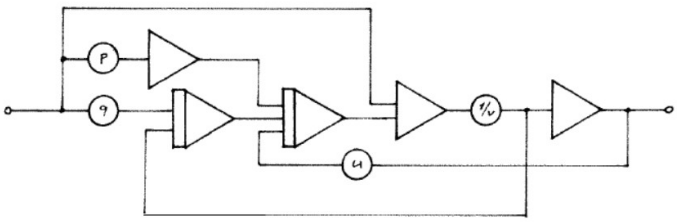

7.4 Description of the program system

Help files for the PDP-8 program system are reprinted in the German version of the thesis. Programs were mostly written by Hans Strasburger, 1977–1979, a few were written by Helmut Zucker (then at the IT department of the MPIP), and Werner Gless, written at around the same time. Languages were Fortran II and some SABR.